

**Apoptotic and Proteomic Study of
Two Bioactive Compounds Isolated from *Sophora flavescens*
on Human Hepatocellular Carcinoma**

CHEUNG Sao Fong

**A Thesis Submitted in Partial Fulfillment of
the Requirement for the Degree of**

**Master of Philosophy
In
Biochemistry**

**The Chinese University of Hong Kong
September 2006**

The Chinese University of Hong Kong holds the copyright of this thesis. Any person(s) intending to use a part or whole of the materials in the thesis in a proposed publication must seek copyright release from the Dean of the Graduate School



THESIS/ ASSESSMENT COMMITTEE

Prof. WAYE Miu Yee, Mary (Chair)

Prof. AU Wing Ngor, Shannon (Thesis Supervisor)

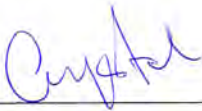
Prof. FUNG Kwok Pui (Thesis Supervisor)

Prof. KWOK Tim Tak (Committee Member)

Prof. CHAN Pui Kwong (External Member)

DECLARATION

I declare that the assignment here submitted is original except for source material explicitly acknowledged. I also acknowledge that I am aware of University policy and regulations on honesty in academic work; and of the disciplinary guidelines and procedures applicable to breaches of such policy and regulations, as contained in the website <http://www.cuhk.edu.hk/policy/academichonesty/>.



Signature

15 Sept, 2006

Date

CHEUNG Sao Fong, Crystal

Name

04073200

Student ID

BCH806R

Course code

Thesis Research

Course title

ACKNOWLEDGEMENTS

With a deep sense of gratitude, I would like to express my sincere thanks to my supervisors, Professor Fung Kwok Pui and Professor Au Wing Ngor, Shannon for their patient guidance throughout my graduate study.

I also wish to thank Professor Kong Siu Kai and Professor Kwok Tim Tak for providing me critical materials in the experiments of apoptosis; as well as Professor Ngai Sai Ming and Miss Helen Tsai (Department of Biology) for their immense assistance in executing the proteomic work.

I am indebted to Mr. Johnny Koon, Miss Karen Chung, Miss Cecilia Chan and Miss Meiji Ma for their invaluable advice and generous technical assistance. Special thanks are due to Mr. Julian Lui, who has always kindly extended timely help in my difficult time. I am also thankful to all my friends in the department. Thanks also go to every current and past members of Room 316, 513 and 514, BMSB and E210, SC for their useful comments and suggestions in my course of studies.

Last but not least, I would like to present my wholehearted thanks to my parents and brother, Keith, who have rendered me enormous encouragement and support during the whole tenure of my research.

This study was supported by earmarked grants from the Research Grant Council (RGC), Hong Kong (Ref. No.: CUHK4399/ 03M).

ABSTRACT

Sophora flavescens is a shrub cultivated widely in northeast Asian countries. *Radix Sophorae* (also known as KuShen), stipulated as the dried roots of this species, is a natural product used in the traditional herbal preparations in China for centuries, being prescribed as an anti-tumor and anti-metastasis agent against hepatocellular carcinoma (HCC). In the earlier time, several bioactive flavonoids were successfully purified and identified from this medicinal herb. Herein, the project focuses to delve into the possible application(s) of the two constituents – Leachianone A and Sophoraflavone J – on HCC treatment by *in vitro* and *in vivo* studies.

Cell viability assay and experiments on cell cycle arrest and apoptotic events showed that the compounds exerted their anti-proliferative activities on hepatoma cells HepG2 and RHepG2 via the induction of apoptosis, with the involvement of both extrinsic (death receptor-mediated) as well as intrinsic (mitochondrial) pathways. Meanwhile, Leachianone A was able to retard the growth of tumor in HepG2-bearing nude mice, as corroborated by the 17% - 54% reduction of tumor size when compared to the control group.

Most importantly, its administration failed to cause any toxicity to the heart and liver tissues of the hosts.

The same set of tests was also conducted with Sophoraflavone J on HepG2 cells, in which cell death was again mediated by apoptosis. In attempt to further define the mechanism(s) underlying its actions, a comparative proteomic approach was employed. Spots with differential expression patterns identified so far included multiple classes of proteins, for instance membrane proteins/ antigens, structural proteins, transcriptional factors, glycolytic enzymes, heat-shock chaperon proteins (HSP), reactive oxygen species (ROS)-related proteins and proteosomes, etc. The findings were confirmed by Western blot analysis and real-time PCR. Preliminary experiments for characterization of the roles of these proteins were done as well. It was hypothesized that Sophoraflavone J brought about cell death through generation of oxidative stresses, which subsequently led to mitochondrial dysfunction.

In an overall, we uncovered that the anti-cancer effects of Leachianone A and Sophoraflavone J were achieved by apoptosis, dependent of the

activation of caspases-3, -8 and -9. Albeit this, cell cycle arrest did not come off throughout the whole treatment process. On the other hand, using proteomics for the molecular dissection of mechanisms, we came up with some novel protein candidates of significance in the understanding the full pictures of disease pathogenesis and recuperation.

論文摘要

氧化苦參碱 (*Sophora flavescens*) 是一種廣泛在東南亞國家培植的灌木。 氧化苦參碱的根部 (又名苦參, KuShen), 約定爲此植物品種的乾燥根, 是一種於中國採用良久作爲傳統草本配方的自然物質, 用作抗肝癌症和抗肝癌症擴散的藥方。 在稍早前的時間, 幾種具生物活性的黃酮類成功由這含藥效的草藥裡被純化和鑑定。 在此, 科研項目集中於沿用體內和體外的研究去探索兩種成份 --- 利奇槐酮 A (Leachianone A) 和槐黃酮 J (Sophoraflavone J) --- 用作爲肝癌症治療的應用可能性。

由一些細胞生存能力的測試和細胞周期停滯及細胞自毀的實驗結果顯示出, 這兩個化合物是透過引發細胞自毀來發揮其於肝癌細胞 HepG2 和 RHepG2 之抗增殖行動, 涉及外在 (死亡感受體) 的和內在 (線粒體) 兩個途徑。 與此同時, 隨著相對於對照群組的 17% 至 54% 腫瘤尺寸減小之證據, 利奇槐酮 A 是能夠減慢腫瘤在帶有 HepG2 肝癌細胞的裸鼠上生長。 而最重要的是, 它的服用不會給寄主的心臟和肝臟組織呈現任何毒性。

相同的測試實驗亦都給槐黃酮 J 於肝癌細胞 HepG2 進行; 結果是, 細胞的死亡相似地是以細胞自毀來引發。 爲嘗試進一步解釋它的行爲的構成機制, 比較性的蛋白質組學方法被利用作研究。 確認為擁有差別的表達形式之點塊包括了多種類別的蛋白, 例如薄膜上的蛋白或抗原, 結構性蛋白, 轉錄因子, 醣酵解過程中的酶, 熱休克伴侶蛋白, 和氧自由基物質有關的蛋白質, 以及蛋白體等等。 這些發現已由免疫印

跡分析和實時螢光定量技術確定。初步用作描述這些蛋白質角色特性的實驗也執行了。建議的是, 槐黃酮 J 憑著產生氧化氣激, 接著引起線粒體官能不良, 從而導致細胞死亡。

整體來說, 我們揭露出利奇槐酮 A 和槐黃酮 J 的抗癌症功效是因細胞自毀而得以實現, 當中是依靠著卡斯帕西斯蛋白酶-3, -8 和-9 的活化。但是, 細胞周期停滯在整個治療過程中並沒有發生。於另一方面, 使用蛋白質組學來解剖分子機制, 我們提出了若干個嶄新的候選蛋白, 重要為疾病的發病原因及康復提供出全面的瞭解。

LIST OF FIGURES AND TABLES

	Figure/ Table Legend	Page
Fig. 1.1.1.1	Statistics of mortality in Hong Kong in 2003.	p. 3
Figure 1.1.4.1.1	Schematic structure of P-glycoprotein and some examples of its substrates.	p. 8
Fig. 1.2.1.1	Photographs taken for the whole plant of <i>Sophora flavescens</i> (A) and its dried root, <i>Radix Sophorae</i> (B, C).	p. 12
Fig. 1.2.2.1	Basic chemical unit of a flavonoid.	p. 14
Fig. 1.2.2.2	Chemical structures of different types of flavonoids, flavanone (A), flavone (B), flavonol (C), isoflavonoid (D), anthocyanin (E) and chalcone (F).	p. 14
Fig. 1.2.3.1	Structures of 6 bioactive flavonoids obtained from the <i>Radix Sophorae</i> .	p. 16
Fig. 1.3.3.1	Outline of the extrinsic (death receptor-mediated) and intrinsic (mitochondrial) pathways.	p. 19
Fig 2.6.4.1	BSA protein standard curve plotted for protein concentration estimation.	p. 52
Fig. 3.1.1	Structures of 6 bioactive flavonoids purified from the <i>Radix Sophorae</i> .	p. 73
Fig. 3.2.1	Effect of Leachianone A on the proliferation of HepG2 cells.	p. 76
Fig. 3.2.2	Effect of Leachianone A on the proliferation of RHepG2 cells.	p. 76
Fig. 3.3.1	Effect of Leachianone A on the proliferation of WRL-68 cells.	p. 78
Fig. 3.4.1	Effect of Sophoraflavone J on the proliferation of HepG2 cells.	p. 80
Fig. 3.5.1	Effect of Sophoraflavone J on the proliferation of WRL-68 cells.	p. 80
Fig. 3.6.1	Effect of cisplatin on the proliferation of HepG2 cells.	p. 83
Fig. 3.6.2	Effect of taxol on the proliferation of HepG2 cells.	p. 83
Fig. 3.6.3	Effect of cisplatin on the proliferation of RHepG2 cells.	p. 84

Fig. 3.6.4	Effect of taxol on the proliferation of RHepG2 cells.	p. 84
Fig. 3.6.5	Effect of cisplatin on the proliferation of WRL-68 cells.	p. 85
Fig. 3.6.6	Effect of taxol on the proliferation of WRL-68 cells.	p. 85
Fig. 4.1.1	A characteristic pattern of untreated cells in the sub-G1, G1/ G0, G2/ M and S phases in the cell cycle analysis.	p. 89
Fig. 4.1.2	Cell cycle analysis of HepG2 cells treated with vehicle or Leachianone A for 48 hours.	p. 91
Fig. 4.1.3	Cell cycle analysis of RHepG2 cells treated with vehicle or Leachianone A for 48 hours.	p. 92
Fig. 4.2.1.1a	Schematic diagram of cell distribution of viable, early apoptotic and later apoptotic/ necrotic cells in annexin V-FITC/ PI staining experiment.	p. 95
Fig. 4.2.1.1b	Density plot of cells exposed to 1 μ M staurosporine for 48 hours.	p. 95
Fig. 4.2.1.2	Annexin V-FITC/ PI staining of HepG2 cells treated with vehicle or Leachianone A for 48 hours.	p. 97
Fig. 4.2.1.3	Annexin V-FITC/ PI staining of RHepG2 cells treated with vehicle or Leachianone A for 48 hours.	p. 98
Fig. 4.2.2.1.1	TUNEL assay of HepG2 cells treated with vehicle or Leachianone A for 48 hours.	p. 101
Fig. 4.2.2.1.2	TUNEL assay of RHepG2 cells treated with vehicle or Leachianone A for 48 hours.	p. 102
Fig. 4.2.2.2.1	Induction of DNA fragmentation in Leachianone A-treated A) HepG2 and B) RHepG2 cells.	p. 104
Fig. 4.3.1.1	Activation of caspases-3, -8 and -9 as well as induction of ICAD and PARP cleavages by Leachianone A in HepG2 and RHepG2 cells.	p. 108
Fig. 4.3.1.2	Study of the enhancement of caspase-3 activity in Leachianone A-treated HepG2 cells.	p. 110
Fig. 4.2.1.3	Study of the enhancement of caspase-3 activity in Leachianone A-treated RHepG2 cells.	p. 111
Fig. 4.3.2.1	Alteration of Expression Levels of Bcl-2 family proteins by Leachianone A in HepG2 and RHepG2 cells.	p. 114
Fig. 4.3.3.1	Study of the loss of mitochondrial membrane potential in Leachianone A-treated HepG2 cells.	p. 117

Fig. 4.3.3.2	Study of the loss of mitochondrial membrane potential in Leachianone A-treated RHepG2 cells.	p. 118
Fig. 4.3.3.3	Release of cytochrome c (cyt c) and apoptosis-inducing factor (AIF) from mitochondria to cytosol in Leachianone A-treated HepG2 and RHepG2 cells.	p. 120
Fig. 4.4.1	Effect of 30-day intra-venous administration of Leachianone A on the size of tumors of HepG2-bearing nude mice.	p. 123-124
Fig. 4.4.2	Evaluation of the toxicity of Leachianone A on heart and liver of the hosts.	p. 125-126
Fig. 5.1.1	Cell cycle analysis of HepG2 cells treated with vehicle or Sophoraflavone J for 48 hours.	p. 134
Fig. 5.1.2	Annexin V-FITC/ PI staining of HepG2 cells treated with vehicle or Sophoraflavone J for 48 hours.	p. 135
Fig. 5.1.3	TUNEL assay of HepG2 cells treated with vehicle or Sophoraflavone J for 48 hours.	p. 136
Fig. 5.1.4	Induction of DNA fragmentation in Sophoraflavone J-treated HepG2 cells.	p. 137
Fig. 5.2.1	Activation of caspases-3, -8 and -9 as well as induction of ICAD and PARP cleavages by Sophoraflavone J in HepG2 cells.	p. 140
Fig. 5.2.2	Study of the enhancement of caspase-3 activity in Sophoraflavone J-treated HepG2 cells.	p. 141
Fig. 5.2.3	Alteration of Expression Levels of Bcl-2 family proteins by Sophoraflavone J in HepG2 cells.	p.142
Fig. 5.2.4	Study of the loss of mitochondrial membrane potential in Sophoraflavone J-treated HepG2 cells.	p. 143
Fig. 5.2.5	Release of cytochrome c (cyt c) and apoptosis-inducing factor (AIF) from mitochondria to cytosol in Sophoraflavone J-treated HepG2 cells.	p. 144
Fig. 5.3.1	Representative overview of 2D-gel images of control and Sophoraflavone J-treated HepG2 cell samples.	p. 150-151
Fig. 5.3.2	Comparison of the protein expression profiles of control and Sophoraflavone J-treated HepG2 cell samples.	p. 152-154
Fig. 5.3.3	Confirmation of the altered expressed protein molecules in Sophoraflavone J-treated HepG2 cells by Western blotting.	p. 158
Fig. 5.3.4	Investigation of modulated mRNA transcripts in Sophoraflavone J-treated HepG2 cells using real-time PCR.	p. 159
Fig. 5.3.5	Change of cellular glutathione level contributed partly to the	p. 166

Sophoraflavone J-induced cell death.

Table 2.1	A list of antibodies employed for Western blot experiment.	p. 29 - 30
Table 2.2	A list of chemicals used, their chemical/ common names, formula, formular weights and the sources to obtain.	p. 30 - 33
Table 2.3	The ingredients needed to prepare the resolving and stacking protein gels.	p. 52
Table 2.4	The procedures involved in a standard silver staining process.	p. 61 - 62
Table 2.5	The ingredients needed to make up a reaction mix for the first-strand cDNA synthesis reaction.	p. 67
Table 3.1	A summary of the results from cell viability assays on the 48-hour exposure of anti-cancer drugs, cisplatin and taxol, to human hepatoma cells and normal liver cells.	p. 82
Table 3.2	A summary of the results from cell viability assays on the exposure of Leachianone A, Sophoraflavone J and anti-cancer drugs, cisplatin and taxol, to human hepatoma cells and normal liver cells for different time periods.	p. 86
Table 4.1	A summary of the results from the apoptotic bioassays for Leachianone A in HepG2 and RHepG2 cells.	p. 128-131
Table 5.1	A summary of the results from the apoptotic bioassays for Sophoraflavone J in HepG2 cells.	p. 145-147
Table 5.2	A complete list of the altered expressed protein molecules in Sophoraflavone J-treated HepG2 cells.	p. 155-156
Table 5.3	A review of the mRNA and protein levels of the 4 candidates in control and Sophoraflavone J-treated HepG2 cells.	p. 160

LIST OF ABBREVIATIONS

$\Delta\Psi_m$	mitochondrial membrane potential
°C	degree Celsius
%	percentage
μg	micro-gram(s)
$\mu\text{g}/\mu\text{l}$	micro-gram(s) per micro-liter
$\mu\text{g}/\text{ml}$	micro-gram(s) per milli-liter
μl	micro-liter(s)
μM	micro-molarity(s)
μm	micro-meter(s)
2-DE	two-dimensional electrophoresis
ABC	ATP-binding cassette
ACN	acetonitrile
AIF	apoptosis-inducing factor
ALT	alanine transaminase
Apaf-1	apoptosis protease-activating factor-1
APS	ammonium persulfate
AST	aspartate transaminase
ATP	adenosine triphosphate
Bcl-2	B-cell lymphoma 2
bp	base pair(s)
BCA solution	bicinchoninic acid solution
BBB	blood-brain barrier
BCRP/ MXR	breast cancer resistance protein
BSA	bovine serum albumin
Ca^{2+}	calcium ion
CAD	caspase-activated DNase
caspase	cysteine-aspartic acid protease
cDNA	complementary deoxyribonucleic acid
CHAPS	3-[(3-cholamidopropyl)-dimethylammonio]-1-propane
CHCA	α -cyano-4-hydroxycinnamic acid

cm	centi-meter(s)
CON	control
cyt c	cytochrome c
Da	dalton
DD	death domain
DEPC	diethyl pyrocarbonate
DEVD	aspartate-glutamate-valine-glutamate
dd.H ₂ O	double distilled water
DISC	death-initiating signaling complex
DMEM	Dulbecco's Modified Eagle's medium
DMSO	dimethylsulfoxide
DNA	deoxyribonucleic acid
DNase	deoxynuclease
dNTP	deoxynucleic triphosphate
Dox	doxorubicin
DR	death receptor
DTT	dithiothreitol
dUTP	deoxyuridine triphosphate
ECL reagent	enhanced chemiluminescence reagent
EF	elongation factor
endo G	endonuclease G
ENO1	alpha enolase
ER	endoplasmic recticulum
FADD	Fas-associating protein with death domain
FBS	fetal bovine serum
FUBI protein	far-upstream element binding protein
FMK	fluoromethyl ketone
g	gram(s)
g/L	gram per liter
GPx	glutathione peroxidase
GRP78	glucose-regulated protein 78
GST	glutathione S-transferase
GSH	glutathione

HCC	hepatocellular carcinoma
HDGF	hepatoma-derived growth factor
HLA	human leukocyte antigen
hnRNP	heterogeneous nuclear ribonucleoprotein
hr	hour(s)
HRP	horseradish peroxidase
HSP70	heat shock protein 70
IAA	iodoacetamide
IC ₅₀	50% inhibitory concentration
ICAD	inhibitor of caspase-activated DNase
IEF	isoelectric focusing
JC-1	5, 5', 6, 6'-tetrachloro-1, 1', 3, 3'- -tetraethylbenzimidazolcarbocyanine iodide
kDa	kilo-dalton(s)
kg	kilo-gram(s)
L	liter(s)
LDH	lactate dehydrogenase
LMP	lysosomal rupture
mA	milli-ampere(s)
MALDI-TOF	matrix-assisted laser desorption ionization time-of-flight
MDR	multi-drug resistance
mg	milli-gram(s)
mg/ml	milli-gram(s) per milli-liter
MHC	major histocompatibility complex
min	minute(s)
ml	milli-liter
mM	milli-molarity(s)
mm	milli-meter(s)
mRNA	messenger ribonucleic acid
MRP	multi-drug resistance protein
MPT	mitochondrial permeability transition
MPTP	mitochondrial permeability transition pore
MS	mass spectrometry

MTT	3-(4, 5-dimethylthiazol-2-yl)-2, 5-diphenyltetrazolium bromide, thiazoyl blue
nm	nano-meter
NMR	nuclear magnetic resonance
PAGE	polyacrylamide gel electrophoresis
PARP	poly-(ADP-ribose) polymerase
PBS	phosphate-buffered saline
PBST	phosphate-buffered saline Tween 20
PCD	programmed cell death
PCR	polymerase chain reaction
Pgp	P-glycoprotein
PI	propidium iodide
pI	isoelectric point
PMSF	phenylmethylsulphonyl fluoride
ppm	part(s) per million
Prx	peroxiredoxin
PS	phosphatidylserine
PS	streptomycin-penicillin
PVDF	poly-vinylidene fluoride
R	region
RNA	ribonucleic acid
RNAi	RNA interference
RNase	ribonuclease A
ROS	reactive oxygen species
rpm	rotation(s) per minute
RPMI medium	Rosewell Park Memorial Institute 1640 medium
SD	standard deviation
SDS	sodium dodecyl sulfate
smac/ DIABLO	second mitochondria-derived activator of caspase/ direct IAP binding protein with low pI
SOD	superoxide dismutase
STS	staurosporine
TAGLN2	transgelin 2

TCM	traditional chinese medicine
TEMED	N, N, N'-tetramethyl-ethylene diamine
TFA	trifluoroacetic acid
TRADD	TNF-related associated death domain
TRE	treated
TUNEL assay	Terminal Deoxynucleotidyl Transferase-mediated dUTP Nick End Labeling assay
U/L	unit(s) per liter
UV	ultra-violet
V	voltage(s)
Vhr	volt-hour(s)
v/v	volume per volume
w/v	weight per volume
X	times

TABLE OF CONTENT

Examination Committee List	i
Declaration	ii
Acknowledgements	iii
Abstract	v
Abstract in Chinese	viii
List of Figures and Tables	x
List of Abbreviations	xix
Table of Content	xxiii
Chapter 1 INTRODUCTION	1
1.1 Human Liver Cancer	1
1.1.1 Incidence of Hepatocellular Carcinoma	1
1.1.2 Causes and Symptoms of Hepatocellular Carcinoma	4
1.1.3 Treatment Options for Hepatocellular Carcinoma	4
1.1.4 Multi-drug Resistance	5
1.1.4.1 Mechanisms of Multi-drug Resistance	5
1.2 Traditional Chinese Medicine	10
1.2.1 <i>Sophora flavescens</i> and Radix <i>Sophorae</i>	10
1.2.2 Flavonoid and its Sub-classification	13
1.2.3 Flavonoid and Human Health	15
1.3 Cell Death	17
1.3.1 Necrosis	17
1.3.2 Apoptosis	17
1.3.3 Signaling Pathways in Apoptosis	18
1.3.3.1 Extrinsic (Death Receptor-mediated) Pathway	20
1.3.3.2 Intrinsic (Mitochondrial) Pathway	21
1.3.3.3 Cysteine Aspartic Acid Proteases	21
1.4 Research Objective(s)	22

Chapter 2	MATERIALS AND METHODS	23
2.1	Materials	23
2.1.1	Cell Lines	23
2.1.1.1	HepG2	24
2.1.1.2	RHepG2	24
2.1.1.3	WRL-68	25
2.1.2	Culture Media	26
2.1.2.1	Rosewell Park Memorial Institute(RPMI) 1640 Medium	26
2.1.2.2	Dulbecco's Modified Eagle's Medium (DMEM)	26
2.1.3	Animals	27
2.2	Traditional Chinese Medicines and Conventional Anti-cancer Drugs	27
2.3	Antibodies	29
2.4	Chemicals	30
2.5	Reagents and Buffers	34
2.5.1	Reagents for Silica Gel Column Chromatography	34
2.5.2	Buffers for Common Use	34
2.5.3	Reagents for Cell Viability Assay	35
2.5.4	Reagents and Buffers for Typical Apoptosis Experiments	35
2.5.4.1	Cell Cycle Analysis	35
2.5.4.2	Terminal Deoxynucleotidyl Transferase-mediated dUTP Nick End Labeling (TUNEL) Assay	35
2.5.4.3	DNA Fragmentation Detection	35
2.5.5	Reagents and Buffers for Western Blot Study	36
2.5.5.1	Whole-cell Protein Extraction	38
2.5.5.2	Mitochondrial and Cytosolic Fraction Protein Extraction	38
2.5.6	Reagents and Buffers for Mitochondrial Transmembrane Potential Depolarization Measurement	39
2.5.7	Reagents and Buffers for <i>in vivo</i> Animal Study	39
2.5.8	Reagents and Buffers for Two-Dimensional Gel Electrophoresis	40
2.5.8.1	Sample Preparation	40
2.5.8.2	First Dimension Gel Electrophoresis – Isoelectric Focusing (IEF)	40
2.5.8.3	Second Dimension Gel Electrophoresis –	40

	SDS-Polyacrylamide Gel Electrophoresis (SDS-PAGE)	
2.5.8.4	Silver Staining	41
2.5.9	Reagents for Mass Spectrometry Preparation	42
2.5.9.1	Destaining	42
2.5.9.2	Trypsin Digestion	42
2.5.9.3	Desalting of Peptide Mixture	43
2.5.10	Reagents and Buffers for Real-Time PCR	43
2.6	Methods	44
2.6.1	Isolation of Bioactive Constituents by Silica Gel Column Chromatography	44
2.6.2	Cell Viability Assay	45
2.6.3	Typical Apoptosis Experiments	45
2.6.3.1	Cell Cycle Analysis	46
2.6.3.2	Annexin V-FITC/ PI Staining Experiment	47
2.6.3.3	Terminal Deoxynucleotidyl Transferase-mediated dUTP Nick End Labeling (TUNEL) Assay	48
2.6.3.4	DNA Fragmentation Reaction	48
2.6.4	Western Blot Study	49
2.6.4.1	Whole-cell Protein Extraction	49
2.6.4.2	Mitochondrial and Cytosolic Fraction Protein Extraction	50
2.6.5	Caspase Activity Determination	54
2.6.6	Mitochondrial Transmembrane Potential Depolarization Measurement	55
2.6.7	<i>in vivo</i> Animal Study	56
2.6.8	Two-Dimensional Gel Electrophoresis	58
2.6.8.1	Sample Preparation	58
2.6.8.2	First Dimension Electrophoresis – Isoelectric Focusing (IEF)	59
2.6.8.3	Second Dimension Electrophoresis – SDS-Polyacrylamide Gel Electrophoresis (SDS-PAGE)	60
2.6.8.4	Silver Staining	61
2.6.9	Mass Spectrometry Preparation	63
2.6.9.1	Destaining and Trypsin Digestion	63
2.6.9.2	Peptide Extraction	63
2.6.9.3	Desalting of Peptide Mixture	64

2.6.10	Real-Time PCR	65
2.6.11	Cellular Glutathione Level Detection	69
2.7	Statistical Analysis	70
Chapter 3	RESULTS AND DISCUSSIONS –	72
	CYTOTOXICITY OF FLAVONOIDS ISOLATED FROM RADIX SOPHORAE	
3.1	Screening of Cytotoxic Flavonoids from <i>Radix Sophorae</i>	72
3.2	Cytotoxicity of Leachianone A on Human Hepatoma Cell Lines	74
3.3	Cytotoxicity of Leachianone A on Human Normal Liver Cell Line	77
3.4	Cytotoxicity of Sophoraflavone J on Human Hepatoma Cell Line	79
3.5	Cytotoxicity of Sophoraflavone J on Human Normal Liver Cell Line	79
3.6	Cytotoxicities of Cisplatin and Taxol on Human Hepatoma as well as Normal Liver Cell Lines	81
3.7	Conclusion	86
Chapter 4	RESULTS AND DISCUSSIONS –	88
	MECHANISTIC STUDY OF LEACHIANONE A-INDUCED CELL DEATH IN HEPATOMA CELLS, HepG2 and RHepG2	
4.1	Promotion of Cell Cycle Arrest	88
4.2	Induction of Apoptosis as Evidenced by Phosphatidylserine Externalization and DNA Fragmentation	93
4.2.1	Occurrence of Phosphatidylserine Externalization	94
4.2.2	DNA Fragmentation Detection	99
4.2.2.1	Terminal Deoxynucleotidyl Transferase(TdT)-mediated dUTP Nick End Labeling (TUNEL) Assay	99
4.2.2.2	DNA Laddering Pattern in Agarose Gel Electrophoresis	103
4.3	Recruitment of Multiple Signaling Pathways in Leachianone A-induced Apoptosis	105
4.3.1	Activation of Caspases-3, -8, and -9	105
4.3.2	Altered Expressions of Bcl-2 Family Proteins	112
4.3.3	Loss of Mitochondrial Membrane Potential	115
4.4	<i>in vivo</i> Tumor Growth Inhibition in HepG2-bearing Nude Mice	121
4.5	Conclusion	127

Chapter 5	RESULTS AND DISCUSSIONS –	132
	MECHANISTIC STUDY OF SOPHORAFLAVONE J-INDUCED CELL DEATH IN	
	HEPATOMA CELLS HepG2	
5.1	Execution of Cellular Apoptosis	133
5.2	Involvement of Multiple Signaling Pathways in Sophoraflavone J-induced Apoptosis	138
5.3	Differential Proteomes of Control and Sophoraflavone J-treated HepG2 Cells	148
5.4	Conclusion	167
Chapter 6	OVERALL CONCLUSION AND FUTURE PERSPECTIVES	169
References		xxiv

CHAPTER 1

INTRODUCTION

1.1 Human Liver Cancer

Liver cancer is defined as an excessive, disorganized cell division of the hepatocytes, which finally leads to the formation of an abnormal clump, known as tumor. Hepatocellular carcinoma (HCC) or called hepatoma represents the majority of malignant liver cancer, as originated from hepatocytes themselves. Cholangiocarcinoma is a discrete type, arising from the bile ducts in liver and proceeding down towards the gallbladder. Some other rare kinds of liver cancer include angiosarcomas (from the blood vessels in the liver), lymphomas (from the immune cells in the liver) and carcinoids (from hormone-making liver cells).

1.1.1 *Incidence of Hepatocellular Carcinoma*

HCC is the most common primary malignant neoplasm of the liver worldwide, occurring as one of the top five cancers in overall frequency. The disease prevails in parts of Asia and Africa; yet appears rife in European countries in

recent years. It accounts for about 6% of all human cancers annually (Nowak *et al.*, 2004). In 2003, hepatocarcinoma ranked high up as the third killer in Hong Kong, causing 14,000 mortalities in total (Fig. 1.1.1.1).

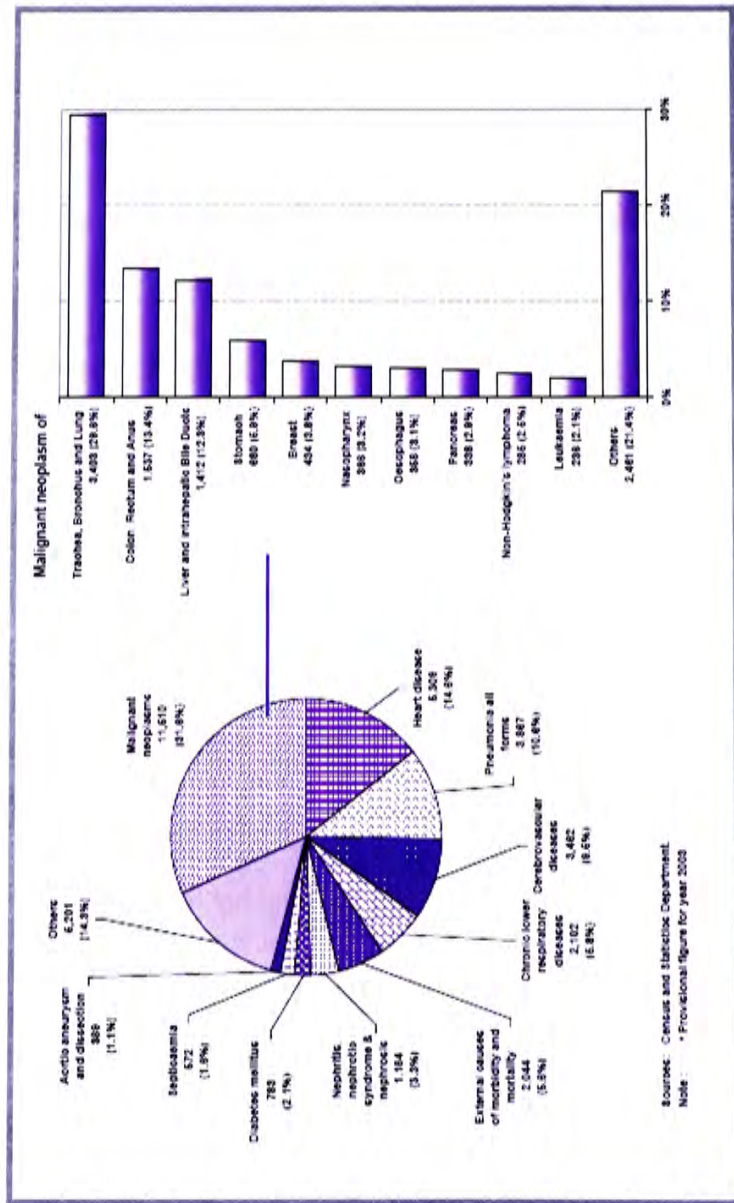


Fig. 1.1.1.1 Statistics of mortality in Hong Kong in 2003.

<http://www.ha.org.hk/hesd/nsapi/>

1.1.2 Causes and Symptoms of Hepatocellular Carcinoma

So far, certain risk factors have been identified to be vastly related to the development of HCC, including infection with chronic viral hepatitis, primarily types B and C; and a diseased condition called cirrhosis, as resulted from haemochromatosis, autoimmune diseases and alcoholism, etc (Omata *et al.*, 2004). In an early cancer stage, the tumor is often too small to cause any signs in patients. As it enlarges to an advanced level, though, abdomen swelling, weight loss, fatigue, pain and para-neoplastic syndromes are confronted. Worse still, spread of cancer gives rise to severe intestinal blockage, bone pain and neurological damage, etc.

1.1.3 Treatment Options for Hepatocellular Carcinoma

Nowadays, standard treatment methods for the HCC patients comprehend surgical resection, systemic radiotherapy and chemotherapy. Unfortunately, only 10% - 20% of patients are suitable for resection (Johnson *et al.*, 2002). And, the response following the radiotherapy and chemotherapy is also not satisfactory at present. It is because the efficacy of the drugs used is hampered by the assortment of adverse side-effects exerted on patients. In addition, development of multi-drug resistance (MDR) property by cancer

cells poses another problem for successful remedy. For these reasons, it comes to an urgent need to explore a new avenue for an effectual therapy against this disease. Currently, natural products with historical medicinal application arise to help address the point.

1.1.4 Multi-drug Resistance

MDR is a generic term for the variety of strategies tumor cells employ to evade the cytotoxic actions of anti-cancer drugs (Simon *et al.*, 1994). Prolonged incubation with a single anti-cancer drug always make the cells become less sensitive and more resistant to a broad spectrum of unrelated drugs, a phenomenon known as cross-resistance (Stavrovskaya *et al.*, 2000).

1.1.4.1 Mechanisms of Multi-drug Resistance

i) Inherent Form of Multi-drug Resistance

Depending on the nature of tumor cells, some possess an ability to counteract the effects of drugs before therapy. This kind of MDR usually comes in the genetically pre-disposed tumor cells; or appears due to the special locations of the tumors. For example, tumors in the brain are impregnable to numbers of therapeutic agents, owing to the presence of

blood-brain barrier (BBB).

ii) Acquired Form of Multi-drug Resistance

For other cells, on the contrary, they attain MDR after therapy. There are several means, by which the tumor cells operate to escape from the annihilation by drugs, ranging from the declined drug accumulation in cells to the abrogation of the onset and execution of apoptosis (Tomida *et al.*, 2002, Blagosklonny *et al.*, 2003).

To start with the defense, MDR cells are basically able to change the lipid compositions of the plasma membrane so as to minimize the diffusion of the drug molecules into the cells. On the other hand, they also simultaneously activate the expression of some transporter proteins for pumping out the toxic substances (Grude *et al.*, 2002). Until now, different superfamilies of proteins are known to be frequently involved in drug efflux: P-glycoprotein (Pgp), multi-drug resistance protein (MRP) and breast cancer resistance protein (BCRP or MXR) (Arceci *et al.*, 2000, Leonard *et al.*, 2003) (Fig. 1.1.4.1.1). Alternatively, cells somehow stimulate the detoxification enzymes, such as glutathione peroxidase (GPx), glutathione S-transferase (GST), and

superoxide dismutase (SOD), which then facilitate the cancellation of the destructive behaviors evoked by the drugs (Lee *et al.*, 1996, Yen *et al.*, 1998, Gouaze *et al.*, 2001).

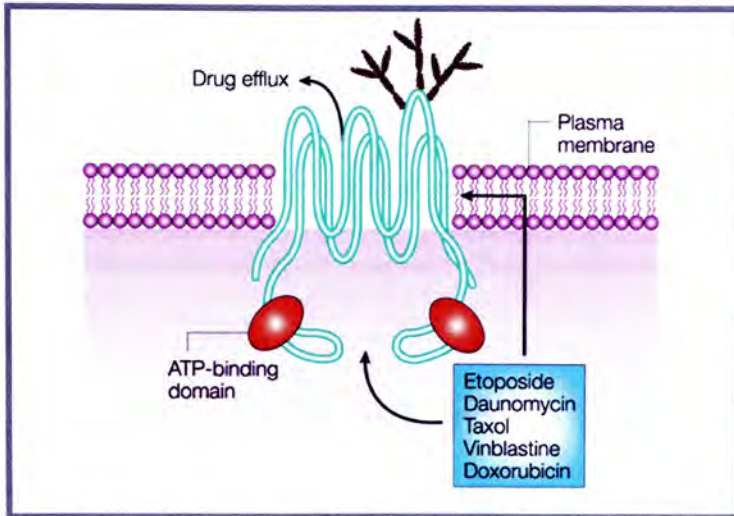


Figure 1.1.4.1.1. Schematic structure of P-glycoprotein and some examples of its substrates. (Adapted from Sorrentino *et al.*, 2002).

P-glycoprotein (P-gp) is a 170 kDa plasma membrane protein encoded by the MDR 1 gene on the chromosome 7 in human. It is member of the ATP-Binding Cassette (ABC) transporters; it possesses 2 homologous and symmetrical halves, each containing an ATP-binding domain and 6 trans-membrane domains separated by a flexible linker polypeptide. The protein thus forms a negatively charged hydrophobic pore of diameter 5nm. It is proposed that cationic lipophilic substrates (including some anti-cancer drugs) are pumped out to the extra-cellular space at the expense of ATP. Hence, it reduces the quantity and activity of the anti-cancer drugs inside the tumor cells.

To secure against cell death, tumor cells deregulate multiple targets in the apoptotic pathways, particularly the tumor-suppressor gene p53 and the anti-apoptotic proteins Bcl-2 and Bcl-X_L (Schott *et al.*, 1995, Walczak *et al.*, 2000, Yu *et al.*, 2004). For long, p53 wild-type gene is believed to be awfully important to both the cell cycle progression and the control of apoptosis (Lowe *et al.*, 1993). Defects and/ or mutations of p53 delay cell-cycle arrest; and abolish the DNA repair process, which otherwise render the cells apoptosis. Sometimes, inadequate Bcl-2 and Bcl-X_L protein expressions are likely to enhance tumor cell survival (Chipuk *et al.*, 2002).

1.2 Traditional Chinese Medicine

Since ancient times, plant-based formulations have been availed as remedial measures against various ailments (Singh *et al.*, 2003). They offer an overwhelming variety of metabolites, which display diverse medicinal and pharmaceutical functions (Gerber *et al.*, 2002). Nearly 80% of the prescriptions today are filled with drugs with active ingredients extracted or derived from plants. For instance, analogues of camptothecin from *Camptotheca acuminata* are commonly taken for small-cell lung and colorectal cancers (Oberlies *et al.*, 2001). Indirubin from *Indigofera tinctoria* as well as harringtonine from *Cephalotaxus hainanensis* own other unique biological activities effective against myelocytic leukemia diseases (Hoessel *et al.*, 1999).

1.2.1 *Sophora flavescens* and *Radix Sophorae*

Sophora flavescens is distributed extensively in China, Japan and Korea (Fig. 1.2.1.1). For many years, the roots of the species are applied in folk medicine as an anti-asthmatic, anti-carcinogenic/ metastatic, anti-inflammatory, anti-pyretic and anti-ulcerative agent (Kang *et al.*, 2000). The herb is characteristic of a bitter taste and a cold nature. Inside the body, it is

attributive to heart, stomach, liver, large intestine and urinary bladder channels.

Previous phytochemical studies of *Radix Sophorae* have reported the isolation of quinolizidine alkaloids, flavonoids and triterpenoids (Kim *et al.*, 2004). Of them all, flavonoids are renowned for their physiological anti-neoplastic activity, being able to bring about the differentiation and/ or growth inhibition in various malignant cancer cells, such as lung, esophageal, colorectal, breast and prostate cancers as well as osteosarcoma (Yamahara *et al.*, 1990, De Naeyer *et al.*, 2004, Xu *et al.*, 2005). While, alkaloids are powerful in relieving the discomfort emanated from common cold and bronchial asthma, etc (Ueng *et al.*, 2005).

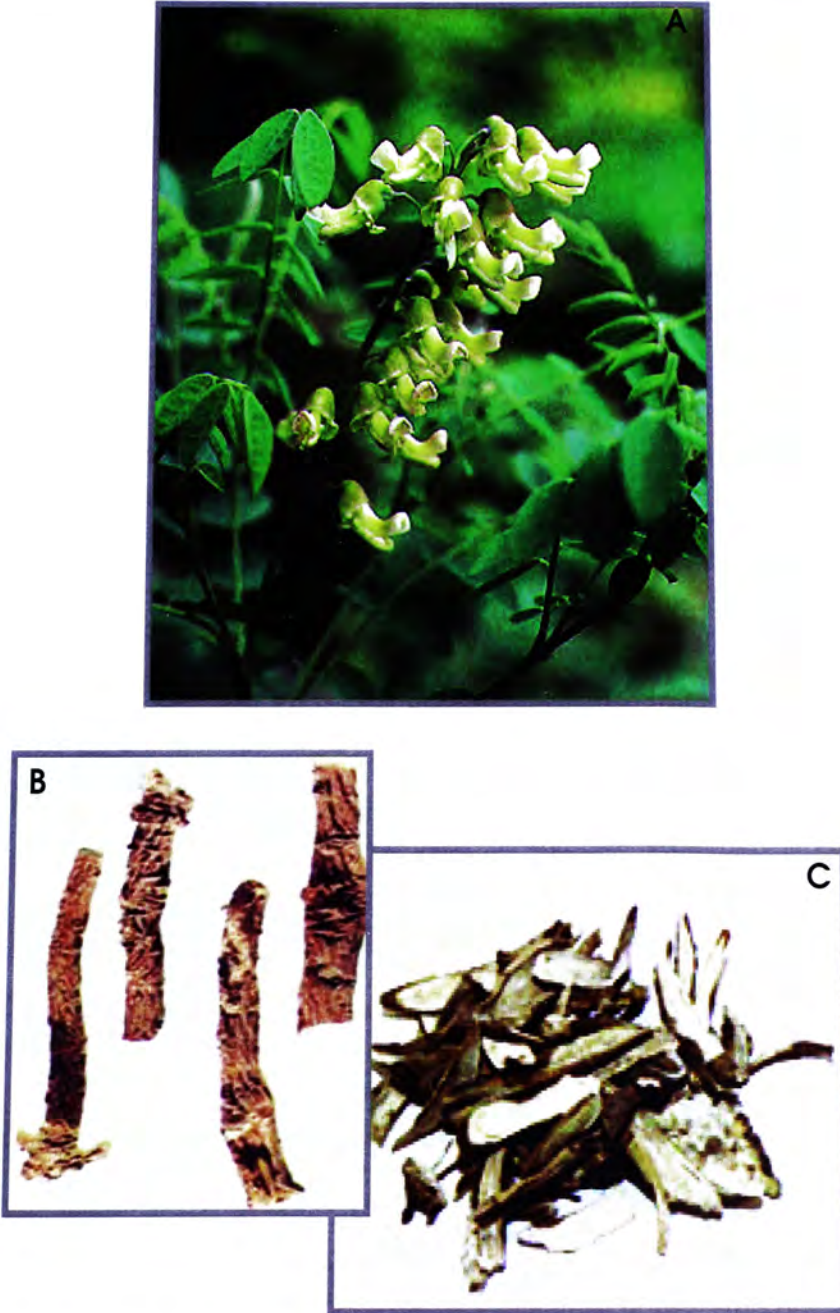


Fig. 1.2.1.1 Photographs taken for the whole plant of *Sophora flavescens* (A) and its dried root, *Radix Sophorae* (B, C).

<http://www.biologie.uni-ulm.de/systax/dendrologie/sophflavfw.htm>

<http://www.familydoctor.com.cn/yd/zcy/gl/ks.htm>

1.2.2 Flavonoid and its Sub-classification

Flavonoid (also referred to as bioflavonoid) designates a class of plant secondary metabolites based around a phenylbenzopyrone structure (Fig. 1.2.2.1). It is ubiquitous in nature; over 5,000 flavonoids have been found in different fruits, vegetables and soy. In accordance with the chemical structures, flavonoids are categorized into six sub-groups: flavanones, flavones, flavonols, isoflavones, anthocyanidins and chalcones (Fig. 1.2.2.2).

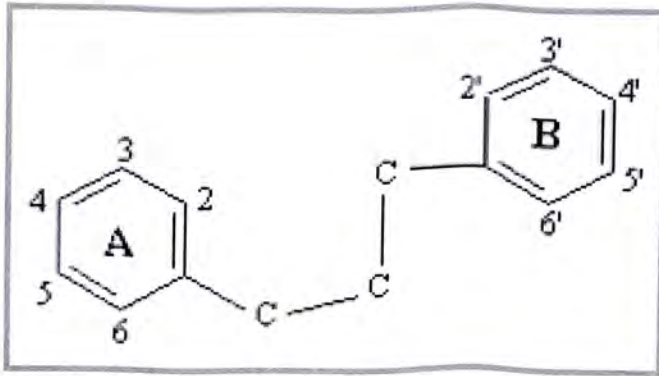


Fig. 1.2.2.1 Basic chemical unit of a flavonoid.

The flavonoid is a polyphenolic compound possessing 15 carbon atoms, with 2 benzene rings joined together by a linear 3-carbon chain.

<http://www.friedli.com/herbs/phytochem/flavonoids.html#intro>

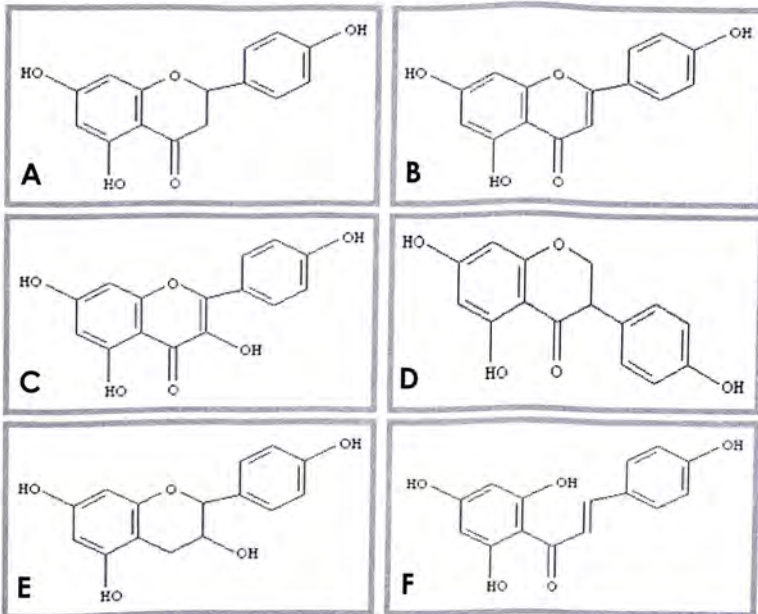


Fig. 1.2.2.2 Chemical structures of different types of flavonoids, flavanone (A), flavone (B), flavonol (C), isoflavonoid (D), anthocyanin (E) and chalcone (F).

<http://www.friedli.com/herbs/phytochem/flavonoids.html#intro>

1.2.3 Flavonoid and Human Health

Consumption of flavonoids has been coupled with loads of beneficial effects on human health, like heart and vascular protection, treatment of menopausal symptoms, etc (Koebnick *et al.*, 2005, Carroll *et al.*, 2006, Stangl *et al.*, 2006, Zaveri *et al.*, 2006). More recently, epidemiological studies have documented the biologically active properties of flavonoids against various kinds of malignancies (Haghiac *et al.*, 2005, Schmidt *et al.*, 2005, Colgate *et al.*, 2006).

In search of the promising compounds against hepatoma, we came across six bioactive flavonoids enriched in *Radix Sophorae*, which were capable of arresting cell growth in human hepatoma cell lines significantly. The present study emphasized on the two constituents called Leachianone A and Sophoraflavone J (Fig. 1.2.3.1). In regard to the classification scheme, they belonged to flavanone and flavone sub-groups, respectively. Both of them herein shared an identical molecular formulae of $C_{26}H_{30}O_6$, with a molecular weight of 438.

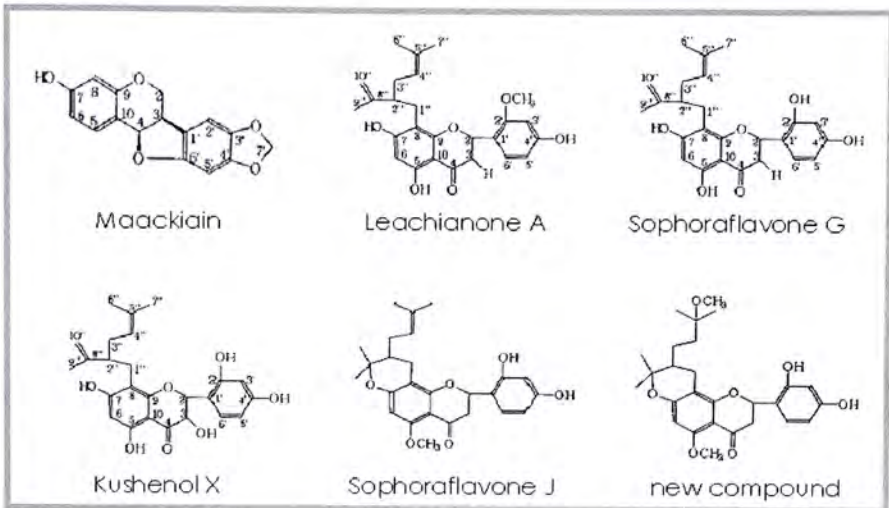


Fig. 1.2.3.1 Structures of 6 bioactive flavonoids obtained from the Radix Sophorae.

1.3 Cell Death

Cell proliferation and death are crucial components of both normal development and pathogenesis, including cancer (Joaquin *et al.*, 2001, Pru *et al.*, 2001). In a broad sense, cells undergo at least two distinct types of cell death; the first one is necrosis and the other, apoptosis. The former is a random issue; the latter, however, is strictly controlled and regulated.

1.3.1 Necrosis

Necrotic cell death is a passive form of degeneration affecting massive cell populations. It is ascribed to accidental and violent tissue injuries; and accompanied by cytoplasm swelling, organelle destruction as well as disruption of plasma membrane, followed by the release of intra-cellular contents. In the end, inflammatory reactions are triggered off.

1.3.2 Apoptosis

Yet, apoptosis is considered as a well-organized cell death program, which embrace the initiation, execution and termination phases. Unlike necrosis, apoptosis takes place in individual cells, as characterized by cell shrinkage, membrane blebbing, maintenance of organelle integrity, chromatin

condensation, DNA fragmentation and lastly ordered removal through phagocytosis (Wyllie *et al.*, 1981, Gupta *et al.*, 2001).

Early in 1970s, apoptosis has been put under the entity of programmed cell death (PCD) (Kerr *et al.*, 1972). PCD, in a few words, dictates a sequence of events of cellular metabolism, which ultimately come off with cell destruction (Guimaraes *et al.*, 2003). Other than apoptosis, autophagy is another type of PCD (Seglen *et al.*, 1992).

1.3.3 Signaling Pathways in Apoptosis

Generally, initiation of apoptosis involves two major pathways, the extrinsic (death receptor-mediated) and the intrinsic (mitochondrial) pathways (Fig. 1.3.3.1).

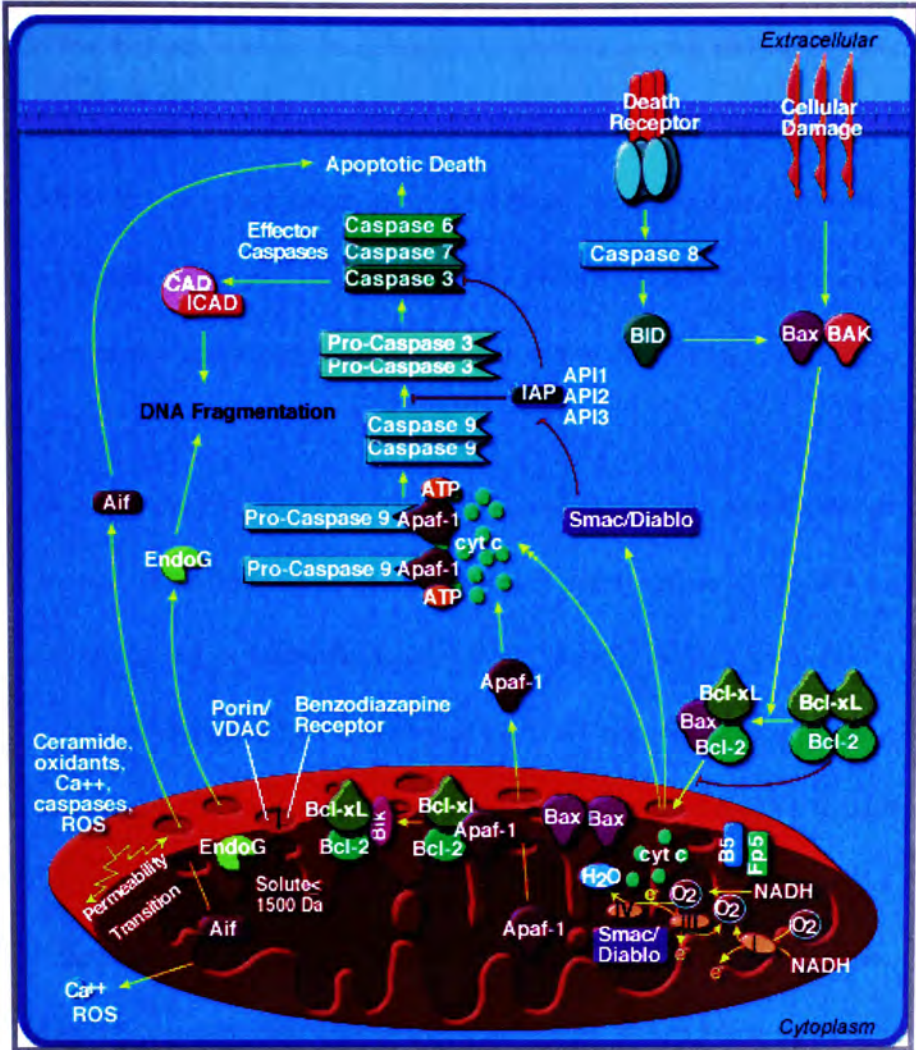


Fig. 1.3.3.1 Outline of the extrinsic (death receptor-mediated) and intrinsic (mitochondrial) pathways.

http://www.biocarta.com/images/FeaturedProducts/h_mitochondriapathway.gif

1.3.3.1 Extrinsic (Death Receptor-mediated) Pathway

In the extrinsic pathway, its activation chiefly relies on the binding of some death ligands onto the death receptors (DR) present on the cell surface. DRs, in fact, are a sub-group of TNF superfamily carrying a specific 80-amino acid long cytoplasmic death domain (DD), which is essential for the induction of apoptotic signal following receptor ligation (Kim *et al.*, 2006).

Soon with the agonist bound, DRs start to oligomerize; and recruit adaptor proteins, such as TNF-related associated death domain (TRADD) or Fas-associating protein with death domain (FADD), through a homophilic interaction between the DD of DR and the DD of adaptor proteins (Sartorius *et al.*, 2001). As such, a death-initiating signaling complex (DISC) is formed to prompt the proteolytic auto-activation of pro-caspase-8. Downstream of caspase-8, apoptosis thus either directly activates the effector caspases, like caspase 3, to in turn elicit the final apoptotic execution phase in type I cells (e.g. BJAB cells); or cleaves the intact Bid protein to generate truncated Bid, which then translocates to the mitochondria and induces activation of intrinsic pathway in type II cells (e.g. Jurkat cells) (Li *et al.*, 1998, Scaffidi *et al.*, 1999).

1.3.3.2 Intrinsic (Mitochondrial) Pathway

In the intrinsic pathway, the primary site of action is mitochondria. During the course of apoptosis, cellular stress spurs pro-apoptotic proteins and represses the anti-apoptotic ones to finish up with the opening of mitochondrial permeability transition pores (MPTP) gated between the outer and inner mitochondrial membranes (Huang *et al.*, 2000). Once opened, release of cytochrome *c* (cyt *c*) enables the complexation of cyt *c*, apoptosis protease-activating factor-1 (Apaf-1) and pro-caspase-9 for apoptosome to activate caspase-9. At the same time, the mitochondrial membrane potential ($\Delta\Psi_m$) is also collapsed. Eventually, caspase cascade continues; and drives the cells to die.

1.3.3.3 Cysteine Aspartic Acid Proteases

Cysteine-aspartic acid proteases (caspases) are vital to the execution of apoptosis in living systems. To achieve rapid activation, they are constitutively expressed in cells as zymogens (pro-caspases) with very low activity. These pro-enzymes consist of a pro-domain, a small subunit and a large subunit. Upon stimulation, they go through proteolytic processings to get rid of the inhibitory unit; and become activated. Active caspase

enzymes then assist in different aspects to accomplish the process of cellular death, depending on their functions. Briefly, initiator caspases (e.g. caspases-8 and -9) work to convert the precursors of effector caspases into mature proteases. While, effector caspases (e.g. caspase-3), when activated, promote the proteolytic cleavage of protein substrates, say inhibitor of caspase-activated DNase (ICAD) and poly-(ADP-ribose) polymerase (PARP); and subsequently result in the morphological and biochemical features in apoptotic cells (Stroh *et al.*, 1998).

1.4 Research Objective(s)

The research project herein aims to deploy two dissimilar approaches to elucidate the anti-proliferative effect of the two flavonoids extracted from *Radix Sophorae*. For Leachianone A, we adopt sets of apoptotic assays to investigate its *in vitro* and *in vivo* cytotoxic activities on HepG2 and RHepG2 cells. Concerning Sophoraflavone J, we focus on the comprehensive comparison of the proteomes between the control and the treated panels of HepG2 cells; and try to find out some key protein candidates associated with the action mechanism of the drug.

CHAPTER 2

MATERIALS AND METHODS

2.1 Materials

2.1.1 Cell Lines

A total of three human cell lines were employed. Two of them, namely HepG2 and RHepG2 were hepatocarcinoma cells chosen herein for anti-tumor activity studies. While, the one left, WRL-68, was from human normal liver tissues; it was taken to evaluate the toxicities of the two flavonoids prepared from the herb *Sophora flavescens* on normal cells.

All the cell lines were purchased from American Type Culture Collection (ATCC), with RHepG2 cells exclusive. Cells were cultivated as monolayer with Rosewell Park Memorial Institute (RPMI) 1640 medium or Dulbecco's Modified Eagle's Medium (DMEM), supplemented with 10% (v/v) heat-inactivated fetal bovine serum (FBS), 100 µg/ml streptomycin and 100 unit/ml penicillin (PS). The cultures were maintained at 37°C in a humidified

atmosphere of 5% carbon dioxide (CO₂). Routine sub-culturing of the cells was performed twice a week. In each passage, the spent medium was discarded; cells were rinsed with phosphate-buffered saline (PBS) once before trypsinization. Centrifugation at 1,500 rpm for three minutes was applied to collect the suspended cells. Then, appropriate aliquots of cell suspension was resuspended in fresh complete medium; and cultivated in new tissue vessels. Cells grown in the exponential growth phase were used for all experiments.

2.1.1.1 HepG2

Human hepatoma cell line HepG2 (ATCC #: HB-8065) was first derived from the liver tumor, which was histologically diagnosed as a well-differentiated hepatoblastoma, in a 15-year-old Caucasian adolescent male. The cells were adherent ones with epithelial morphology. Cultivation of cells were carried out in the complete RPMI 1640 medium, as supplemented with 10% (v/v) FBS (Gibco) and 1% (v/v) PS (Gibco). And, the cultures were maintained at 37°C in a humidified atmosphere of 5% CO₂.

2.1.1.2 RHepG2

RHepG2 was a multi-drug resistant counterpart of HepG2, as previously developed in our laboratory. It was achieved by incubating its parental cells HepG2 with a stepwise increase in the doxorubicin (Dox) concentration from 0.1 μM to 100 μM . In the selection process, Dox-sensitive cells were removed; and the resistant ones were continuously cultivated with a rising concentration of Dox. Finally, a pure population of Dox-resistant cells was obtained. The resistant cells were thereafter kept in the complete RPMI 1640 medium, with 1.2 μM Dox added. The multi-drug resistance property of RHepG2 cells was primarily attributed to the up-regulation of MDR1 gene and the over-expression of P-glycoprotein (Pgp), as illustrated respectively in the Northern blot study and Western blot analysis (Chan *et al.*, 2000).

2.1.1.3 WRL-68

Hepatic epithelial cell line WRL-68 (ATCC #: CL-48) was originated from the normal liver tissue of a fetus. This cell line basically preserved the morphologic structure similar to hepatocytes and hepatic primary cultures. Cell cultures were supported in the standard DMEM medium supplemented with 10% (v/v) FBS and 1% (v/v) PS.

2.1.2 Culture Media

All the media used were purchased in powder form; reconstitution was done following the supplier's instructions. Firstly, contents of each medium pouch were dissolved in 1 L of deionized or double distilled water (dd.H₂O). Then, indicated amount of sodium bicarbonate (NaHCO₃) was added (2 g/L for RPMI and 1.5 g/L for DMEM); and the pH was adjusted to 7.2 at 25 °C. Afterwards, the medium was sterilized by filtration through a 0.22 µm cellulose membrane bottle-top filter. Sterilized medium was thus stored at 4°C until use. Lastly, complete medium was prepared by the introduction of 10%(v/v) FBS and 1%(v/v) PS to the sterilized plain medium.

2.1.2.1 Rosewell Park Memorial Institute (RPMI) 1640 Medium

RPMI 1640 (Gibco), consisting of phenol red, 4 mM L-glutamine and 0.5 mM HEPES, was used to cultivate the two human liver cancer cell lines, HepG2 and RHepG2. In some experiments, phenol red-free RPMI 1640 medium was utilized to prevent any interference of phenol red to the assay results.

2.1.2.2 Dulbecco's Modified Eagle's Medium (DMEM)

DMEM (Gibco), consisting of phenol red, 4 mM L-glutamine and 4.5 g/L

glucose, was used, on the other hand, to cultivate the human normal liver cells, WRL-68.

2.1.3 Animals

Four- to six-week-old inbred male nude mice each weighing 20 g to 25 g were ordered from the Laboratory Animal Services Centre (LASEC) at the Chinese University of Hong Kong. Procedures involving the care and use of animals were conducted in accordance with the guidelines listed in the Animals (Control of Experiments) Ordinance.

2.2 Traditional Chinese Medicines and Conventional Anti-cancer Drugs

Radix *Sophorae* (also known as KuShen), stipulated as the dried roots of the herbal species *Sophora flavescens* (voucher number 2004-2531), was obtained in Guangzhou of mainland China. The identity of the plant was authenticated from its appearance, odor and some other special in-built features by experienced technicians (Mr. Hon PM and Mr. Lau CP) from the Institute of Chinese Medicine (ICM), the Chinese University of Hong Kong. Purification by silica gel column chromatography yielded six different

bioactive compounds herein (see Chapter 1). These flavonoids had been mostly encountered by several research groups working on this herb previously. Of them all, Leachianone A and the novel constituent, named Sophoraflavone J, were selected for further studies in the project.

Lyophilized powder of both **Leachianone A** and **Sophoraflavone J** was dissolved in absolute ethanol, filtered and then stored at -20°C . Stock concentration was kept at $690\ \mu\text{M}$ (10 mg/ml). For all experiments, the final concentrations of the tested compound(s) were prepared by diluting the stock with complete RPMI or DMEM medium.

Cis-platinum(II) diammine dichloride (DCPP), or called **cisplatin**, was prepared by dissolving in autoclaved PBS to give a stock concentration of 500 mM. Thereafter, the solution was frozen at -20°C for later use.

Paclitaxel, also known as **taxol**, was prepared by dissolving in autoclaved PBS to give a stock concentration of 50 mM. Thereafter, the solution was frozen at -20°C for later use.

Doxorubicin (Dox) was prepared by dissolving in sterilized PBS for a stock concentration of 17.24 mM. The solution was aliquoted; and stored at -20°C until use. Working concentration was obtained by diluting the stock solution with PBS to 1 mM.

Staurosporine (STS) was prepared by dissolving in sterilized PBS; the stock concentration was set as 1 mM. The solution was kept as small aliquots at -20°C until use. Working concentration was obtained by diluting the stock solution with PBS to 1 μM.

2.3 Antibodies

Antibody	Species	Dilution used	Supplier
Primary Antibodies			
anti-apoptosis inducing factor, AIF	mouse monoclonal	1 : 2000	Santa Cruz Biotechnology
anti-bad	rabbit polyclonal	1 : 1000	Santa Cruz Biotechnology
anti-bax	mouse monoclonal	1 : 1000	Santa Cruz Biotechnology
anti-bcl-2	mouse monoclonal	1 : 1000	Santa Cruz Biotechnology
anti-bcl- XL	mouse monoclonal	1 : 1000	Zymed
anti-beta-actin	mouse	1 : 5000	Sigma

	monoclonal		
anti-bid	rabbit polyclonal	1 : 1000	Santa Cruz Biotechnology
anti-cytochrome c	mouse monoclonal	1 : 1000	Pharmingen
anti-enolase	goat polyclonal	1 : 1000	Santa Cruz Biotechnology
anti-glucose regulated protein 75, GRP75	goat monoclonal	1 : 1000	Santa Cruz Biotechnology
anti-glucose regulated protein 78, GRP78	mouse monoclonal	1 : 1000	Zymed
anti-heat shock protein 70, HSP 70	mouse monoclonal	1 : 1000	Zymed
anti-inhibitor of caspase activated DNase, ICAD	rabbit polyclonal	1 : 2000	Santa Cruz Biotechnology
anti-poly-(ADP-ribose) polymerase, PARP	rabbit polyclonal	1 : 2000	Santa Cruz Biotechnology
anti-procaspase-3	mouse monoclonal	1 : 500	Santa Cruz Biotechnology
anti-procaspase-8	mouse monoclonal	1 : 1000	Calbiochem
anti-procaspase-9	mouse monoclonal	1 : 1000	Stressgen
Secondary Antibodies			
anti-mouse IgG-HRP	donkey	1 : 2000	Santa Cruz Biotechnology
anti-goat IgG-HRP	donkey	1 : 2000	Santa Cruz Biotechnology
anti-rabbit IgG-HRP	donkey	1 : 2000	Santa Cruz Biotechnology

Table 2.1 A list of antibodies employed for Western blot experiment.

2.4 Chemicals

Name and Formula of Chemical	Molecular	Source
------------------------------	-----------	--------

	Weight	
100bp DNA marker	---	Genepath Technology
2-mercaptoethanol (β -ME; C ₂ H ₆ OS)	78.1	Sigma-Aldrich
3-[[3-cholamidopropyl]-dimethylammonio]-1-propane (CHAPS; C ₃₂ H ₅₈ N ₂ O ₇ S)	614.89	USB
3-(4, 5-dimethylthiazol-2-yl)-2, 5-diphenyltetrazolium bromide, thiazoyl blue (MTT; C ₁₈ H ₁₆ N ₅ SBr)	414.3	Sigma-Aldrich
5, 5', 6, 6'-tetrachloro-1, 1', 3, 3'-tetraethylbenzimidazolcarbocyanine iodide (JC-1)	652	Molecular Probes
α -cyano-4-hydroxycinnamic acid (CHCA)	---	Amersham Biosciences
acetic acid (CH ₃ COOH)	60.05	Merck
acetonitrile (ACN; CH ₃ CN)	41.05	Amersham Biosciences
acrylamide/ bis-acrylamide (30% solution, mix ratio 37.5:1)	---	Sigma-Aldrich
agarose	---	USB
albumin, bovine (BSA)	---	Sigma-Aldrich
ammonium bicarbonate (CH ₂ O ₃ H ₃ N)	79.06	Sigma-Aldrich
ammonium persulfate (APS; (NH ₄) ₂ S ₂ O ₈)	228.2	Bio-Rad
annexin V-FITC	---	Trevigen
apologix carboxy-fluorescein caspase detection kit	---	Edward-Keller
aprotinin	6500	Sigma-Aldrich
benzamidine, hydrochloride hydrate (C ₇ H ₈ N ₂ HCl)	156.61	Sigma-Aldrich
bicinchoninic acid (BCA) solution	---	Sigma-Aldrich
boric acid (H ₃ BO ₃)	61.83	USB
bromophenol blue, sodium salt (C ₁₉ H ₉ Br ₄ O ₅ Na)	691.9	Sigma-Aldrich
cis-platinum(II) diammine dichloride or cisplatin (CDDP; Pt(NH ₃) ₂ Cl ₂)	300	Sigma-Aldrich
chloroform	---	Sigma-Aldrich
commassie brilliant blue R-250 (C ₄₅ H ₄₄ N ₅ O ₇ S ₂ Na)	825.99	USB
copper(II) sulfate pentahydrate (CuSO ₄ .5H ₂ O)	249.68	Sigma-Aldrich
diethyl pyrocarbonate (DEPC; C ₆ H ₁₀ O ₅)	162.1	Sigma-Aldrich
dithiothreitol (DTT; HSCH ₂ (CHOH) ₂ CH ₂ SH)	164.24	Sigma-Aldrich

digitonin (C ₂₂ H ₂₆ N ₂ O ₄ S)	1228	Sigma-Aldrich
dimethylsulfoxide (DMSO; CH ₃ SOCH ₃)	78.13	Invitrogen
doxorubicin (DOX; C ₂₇ H ₂₉ N ₁₁ HCl)	580.0	Sigma-Aldrich
drystrip cover fluid	---	Amersham Biosciences
Dulbecco's Modified Eagle's Medium (DMEM)	---	Gibco
enhanced chemiluminescence reagents (ECL)	---	Amersham Biosciences
ethanol (C ₂ H ₅ OH)	46.07	Merck
ethidium bromide (EtBr)	394	Molecular Probes
ethyl acetate (CH ₃ COOC ₂ H ₅)	88.11	Lab-Scan
ethylenediaminetetraacetic acid (EDTA; C ₁₀ H ₁₆ N ₂ O ₈)	292.2	Sigma-Aldrich
fetal bovine serum (FBS)	---	Gibco
formaldehyde 37% solution or formalin (CH ₂ O)	30.03	Sigma-Aldrich
glutathione apoptosis detection kit, fluorometric	---	Calbiochem
glycerol (HOCH ₂ CH(OH)CH ₂ OH)	92.09	USB
glycine (H ₂ NCH ₂ CO ₂ H)	75.07	USB
hydrochloric acid (HCl)	36.45	BDH
<i>in situ</i> cell death detection kit, fluorescein	---	Roche
iodoacetamide (IAA; C ₂ H ₄ I ₂ NO)	184.96	Sigma-Aldrich
isopropanol ((CH ₃) ₂ CHOH)	---	Merck
leupeptin (C ₂₀ H ₃₈ N ₆ O ₄)	463	Sigma-Aldrich
magnesium chloride, hexahydrate (MgCl ₂ . 6H ₂ O)	203.30	USB
methanol (CH ₃ OH)	32.1	Merck
n-hexane (CH ₃ (CH ₂) ₄ CH ₃)	86.18	Lab-Scan
N, N, N'-tetramethyl-ethylene diamine (TEMED)	116.21	Bio-Rad
non-fat milk powder	---	Nestle
paclitaxel or taxol (C ₄₇ H ₅₁ NO ₁₄)	853.9	Sigma-Aldrich
paraformaldehyde	30.03	Sigma-Aldrich
penicillin-streptomycin (PS)	---	Gibco
phenylmethylsulphonyl fluoride (PMSF; C ₇ H ₇ FO ₂ S)	174.19	USB

phenol-chloroform-isoamyl alcohol (mix ratio 25:24:1)	---	Invitrogen
potassium chloride (KCl)	74.55	Sigma-Aldrich
potassium phosphate, dibasic anhydrous (K ₂ HPO ₄)	174.18	USB
potassium phosphate, monobasic anhydrous (KH ₂ PO ₄)	136.09	USB
potassium ferricyanide (K ₃ Fe(CN) ₆)	329.24	Sigma-Aldrich
propidium iodide (PI)	668.4	Sigma-Aldrich
proteinase K, 16U/mg protein	---	Sigma-Aldrich
protein rainbow marker (full-range)	---	Invitrogen
ribonuclease A, 102U/mg protein (RNase A)	---	Sigma-Aldrich
Rosewell Park Memorial Institute (RPMI) 1640	---	Gibco
sequencing grade modified trypsin	---	Promega
sheath fluid	---	USB
silica gel	---	Merck
silver nitrate (AgNO ₃)	169.9	Sigma-Aldrich
sodium acetate (CH ₃ COONa)	82.03	USB
sodium bicarbonate (NaHCO ₃)	84.01	Sigma-Aldrich
sodium carbonate (Na ₂ CO ₃)	105.99	Sigma-Aldrich
sodium chloride (NaCl)	58.44	USB
sodium citrate, trisodium salt HOC(COONa)(CH ₂ COONa) ₂ · 2H ₂ O	294.1	Sigma-Aldrich
sodium dodecyl sulfate (SDS; CH ₃ (CH ₂) ₁₁ SO ₄ Na)	288.38	USB
sodium hydroxide (NaOH)	40.00	Sigma-Aldrich
sodium phosphate, dibasic heptahydrate (Na ₂ HPO ₄ · 7H ₂ O)	268.07	USB
sodium phosphate, monobasic monohydrate (NaH ₂ PO ₄ · H ₂ O)	137.99	USB
sodium thiosulphate (Na ₂ S ₂ O ₃ · 5H ₂ O)	248.19	USB
sodium orthovanadate (Na ₃ VO ₄)	183.9	Sigma-Aldrich
staurosporine (STS)	466.5	Calbiochem
sucrose (C ₁₂ H ₂₂ O ₁₁)	342.3	Sigma-Aldrich
trifluoroacetic acid (TFA; CF ₃ COOH)	114.02	Sigma-Aldrich
tris (NH ₂ C(CH ₂ OH) ₃)	121.14	USB

triton X-100	---	USB
TRIzol reagent	---	Invitrogen
trypan blue solution	---	Sigma-Aldrich
trypsin-EDTA	---	Gibco
tween 20, polyoxyethylene sorbitan monolaurate	---	USB
urea (NH ₂ CONH ₂)	60.06	USB
xylene cyanol FF (C ₂₅ H ₂₇ N ₂ O ₆ S ₂ Na)	538.6	Sigma-Aldrich

Table 2.2 A list of chemicals used, their chemical/ common names, formula, formular weights and the sources to obtain.

2.5 Reagents and Buffers

Buffers were prepared by dissolving chemicals in dd.H₂O; and titrated to suitable pH with either HCl or NaOH, unless otherwise specified.

2.5.1 Reagents for Silica Gel Column Chromatography

Silica gel column was prepared by mixing every 1 g silica gel with 4 ml stationary phase solvent, ethyl acetate.

2.5.2 Buffers for Common Use

PBS was composed of 2 mM KH₂PO₄, 2.7 mM KCl, 10 mM Na₂HPO₄ and 137 mM NaCl; its pH was titrated to 7.4. Afterwards, it was autoclaved for sterilization; and stored at 4°C.

2.5.3 Reagents for Cell Viability Assay

MTT solution was prepared by dissolving the MTT powder in PBS to give a concentration of 5 mg/ml. The resulting solution was filtered through a filter paper to remove precipitates. At last, MTT solution was kept at 4°C for use in a later time.

2.5.4 Reagents and Buffers for Typical Apoptosis Experiments

2.5.4.1 Cell Cycle Analysis

PI stain solution was prepared by dissolving PI (20 µg/ml), RNase A (10 µg/ml) and 1% (v/v) Triton X-100 in PBS.

2.5.4.2 Terminal Deoxynucleotidyl Transferase-mediated dUTP Nick End

Labeling (TUNEL) Assay

Fixation buffer was prepared by dissolving 4% (w/v) paraformaldehyde in PBS.

Permeabilization buffer was prepared by dissolving 0.1% (v/v) Triton X-100 in 0.1% (w/v) sodium citrate.

2.5.4.3 DNA Fragmentation Detection

DNA lysis buffer was composed of 100 mM EDTA, 200 mM Tris-HCl (pH8.3) and 1% SDS.

Tris-EDTA (TE) buffer was composed of 1 mM EDTA and 10 mM Tris-HCl (pH7.0).

Proteinase K was dissolved in dd.H₂O with 10 mg/ml as a stock concentration. It was kept at -20°C until use.

Ribonuclease A was dissolved in TE buffer with 0.2 mg/ml as a stock concentration. Also, it was kept at -20°C for later use.

1 X Tris-Borate-EDTA (TBE) buffer was composed of 89 mM boric acid, 2 mM EDTA and 89 mM Tris-HCl (pH8.0).

6 X DNA loading dye was composed of 40% (w/v) sucrose, 0.25% (w/v) bromophenol blue and 0.25% (w/v) xylene cyanol FF.

2.5.5 Reagents and Buffers for Western Blot Study

4 X resolving gel buffer was composed of 1.5 M Tris-base and 14 mM SDS.

The buffer pH was adjusted to 8.8.

4 X stacking gel buffer was composed of 0.5 M Tris-base and 14 mM SDS. The buffer pH was adjusted to 6.8.

1 X SDS running buffer was composed of 250 mM glycine, 25 mM Tris-base (pH8.3) and 0.1% (w/v) SDS.

6 X SDS loading dye was composed of 300 mM Tris-HCl (pH6.8), 600 mM DTT, 60% (v/v) glycerol, 12% (w/v) SDS and 0.6% (w/v) bromophenol blue.

1 x electro-blotting buffer (E-blot Buffer) was composed of 39 mM glycine, 48 mM Tris-base, 20% (v/v) methanol and 0.0375% (w/v) SDS. Buffer was calibrated to pH 8.3 for use. Freshly prepared buffer was always preferred for the experiments.

Commassie blue staining solution was prepared by mixing acetic acid, ethanol and dd.H₂O in the ratio of 1:4.5:4.5, with 0.25% (w/v) commassie brilliant blue R-250 added.

De-staining solution was prepared by mixing acetic acid, ethanol and dd.H₂O in the ratio of 1:4.5:4.5.

1 x PBS-Tween 20 (PBS-T) was composed of 2 mM KH₂PO₄, 2.7 mM KCl, 10 mM Na₂HPO₄, 137 mM NaCl and 0.002% (v/v) Tween-20. Buffer was then titrated to pH 7.4 for use.

Protein standards (2 mg/ml – 10 mg/ml) were prepared by dissolving 0.02 g – 0.1 g BSA in 10 ml PBS. The standards were kept at -20°C until use.

BCA assay solution was prepared with reagents A and B mixed in a ratio of 49:1. Reagent A (bicinchoninic acid solution) was purchased ready to use. Reagent B was prepared by dissolving 4% (v/v) CuSO₄.5H₂O in dd.H₂O.

2.5.5.1 Whole-cell Protein Extraction

Cell lysis buffer was composed of 4.9 M MgCl₂, 100 mM NaVO₃ and 10% (v/v) Triton X-100. All these components were dissolved in PBS; and the buffer pH was titrated to 7.4. Prior to use, aprotinin (2.1 mg/ml), leupeptin (1.0 mg/ml) and PMSF (0.2 mg/ml) were freshly introduced to the buffer.

2.5.5.2 Mitochondrial and Cytosolic Fraction Protein Extraction

Lysis buffer was basically composed of 75 mM NaCl, 1 mM NaH₂PO₄, 8 mM Na₂HPO₄ and 250 mM sucrose. Various concentrations of digitonin were included in the buffer herein for cell lysis – 0.5 mg/ml for cytosolic and 5 mg/ml for mitochondrial protein fractions. All the chemicals were dissolved in PBS. Again, the buffer pH was titrated to 7.4. Just before use, aprotinin (2.1 mg/ml), leupeptin (1.0 mg/ml) and PMSF (0.2 mg/ml) were freshly introduced to the buffer.

2.5.6 Reagents and Buffers for Mitochondrial Transmembrane Potential Depolarization Measurement

JC-1 dye was dissolved in DMSO for a stock concentration of 2.5 mM. The dye solution was protected from light; and stored at 4°C for later use.

2.5.7 Reagents and Buffers for in vivo Animal Study

Saline was composed of 0.9% (w/v) NaCl. It was kept at 4°C until use.

Pentobarbital was dissolved in PBS with a concentration of 25 mg/ml. It was protected from light; and kept at 4°C until use.

2.5.8 Reagents and Buffers for Two-Dimensional Gel Electrophoresis

2.5.8.1 Sample Preparation

Lysis buffer (LB) was composed of 40 mM DTT, 8 M urea and 4% (w/v) CHAPS.

It was then aliquoted; and frozen at -20°C.

2.5.8.2 First Dimension Gel Electrophoresis – Isoelectric Focusing (IEF)

Rehydration buffer (RB) was composed of 8 M urea, 2% (w/v) CHAPS and 0.002% (w/v) bromophenol blue. The buffer was kept as small aliquots at -20°C. Upon used, 1% (w/v) DTT and 1% (v/v) IPG buffer were freshly added to the buffer.

Bradford protein assay reagent was prepared with the reagent diluted in dd.H₂O, thus to have 10% (v/v) as the working concentration.

2.5.8.3 Second Dimension Gel Electrophoresis – SDS-Polyacrylamide Gel Electrophoresis (SDS-PAGE)

Equilibration buffer (EB) was composed of 75 mM Tris-HCl (pH8.8), 6 M urea, 29.3% (v/v) glycerol, 2% (w/v) SDS and 0.002% (w/v) bromophenol blue.

Equilibration buffer A was prepared with 1% (w/v) DTT freshly introduced to the EB.

Equilibration buffer B was prepared with 2.5% (w/v) IAA freshly introduced to the EB.

Agarose sealing solution was prepared by dissolving 0.5% (w/v) agarose and 0.002 (w/v) bromophenol blue in SDS buffer.

2.5.8.4 Silver Staining

Fixation solution was composed of 10% (v/v) acetic acid and 40% (v/v) ethanol.

Sensitizing solution was composed of 6.8% (w/v) sodium acetate, 5% (w/v) sodium thiosulphate and 30% (v/v) ethanol.

Silver nitrate solution was prepared by dissolving 2.5% (w/v) silver nitrate in nano pure water.

Developing solution was composed of 2.5% (w/v) sodium carbonate and 0.1% (v/v) 37% formaldehyde.

Stopping solution was prepared by dissolving 1.5% (w/v) EDTA in nano pure water.

Storage solution was composed of 12% (v/v) acetic acid and 40% (v/v) ethanol.

2.5.9 Reagents for Mass Spectrometry Preparation

2.5.9.1 Destaining

Destaining solution was prepared by mixing 30 mM potassium ferricyanide with 100 mM sodium thiosulphate in a ratio 1:1, prior to use.

2.5.9.2 Trypsin Digestion

Gel equilibration solution was composed of 200 mM ammonium bicarbonate. The solution was generally stored at 4°C.

Trypsin enzyme was dissolved in 50 mM ammonium bicarbonate to give a

concentration of 40 ng/ μ l. The enzyme so obtained was then frozen at -20°C.

2.5.9.3 Desalting of Peptide Mixture

Resuspension solution [0.1% (v/v) TFA] was prepared from the serial dilutions of 100% TFA to 10%, then to 1%, and finally to 0.1% with nano pure water.

Wetting solution [50% (v/v) ACN] was prepared by mixing equal volumes of 100% ACN and nano pure water.

Elution solution was prepared to have 50% (v/v) ACN and 0.1% (v/v) TFA present in nano pure water.

CHCA matrix was dissolved in a solution containing 50% (v/v) ACN and 0.5% (v/v) TFA until saturation.

2.5.10 Reagents and Buffers for Real-Time PCR

DEPC-H₂O was prepared with 0.1% (v/v) DEPC dissolved in dd.H₂O. The resulting solution was sterilized by autoclave.

2.6 Methods

2.6.1 *Isolation of Bioactive Constituents by Silica Gel Column Chromatography*

The dried roots of the herb (about 4 kg) were first soaked and boiled in 4 L absolute ethanol for two hours. The sample was then filtered; whereas the residue was further extracted under the same condition twice. The filtrates collected from three separate extractions were thus combined, concentrated and partitioned between 1:1 ethyl acetate : water three times to give an ethyl acetate fraction of 1.3 L. This was followed by evaporating the solution to dryness under a reduced pressure, so that a sample weighing about 136 g was resulted.

The crude extract was next subjected to silica gel column chromatography (20 cm x 8.5 cm; 8.5 ml/minute), using 1:1 ethyl acetate : hexane as the solvent system. The semi-purified Leachianone A- and Sophoraflavone J-containing fractions were allowed to dry under vacuum to confer a yield of about 37.24 g and 2.08 g, respectively. The purity of the fractions was monitored and judged by ways of the paper chromatography, in which the fractioned substance was assigned to run alongside the standards on the

paper for colour and displacement comparison. Fewer spots denoted a relatively pure chemical fraction. Further purification of the two target components then came to make use of different strategies. For Leachianone A fraction, it was applied to another silica gel column of smaller pore size (24 cm x 5 cm; 4 ml/minute), with 1:5 ethyl acetate : hexane as the solvent system. While, fraction of Sophoraflavone J was passed to the reversed phase high-performance liquid chromatography (HPLC), with 1:1 acetonitrile : water as the solvent system. In the end of the process, 469.2 mg of Leachianone A and 56.7 mg of Sophoraflavone J of high purity were obtained.

2.6.2 Cell Viability Assay

Cells (1×10^4 per well) were seeded in 96-well flat-bottom microplates (Iwaki); and cultivated in a humidified incubator for adhesion overnight. After that, cells were exposed to various concentrations of Leachianone A and Sophoraflavone J (0 $\mu\text{g/ml}$ – 20 $\mu\text{g/ml}$); and continued for three different time durations (24 hr, 48 hr and 72 hr). Following the incubation, the media were discarded; 30 μl of MTT solution was subsequently added to the wells. The plate was thus allowed to stand at 37°C in the dark for additional three hours.

The MTT-formazan crystals so formed were dissolved in 100 μ l DMSO; and the absorbance was measured specto-photometrically at 540 nm using an ELISA plate reader (Bio-Rad). The cell viability was expressed as the optical density ratio of the treatment to control (PBS-treated cells) calculated from the absorbance values.

2.6.3 Typical Apoptosis Experiments

2.6.3.1 Cell Cycle Analysis

Cells (3×10^5 per well) were seeded in 6-well plates (Iwaki); and exposed to different drug(s) concentrations for 48 hours. They were then harvested, washed and fixed with 70% ice-cold ethanol at 4°C overnight. Afterwards, cells were washed twice with PBS; and incubated in 1 ml PI stain solution containing 10 μ g/ml RNase A at 37°C in the dark for 30 minutes. Fluorescence signals emitted from the PI-DNA complex were collected at FL-2 channel in a log scale for 10,000 events, using the FACSort flow cytometer (Becton Dickinson). Data acquired were analyzed by the WinMDI software (version 2.8), downloaded at <http://facs.scripps.edu/software.html> (Becton Dickinson).

2.6.3.2 Annexin V-FITC/ PI Staining Experiment

Cells (3×10^5 per well) in 6-well plates (Iwaki) under treatments with different concentrations of drug(s) for 48 hours were collected, washed and stained, according to the manufacturer's protocol (Trevigen). In brief, the cells were washed twice with $400 \mu\text{l}$ $1 \times$ binding buffer; and then incubated in $100 \mu\text{l}$ reagent mix containing $1 \mu\text{l}$ annexin V-FITC conjugate and $10 \mu\text{l}$ PI in the dark for 15 minutes at room temperature. Thereafter, the samples were subjected to FACSsort flow cytometric measurement (Becton Dickinson). Again, a total of 10,000 events were acquired for each sample given. Both FL-1 and FL-3 channels, set at log scales, were selected for the detection of signals from annexin V-FITC and PI, respectively. Result interpretation was done with a contour plot by the WinMDI software (Becton Dickinson).

2.6.3.3 Terminal Deoxynucleotidyl Transferase-mediated dUTP Nick End Labeling (TUNEL) Assay

The TUNEL assay for *in situ* detection of apoptosis was performed with the *in situ* Cell Death Detection Kit, Fluorescein (Roche). After 48-hour drug(s) treatment, cells (1×10^6) were first put in the fixation buffer at 25°C for one hour. Fixed cells were then transferred to the permeabilization buffer; and

incubated with the fluorescein-conjugated dUTP in a terminal deoxynucleotidyl transferase-catalyzed reaction at 37°C in the dark for another hour. Finally, the samples were washed twice; and resuspended in 500 μ l PBS ready for subsequent FACSort flow cytometric analysis (Becton Dickinson). 10,000 representative events were collected at FL-1 channel in a log scale for each of the samples herein. Signals resulted from the labeled DNA breaks were evaluated and presented as a histogram using the WinMDI software.

2.6.3.4 DNA Fragmentation Reaction

i) Genomic DNA Extraction

Cells (1×10^6) obtained following the indicated periods of drug(s) treatment were resuspended in 400 μ l cell lysis buffer with 10 μ l proteinase K (20 mg/ml) added; and kept at 37°C overnight for complete digestion. On the next day, 150 μ l saturated sodium chloride solution was introduced; the samples were mixed vigorously by vortex. Centrifugation at 14,000 rpm (Eppendorf) for 20 minutes was applied to collect the supernatant. After so, genomic DNA was extracted with an equal volume of 25:24:1 phenol-chloroform-isoamyl alcohol twice. The extracted DNA was then precipitated with 1 ml ice-cold

absolute ethanol at -20°C for 30 minutes. The DNA so resulted was recovered by centrifugation, rinsed with cold 75% ethanol once and allowed to air dry. Lastly, the DNA samples were dissolved in $20\ \mu\text{l}$ TE buffer containing $0.2\ \text{mg/ml}$ RNase A.

ii) Agarose Gel Electrophoresis

2% (w/v) agarose gel was then prepared by melting 1 g agarose in 50 ml 1 x TBE buffer containing $0.5\ \mu\text{g/ml}$ EB. Equal amount of samples, say $20\ \mu\text{g}$, pre-mixed with DNA loading dye were loaded to the agarose gel; and electrophoresis was performed at constant voltage of 80 V for 45 minutes. Upon finished, the DNA laddering pattern was visualized under UV illumination (Alpha Innotech); and the image was recorded.

2.6.4 Western Blot Study

2.6.4.1 Whole-cell Protein Extraction

i) Protein Preparation

Cells (1×10^6) grown in $100\ \text{mm}^3$ Perti dishes (Iwaki) were disrupted in $300\ \mu\text{l}$ lysis buffer on ice for 30 minutes. The lysates were then boiled for 10 minutes; and centrifuged at 14,000 rpm (Eppendorf) for 15 minutes. In the end, the

supernatants were saved for Western blot study.

2.6.4.2 Mitochondrial and Cytosolic Fraction Protein Extraction

i) Protein Preparation

Control and treated panels of cells (4×10^6) in 150 cm³ culture flasks (Iwaki) were harvested, washed and resuspended in 50 μ l buffer A (containing 0.5 mg/ml digitonin). The resulting cell suspensions were mixed by vortex; and then centrifuged at 10,000 rpm (Eppendorf) for one minute. The supernatants (S1) were collected. After that, the pellets remained were resuspended in 50 μ l buffer B (containing 5 mg/ml digitonin). Again, the cell suspensions were mixed; and centrifuged at 10,000 rpm (Eppendorf) for one minute for new supernatants (S2). S1 and S2 isolated herein represented the cytosolic and mitochondrial fractions, respectively (Ko *et al.*, 2000).

ii) Protein Quantification and Standardization by BCA assay

BCA assay was adopted to determine the protein concentration of samples in a 96-well plate format. In the first place, protein standards with different amounts of BSA (0, 2, 4, 6, 8 and 10 mg/ml) were introduced to the wells. For the part of testing samples, 1 μ l protein was mixed with 9 μ l PBS in each single

well. Three replicates of BSA standards and samples were included totally. After so, 200 μ l BCA mixture consisting of BCA and $\text{CuSO}_4 \cdot 5\text{H}_2\text{O}$ solutions pre-mixed in a ratio 49:1 was added. The plate was then left at 37°C for 30 minutes; absorbance was recorded at 540 nm by a microplate reader (Bio-Rad). In doing so, a standard curve was established, with x-axis representing the concentration of BSA and the y-axis as the measured absorbance values at 540 nm. An equation was thereby developed for the direct calculation of protein quantity present in the samples. Fig 2.1 showed a standard BSA curve.

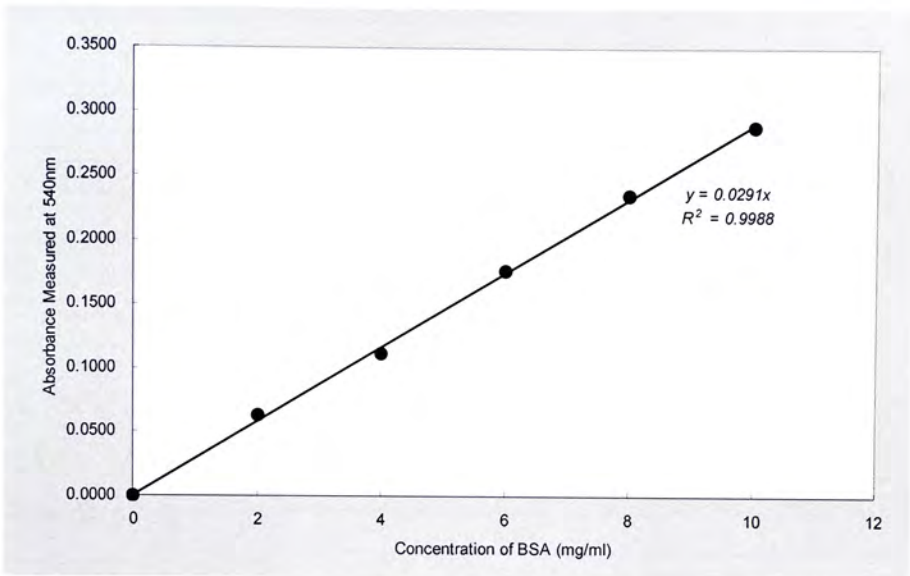


Fig 2.6.4.1 BSA protein standard curve plotted for protein concentration estimation.

iii) SDS-Polyacrylamide Gel Electrophoresis

The apparatus of Mini-Protean III cell (Bio-Rad) for SDS-PAGE was set up according to the supplier's instructions. With reference to the molecular weight of the target protein(s), different percentages of resolving gels and stacking gel were employed. The gel composition was given in Table 2.3.

	Resolving Gel			Stacking Gel
	10%	12%	15%	5%
dd.H₂O	1.90 ml	1.60 ml	1.10 ml	1.40 ml
4 x resolving gel buffer	1.35 ml	1.35 ml	1.35 ml	---
4 x stacking gel buffer	---	---	---	0.25 ml
30% acrylamide	1.70 ml	2.00 ml	2.50 ml	0.33 ml
TEMED	50 μ l	50 μ l	50 μ l	20 μ l
APS	2 μ l	2 μ l	2 μ l	2 μ l

Table 2.3 The ingredients needed to prepare the resolving and stacking protein gels.

Protein samples obtained in the earlier time were boiled in a thermocycler (Progene) for five minutes for heat denaturation. Subsequently, an aliquot of the denatured supernatant containing 30 μ g protein, mixed with SDS loading dye, was resolved by a SDS-polyacrylamide gel. Electrophoresis was performed at a constant voltage of 220 V for 45 minutes. Upon finished, the gel was removed from the electrophoresis cell; and passed to the

succeeding electro-blotting steps.

iv) Electroblothing of Proteins

The electro-blotting of proteins was carried out with the use of Mini Trans-Blot Cell, a tank transfer system (Bio-Rad).

Prior to the electro-blotting process, the dry 0.45 μm poly-vinylidene fluoride (PVDF) membrane (Millipore) was rehydrated with absolute methanol; and then immersed in the E-blot buffer. 1 mm filter paper (Whatman) was soaked together in the E-blot buffer for use. The tank transfer system for electro-blotting was next assembled in the sequence: cathode, fiber pad, 3 x filter paper, SDS-polyacrylamide gel, PVDF membrane, 3 x filter paper, fiber pad, anode. At last, electro-blotting was performed with a constant current at 200 mA for one hour to ensure complete transfer of proteins onto the PVDF membrane.

v) Probing of Proteins with Antibodies

As the procedure got accomplished, the membrane was brought to non-specific blocking with 10% (v/v) skimmed milk in PBS-T for two hours at

room temperature. Later on, the blot was probed with specific primary antibody at 4°C overnight. On the next day, the antibody was discarded; the blot was washed with PBS-T three times for 15 minutes each. HRP-conjugated secondary antibody was then loaded to the blot for another hour at 4°C. (Antibodies used so far were listed in Table 2.1.) In final, the blot was washed with PBS-T twice; and subjected to the enhanced chemiluminescence assay (Amersham Biosciences).

vi) Enhanced Chemiluminescence (ECL) Detection

ECL assay was conducted by mixing the ECL reagents one and two in a ratio of 25:1, as stated in the protocol. The membrane was exposed to the ECL reagent mixture for one minute at room temperature. Following that, the whole membrane was preserved between two layers of transparency; and developed on Fuji Medical x-ray film (Fuji). Films were processed in a film processor (Kodak).

2.6.5 Caspase Activity Determination

Quantitative measurement of caspase activity was achieved using the ApoLogix Carboxy-Fluorescein Caspase Detection Kit (Cell Technology). In

the assay, firstly, cells (3×10^5) were harvested, washed and resuspended in 300 μ l complete medium, with 10 μ l 1 x working FAM-peptide-FMK-solution added. The resulting suspensions were kept at 37°C in the dark with constant shaking for an hour. Shortly after, the samples were rinsed with the wash buffer twice; and then proceeded to the FACSort flow cytometric detection (Becton Dickinson). Fluorescence signals were mainly collected at FL-1 channel to acquire 10,000 events.

2.6.6 Mitochondrial Transmembrane Potential Depolarization

Measurement

Cells (3×10^5) from the respective control and treated groups were collected; and subsequently washed with PBS twice. The cell pellets were next resuspended in 500 μ l plain medium containing 2.5 μ M JC-1 dye; and the suspensions were allowed to stand in the dark for 15 minutes at room temperature. Eventually, the mitochondrial depolarization patterns of the cells were examined by means of FACSort flow cytometry (Becton Dickinson). Channels FL-1 and FL-3 were employed for a simultaneous detection of green and red fluorescence signals from the monomeric and aggregated forms of JC-1, respectively.

2.6.7 *in vivo* Animal Study

i) *in vivo* drug administration

1×10^7 human hepatoma cells, HepG2, in 0.2 ml PBS were subcutaneously inoculated between the scapulae of the male nude mice. After solid tumor formation (i.e. tumor volume reached 200 mm³), the tumor-bearing nude mice were then randomized into three experimental groups, each having 8 mice. The control mice were given 0.2 ml 5% ethanol each on alternate days for 30-day duration. While, the 2 treatment groups were intra-venously injected with the doses of 20 mg/kg/day and 30 mg/kg/day of drug (Leachianone A), respectively.

ii) Plasma Enzyme Activities Evaluation

In the end of the experiment, all the animals were sacrificed; their tumors were dissected and weighed. The tumor inhibitory rates were calculated from the formulae: (mean tumor weight of control nude mice – mean tumor weight of treated nude mice) / mean tumor weight of control nude mice x 100 %. Plasma levels of creatine kinase (CK), lactate dehydrogenase (LDH), alanine transaminase (ALT) and aspartate transaminase (AST) in all three groups of mice were also determined at the same time, as instructed by the

assay protocol provided (Stanbio). In short, indicated volumes of plasma samples were incubated with the test reagents at 37°C for one to three minutes. Then, the absorbance was read at a particular wavelength by a spectro-photometer (Beckman), depending on the type of assay performed.

The enzymatic activities were calculated using the formula:

plasma enzymatic activity (U/L) = $(\Delta A \text{ per min} \times TV \times 1000) / (6.22 \times LP \times SV)$, where

$\Delta A \text{ per min}$ = change in absorbance per minute at a particular wavelength,

TV = total reaction volume (in ml),

LP = light path,

SV = sample volume,

6.22 = milli-molar absorptivity of NADPH, and

1000 = conversion of units per ml to per liter.

In another way round, the formula were expressed as:

CK (U/L) = $\Delta A \text{ per min} \times 8200$

LDH (U/L) = $\Delta A \text{ per min} \times 3376$

AST (U/L) = $\Delta A \text{ per min} \times 1768$

ALT (U/L) = $\Delta A \text{ per min} \times 1768$

2.6.8 Two-Dimensional Gel Electrophoresis

2.6.8.1 Sample Preparation

Soon after the drug(s) incubation, the washed cell pellets (1×10^6) were disrupted in 300 μ l denaturing lysis buffer on ice for 30 minutes. Cellular debris was removed by centrifugation (Eppendorf) at 14,000 rpm for 10 minutes to release the protein content at 4°C. Sample solutions resulted were then subjected to the treatment with 2D Clean-up kit (Amersham Biosciences) to eliminate any interfering substances.

The clean-up process was done in the way as described in the user's manual with some modifications. It began with mixing the samples with three volumes of precipitant by vigorous vortex, followed by standing on ice for 15 minutes. Thereafter, an equal volume of co-precipitant was introduced to the mixtures; and the proteins were precipitated out by centrifugation at 14,000 rpm (Eppendorf) for 10 minutes at 4°C. The supernatants were aspirated immediately. While, the pellets were washed with 200 μ l co-precipitant once; and then resuspended in 50 μ l dd.H₂O. 1 ml pre-chilled wash buffer, together with 5 μ l wash additive, was added to the pellet. The solution was left at -20°C for one hour. Afterwards, the proteins were

precipitated out again by centrifugation at 14,000 rpm (Eppendorf) for 10 minutes at 4°C. The supernatants were decanted; whereas the pellets were dried briefly. Eventually, the dried pellets were solubilized in 250 μ l rehydration buffer; and applied directly to the Immobiline Drystrip gel (Amersham Biosciences).

2.6.8.2 First Dimension Electrophoresis – Isoelectric Focusing (IEF)

Before isoelectric focusing, protein concentration of the samples was estimated with the use of 2D Quant kit (Amersham Biosciences), which was compatible to most of the detergents and reductants, like urea, CHAPS and DTT, etc. Accordingly, equal amounts of proteins, say 300 μ g, were loaded onto the corresponding strip holders. IEF Immobiline Drystrips (13 cm; linear pH 3-10 gradient), with gel facing down, were subsequently inserted into the grooves. Any air bubbles trapped in-between the gel and the holder were carefully dispersed. After a while, 1 ml IPG Cover Fluid (Amersham Biosciences) was evenly distributed onto the entire strip, so as to minimize sample evaporation and urea crystallization.

The strips in the strip holders were hence placed on the Ettan IPGphor II

system platform (Amersham Biosciences). Rehydration and protein absorption to the strips were initiated under a low voltage of 30 V (step-and-hold) for 12 hours. Isoelectric focusing was then followed with the condition: 500 V (step-and-hold) for one hour, 1,000 V (step-and-hold) for one hour and 8,000 V (step-and-hold) for two hours. The current used was limited to 50 μ A per gel strip; and the temperature was maintained at 20°C throughout the experiment. The total product of time x voltage was set at 17 Vhrs for each strip.

2.6.8.3 Second Dimension Electrophoresis – SDS-Polyacrylamide Gel Electrophoresis (SDS-PAGE)

The focused IEF strips were next proceeded to the two-step equilibration procedure, in which the strips were incubated in equilibration buffers A (containing 1% DTT) and B (containing 2.5% IAA) sequentially for 15 minutes at room temperature with gentle rocking. On completion, excessive equilibration buffer was tapped off; the equilibrated IEF strips were ready for the second-dimension run.

In the second-dimension gel electrophoresis, the SE 600 Ruby Standard

Vertical Unit (Amersham Biosciences) was utilized. Once the SDS-polyacrylamide gels (12%) were prepared, the IEF strips were put down onto the gel surface; and a piece of filter paper soaked with protein marker (Invitrogen) was positioned aside for size indication. 1 ml pre-warmed sealing agarose solution was overlaid onto the gels; and allowed to solidify for five minutes at room temperature, in order to fill the narrow gaps between the gel edges and lateral spacers to prevent leakages. When all these were finished, electrophoresis was carried out under cooling at a constant voltage of 200 V for six hours, until the bromophenol blue dye-front reached the bottom of the gel.

2.6.8.4 Silver Staining

After electrophoresis, protein spots on the gels were visualized by a silver staining method. The general procedures were tabulated below (Table 2.4).

Step	Solution	Amount for Each Gel	Duration
fixation	fixation solution (10% (v/v) acetic acid and 40% (v/v) ethanol)	250ml	overnight
sensitizing	sensitizing solution (6.8% (w/v) sodium acetate,	250ml	1 hr

	5% (w/v) sodium thiosulphate and 30% (v/v) ethanol		
washing	nano pure water	~ 500ml	5 x 8 mins
silver nitrate	silver nitrate solution (2.5% (w/v) silver nitrate)	200ml	1 hr
washing	nano pure water	~ 500ml	4 x 1 min
developing	developing solution (2.5% (w/v) sodium carbonate and 0.1% (v/v) 37% formaldehyde)	250ml	depends, until protein spots appear
stopping	stopping solution (1.5% (w/v) EDTA)	250ml	30 mins
washing	nano pure water	~ 500ml	2 x 5 mins
storage	storage solution (12% (v/v) acetic acid and 40% (v/v) ethanol)	250ml	up to 1 month at 4°C

Table 2.4 The procedures involved in a standard silver staining process.

The developed gel images were soon scanned and recorded by the Image Scanner II (Amersham Biosciences), equipped with the LabScan software (version 3.0) (Amersham Biosciences). To tackle with the problems of experimental variations, comparative analysis was made between replicated sets of control and treated samples, using the computer software ImageMaster 2D Platinum (version 5.0) (Amersham Biosciences). Protein spots with differential expression pattern (at least two-fold difference)

identified were excised out manually; and kept frozen at -80°C until further processing.

2.6.9 Mass Spectrometry Preparation

2.6.9.1 Destaining and Trypsin Digestion

Subsequent preparation work for the peptide mass fingerprinting involved multiple steps, as depicted as follows. First of all, 100 μl fresh destaining solution was introduced to the gel slices, incubated for 15 minutes with frequent shaking and agitation. As a clear background was attained, they were washed with a large volume of nano pure water three times. After that, the gel pieces were immersed in 200 mM NH_4CO_3 solution for 10 minutes; this process was repeated once. The equilibration solution was discarded. In the meantime, 300 μl 100% (v/v) ACN was added to dehydrate the gel masses for five minutes twice. At this point, shrank white and opaque spots were left behind. They were dried in the SpeedVac concentrator (Savant) shortly for one to two minutes. Lastly, the gel blocks were digested by trypsin in the presence of 50 mM NH_4CO_3 at 30°C overnight.

2.6.9.2 Peptide Extraction

The tryptic digests containing mixtures of peptides were subsequently mixed with 50 μ l 50 mM NH_4CO_3 ; all the liquids were saved and transferred to a new tube. Further extractions were done with 100 μ l 50% (v/v) ACN/ 5% (v/v) TFA solution twice; and 50 μ l 100% (v/v) ACN once, for 10 minutes each time in an ultra-sonic water bath. Finally, all the supernatants were pooled together; and brought to the SpeedVac concentrator (Savant) for drying at 16°C for five hours.

2.6.9.3 Desalting of Peptide Mixture

Next, the dried samples were reconstituted with 10 μ l 0.1% TFA (v/v) solution. Purification and concentration procedures were carried out with the aid of ZipTip C-18 Pipette Tips (Millipore). For use, ZipTip tips (Millipore) were wetted with 10 μ l 50% (v/v) ACN solution twice; and then washed with 10 μ l 0.1% TFA (v/v) solution three times ready for sample binding. Peptides were bound onto the tips by drawing and dispensing the content for 20 cycles. Later on, the tips were washed three times; the bound peptides were eluted in 2 μ l 50% (v/v) ACN/ 0.1% (v/v) TFA solution. In the end, 1 μ l saturated CHCA matrix was loaded to the samples; the whole mixtures were thereby spotted directly onto the MALDI-target (Applied Biosystems).

Data for each sample spot on the MALDI plate (Applied Biosystems) were acquired employing the 4700 Proteomics Analyzer and 4700 Explorer softwares (Applied Biosystems). Combined MS and MS/MS analysis was basically conducted by the Mascot based GPS Explorer Software Remote Access Client (Applied Biosystems), in which the error tolerance for peptide mass was set to be 50 ppm; and the possible missed cleavage of trypsin was one. For MALDI peptide mapping, both the Swiss-Prot (<http://us.expasy.org>) as well as NCBI nr (<http://www.ncbi.nlm.nih.gov>) databases were searched. Only as the proteins got more than four peptides matched were considered as significant.

2.6.10 Real-Time PCR

i) RNA Extraction

Subsequent to the drug(s) exposure, cells (1×10^6) were rinsed once with PBS; and lysed directly in 2 ml TRIzol reagent (Invitrogen) on ice for five minutes. Then, 400 μ l chloroform (Invitrogen) was introduced to the lysates; the mixtures were mixed vigorously for 15 seconds and let stand on ice for three minutes. After that, the samples were centrifuged at 14,000 rpm (Eppendorf) for 15 minutes at 4°C; three layers were thus formed: a lower red chloroform

layer, an inter-phase layer as well as an upper colourless aqueous layer containing RNA exclusively. Colourless phase was aspirated to a new tube instantly, to which 500 μ l isopropanol was added. The solution was placed at -20°C overnight for RNA precipitation. On the day after, the tube was taken to centrifugation at 14,000 rpm (Eppendorf) for 15 minutes at 4°C to separate RNA from the organic solvents. The RNA pellet was washed with ice-cold 75% ethanol once, followed by air-dried at room temperature. In final, 30 μ l DEPC- H_2O was used to dissolve the pellet ready for the coming part of assay.

ii) First-Strand cDNA Synthesis

First-strand cDNA was reverse-transcribed from the total RNA pool in a reaction catalyzed by the SuperScript-III RT enzyme (Invitrogen). The reaction mix consisted of the components listed below (Table 2.5).

5 x cDNA synthesis buffer	4 μ l
oligo T primer (0.05 mM)	1 μ l
dNTP mix (10 mM)	2 μ l
RNA (2 μ g)	x μ l
DTT (100 mM)	1 μ l
RNaseOUT (40 U/ μ l)	1 μ l
SuperScript-III RT (200 U/ μ l)	1 μ l
DEPC-H ₂ O	(10 - x) μ l
TOTAL	20 μl

Table 2.5 The ingredients needed to make up a reaction mix for the first-strand cDNA synthesis reaction.

Reverse transcription reaction was carried out in a thermocycler (Progene), as started at 50°C for 60 minutes and terminated at 85°C for five minutes. When done, 1 μ l RNase H (Invitrogen) was added; the mix was then incubated at 37°C for 20 minutes. cDNA synthesized herein was either used for the real-time PCR analysis immediately, or placed at -20°C for temporary storage.

iii) Real-Time PCR

In general, all the real-time PCR assays were performed in a total volume of 20 μ l in a 96-well plate format by the ABI PRISM 7700 sequence detection system (Applied Biosystems). Reaction mixtures for each assay contained 1

μl 20 x gene expression assay mix (TaqMan), 9 μl diluted cDNA and 10 μl 2 x universal PCR master mix (TaqMan). While, the thermocycling conditions were set as: one cycle at 50°C for two minutes and 95°C for 10 minutes; 40 cycles at 95°C for 15 seconds and 60°C for one minute, according to the guidelines from the manufacturer.

For each investigated gene, triplicates of experiments were included to ensure the reproducibility of results. Relative abundance of the gene transcripts in samples was determined after normalization with the control gene, beta-actin.

iv) Data Analysis

In fact, the basis of gene copy quantification by real-time PCR fundamentally relied on the threshold cycle, C_T , as referred to the cycle number, at which the fluorescence emitted exceeded the fixed threshold. C_T value, as determined by the Sequence Detection Systems (version 1.9) (Applied Biosystems), was inversely proportional to the initial amount of target template. And, the expression level of the target gene, represented by the term – mean fold change, was calculated from the formulae (Livak *et al.*,

2001):

mean fold change = $2^{-\Delta\Delta CT}$, where

$\Delta\Delta CT$ = ΔCT of the target gene in drug-treated sample – ΔCT of the target gene in the control sample, and

ΔCT = CT of the target gene – CT of beta-actin.

Mean fold change of the target gene revealed its amount difference in the treated sample(s) relative to the control one; whereas mean fold change of the control sample was set to be one. For down-regulation of the target gene, the mean-fold-change value ranged from zero to one; in case of up-regulation, however, the value was greater than one.

2.6.11 Cellular Glutathione Level Detection

The detection of the changes in glutathione level of apoptotic cells was chiefly accomplished by the Glutathione Apoptosis Detection Kit, Fluorometric (Calbiochem). In a few words, cells were resuspended in 100 μ l ice-cold cell lysis buffer; and continued on ice for 10 minutes. Then, the supernatants were pipetted to the wells of a 96-well flat-bottom microplate, in which 2 μ l MCB and 2 μ l GST reagents were present. After so, the plate

was incubated at 37°C for 30 minutes. The fluorescence was subsequently measured at 380 nm/ 460 nm using a fluorometer (Beckman).

2.7 Statistical Analysis

Values were expressed as the mean \pm standard deviation (SD). A significant difference from the respective controls for each experimental test condition was assessed using Student's unpaired t-test, with p values of < 0.01 or < 0.05 being regarded as statistically significant.

CHAPTER 3

RESULTS and DISCUSSION --

CYTOTOXICITY OF FLAVONOIDS ISOLATED FROM RADIX SOPHORAE

3.1 Screening of Cytotoxic Flavonoids from Radix Sophorae

Given Radix Sophorae being frequently prescribed against liver diseases in alternate clinical practice, we attempted to screen for the active principle(s), which accounted for these medicinal effects herein. Previously, a bioassay-guided fractionation and purification of Radix Sophorae was conducted by our group, from which six flavonoid constituents were found to exhibit potent cytotoxicities on hepatoma cells *in vitro* (unpublished data). Their identities were revealed by nuclear magnetic resonance (NMR) and mass spectrometric (MS) analyses. Their structures are shown in Fig. 3.1.1.

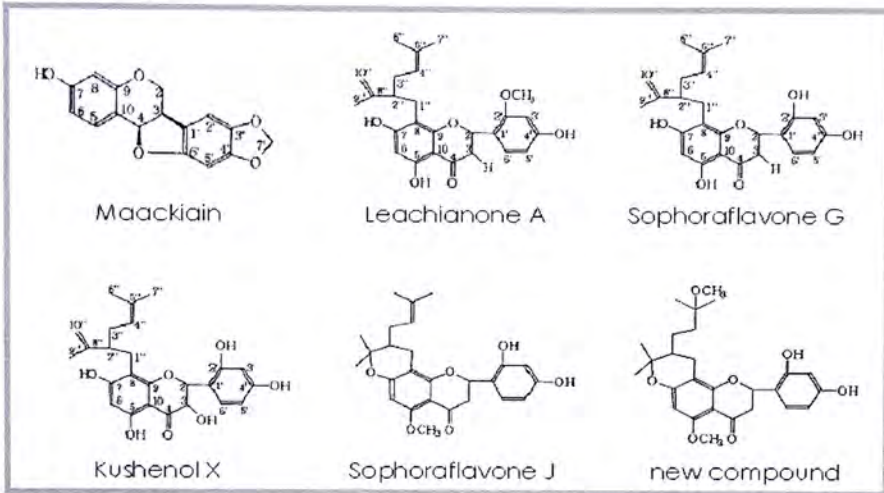


Fig. 3.1.1 Structures of 6 bioactive flavonoids purified from the Radix *Sophorae*.

Among them, the two components, namely Leachianone A and Sophoraflavone J, were our study targets. Their anti-tumor activities were first accessed by their ability to suppress growth of hepatoma cells *in vitro*.

MTT assay is a standard quantitative colorimetric test for the determination of cell survival and proliferation (Mosmann *et al.*, 1983). It is based on the capability of a mitochondrial dehydrogenase enzyme to cleave the tetrazolium rings of the MTT salt; and form dark purple formazan crystals, which are largely impermeable to cell membranes, thereby resulting in their accumulation within the healthy cells (Pagliacci *et al.*, 1993). In this sense, the number of viable cells is directly proportional to the level of the formazan products generated.

3.2 Cytotoxicity of Leachianone A on Human Hepatoma Cell Lines

Initially, the cytotoxicity of Leachianone A on HepG2 cells and its resistant counterpart RHepG2 cells was investigated. Under the experimental conditions, Leachianone A treatment caused an inhibition on the proliferation of both hepatoma cells dose-dependently. The IC_{50} (50% inhibitory concentration) values of 24-, 48- and 72-hour incubations for HepG2 and

RHepG2 cells were calculated as 6.9 $\mu\text{g/ml}$, 3.4 $\mu\text{g/ml}$ and 2.8 $\mu\text{g/ml}$; as well as 3.8 $\mu\text{g/ml}$, 1.4 $\mu\text{g/ml}$ and 1.4 $\mu\text{g/ml}$ respectively, from the dose-response curve (Fig. 3.2.1 & 3.2.2). In both cases, profound cytotoxic activity of Leachianone A was observed at 48-hour culture.

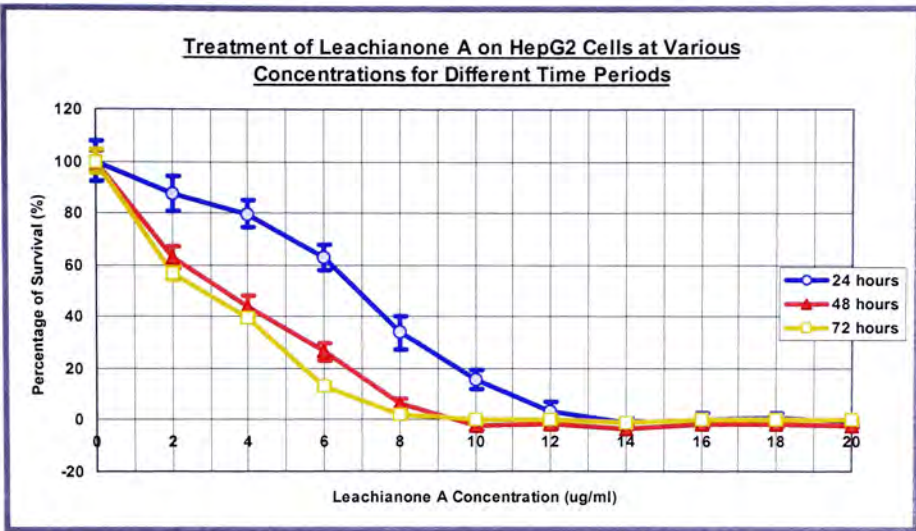


Fig. 3.2.1 Effect of Leachianone A on the proliferation of HepG2 cells.

Cells (1×10^4) were seeded in 96-well plates and incubated with different concentrations of Leachianone A for 24, 48 and 72 hours at 37°C, 5% CO₂. Cell viability was determined by MTT assay. Results are mean \pm SD of 5 determinations.

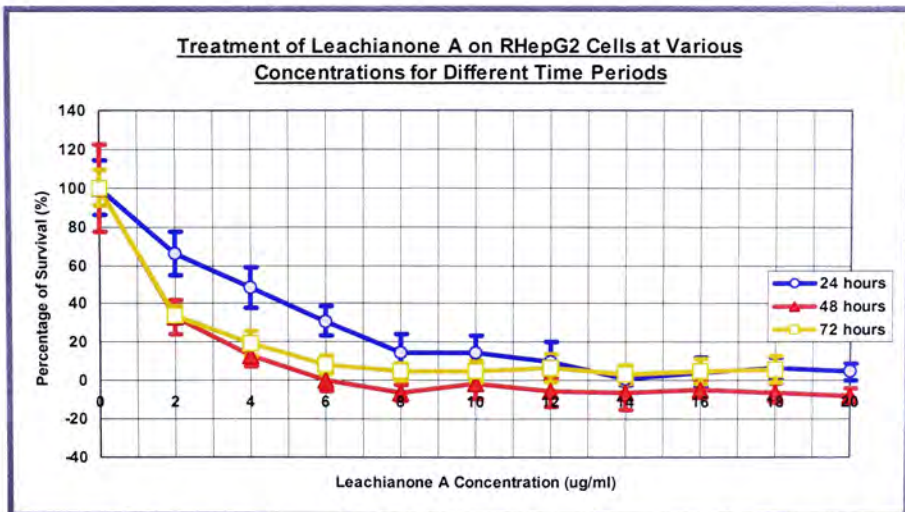


Fig. 3.2.2 Effect of Leachianone A on the proliferation of RHepG2 cells.

Cells (1×10^4) were seeded in 96-well plates and incubated with different concentrations of Leachianone A for 24, 48 and 72 hours at 37°C, 5% CO₂. Cell viability was determined by MTT assay. Results are mean \pm SD of 5 determinations.

3.3 Cytotoxicity of Leachianone A on Human Normal Liver Cell Line

To define if the compound exerted its action specifically on the tumor cells, a human normal liver cell line WRL-68 was also included as a parallel experiment. Upon addition of increasing concentrations (0 $\mu\text{g/ml}$ – 20 $\mu\text{g/ml}$) of Leachianone A for 48 hours, there was a dose-dependent reduction in the cell viability, with an IC_{50} value found to be 9.5 $\mu\text{g/ml}$ (Fig. 3.3.1). Despite this, the percentage of cell survival still maintained high up at 95% when challenged with the effectual dosages (1.4 $\mu\text{g/ml}$ – 2.8 $\mu\text{g/ml}$) of Leachianone A against cancer cells.

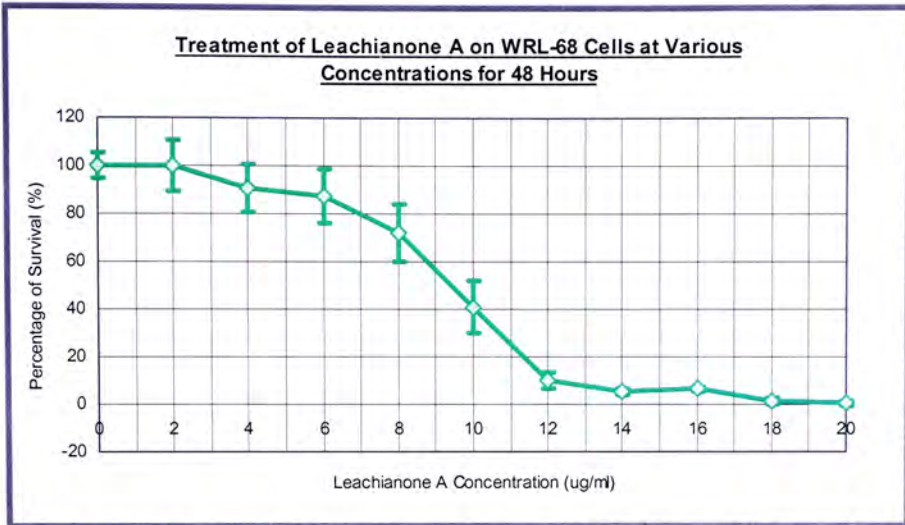


Fig. 3.3.1 Effect of Leachianone A on the proliferation of WRL-68 cells. Cells (1×10^4) were seeded in 96-well plates and incubated with different concentrations of Leachianone A for 48 hours at 37°C , 5% CO_2 . Cell viability was determined by MTT assay. Results are mean \pm SD of 5 determinations.

3.4 Cytotoxicity of Sophoraflavone J on Human Hepatoma Cell Line

Next, the cytotoxicity of Sophoraflavone J on HepG2 cells was examined. From the experiment, Sophoraflavone J brought about 50% cell death at a concentration of 8.1 $\mu\text{g/ml}$ following 24-hour, 5.5 $\mu\text{g/ml}$ following 48-hour and 5.3 $\mu\text{g/ml}$ following 72-hour incubations (Fig. 3.4.1). Again, the data indicated that the maximal inhibitory effect was attained at 48 hours.

Because of the scarce amount of Sophoraflavone J extracted, the cytotoxicity test on RHepG2 cells was lacking at the moment.

3.5 Cytotoxicity of Sophoraflavone J on Human Normal Liver Cell Line

In the situation of WRL-68 cells, similarly, presence of Sophoraflavone J arrested cell growth after 48 hours. 50% survival rate of cells was detected at a concentration of 8.8 $\mu\text{g/ml}$, being much higher than the one (5.5 $\mu\text{g/ml}$) for HepG2 cells (Fig. 3.5.1).

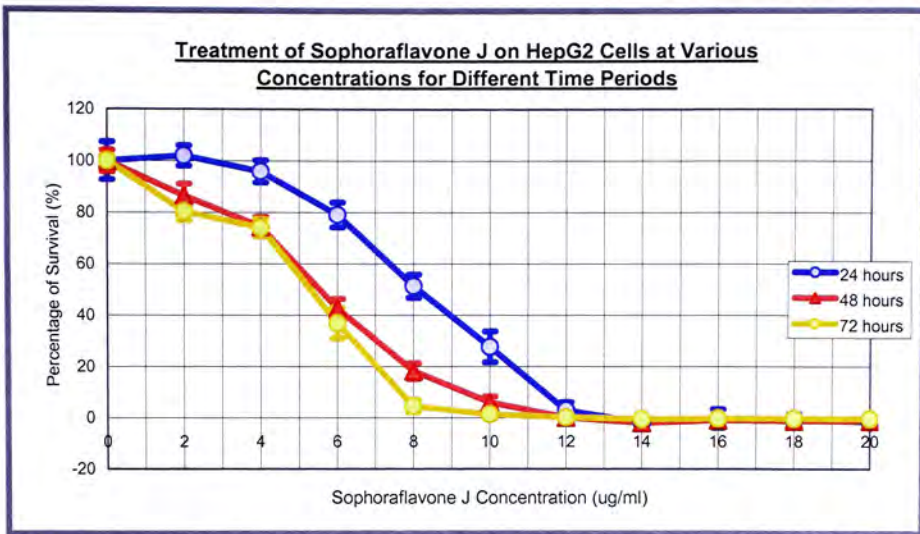


Fig. 3.4.1 Effect of Sophoraflavone J on the proliferation of HepG2 cells. Cells (1×10^4) were seeded in 96-well plates and incubated with different concentrations of Sophoraflavone J for 24, 48 and 72 hours at 37°C, 5% CO₂. Cell viability was determined by MTT assay. Results are mean \pm SD of 5 determinations.

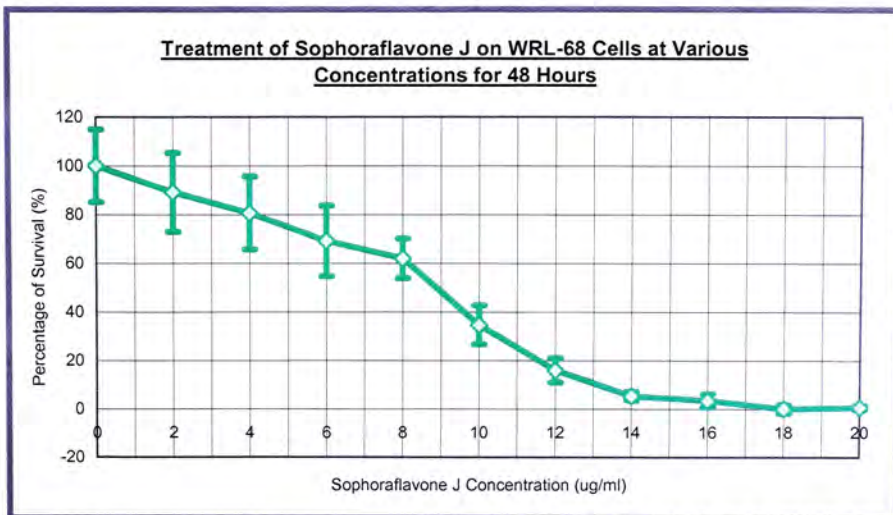


Fig. 3.5.1 Effect of Sophoraflavone J on the proliferation of WRL-68 cells. Cells (1×10^4) were seeded in 96-well plates and incubated with different concentrations of Sophoraflavone J for 48 hours at 37°C, 5% CO₂. Cell viability was determined by MTT assay. Results are mean \pm SD of 5 determinations.

3.6 Cytotoxicities of Cisplatin and Taxol on Human Hepatoma as well as Normal Liver Cell Lines

Aside from these, some conventional anti-cancer agents, for instances cisplatin and taxol, were assayed herein to allow comparisons with the two potential candidates. The former one, cisplatin, is well-known as a DNA-damaging agent; it binds primarily to the guanine residues in DNA to form intra- and inter-strand adducts; as well as DNA-protein cross-linking complexes (Huang *et al.*, 1994, Wang *et al.*, 2006). Cisplatin-modified adducts always change the conformation of DNA-attracting nuclear proteins severely, especially those containing high mobility group domain, so that the DNA buried inside these proteins is poorly repaired (Zamble *et al.*, 1996). While, the action of taxol is rather distinct. This natural diterpenoid attaches on the β -subunit of tubulin; and promotes the assembly of stable but non-functional micro-tubule bundles, which ultimately interfere the mitosis in G2/ M-phase junction (Jordan *et al.*, 1996, Frankel *et al.*, 1997, Rieder *et al.*, 2000).

Likewise, various concentrations of cisplatin and taxol (0 μ M – 100 μ M) were introduced to the HepG2, RHepG2 and WRL-68 cells continued for 48 hours. At the end of the incubation period, cell proliferation was measured using MTT

assay. The drug concentrations required to inhibit cell growth by 50% were listed below (Table 3.1).

	Cisplatin	Taxol
HepG2 cells	12.5 μM	6 μM
RHepG2 cells	17 μM	13 μM
WRL-68 cells	23.5 μM	6 μM

Table 3.1 A summary of the results from cell viability assays on the 48-hour exposure of anti-cancer drugs, cisplatin and taxol, to human hepatoma cells and normal liver cells.

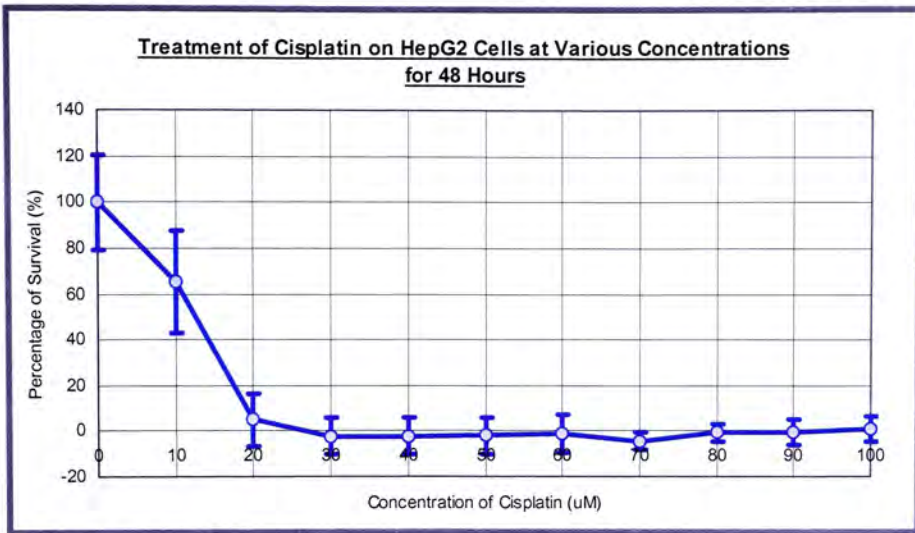


Fig. 3.6.1 Effect of cisplatin on the proliferation of HepG2 cells.

Cells (1×10^4) were seeded in 96-well plates and incubated with different concentrations of cisplatin for 48 hours at 37°C , 5% CO_2 . Cell viability was determined by MTT assay. Results are mean \pm SD of 6 determinations.

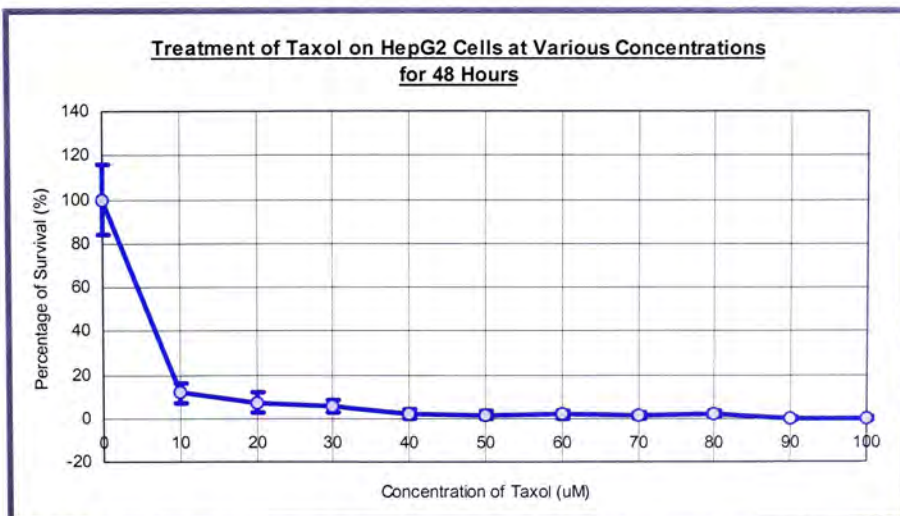


Fig. 3.6.2 Effect of taxol on the proliferation of HepG2 cells.

Cells (1×10^4) were seeded in 96-well plates and incubated with different concentrations of taxol for 48 hours at 37°C , 5% CO_2 . Cell viability was determined by MTT assay. Results are mean \pm SD of 6 determinations.

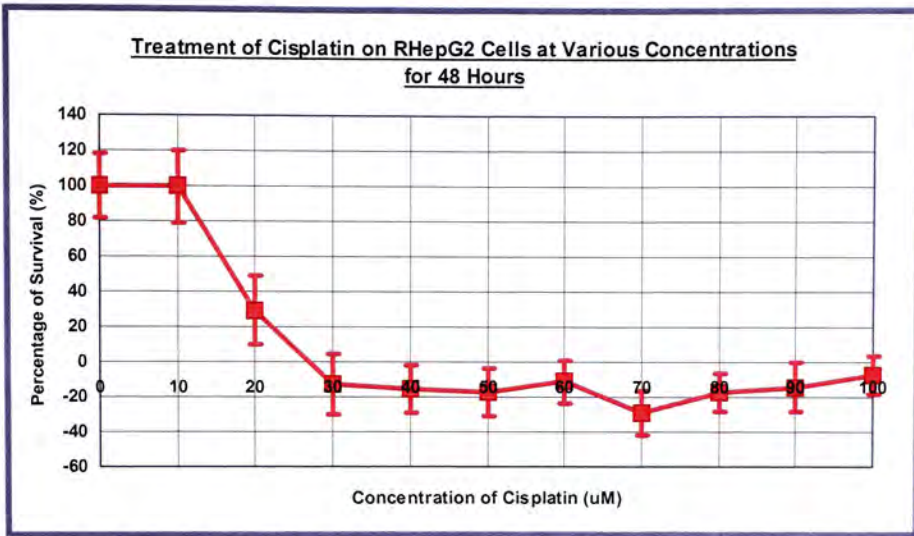


Fig. 3.6.3 Effect of cisplatin on the proliferation of RHEPG2 cells.

Cells (1×10^4) were seeded in 96-well plates and incubated with different concentrations of cisplatin for 48 hours at 37°C, 5% CO₂. Cell viability was determined by MTT assay. Results are mean \pm SD of 6 determinations.

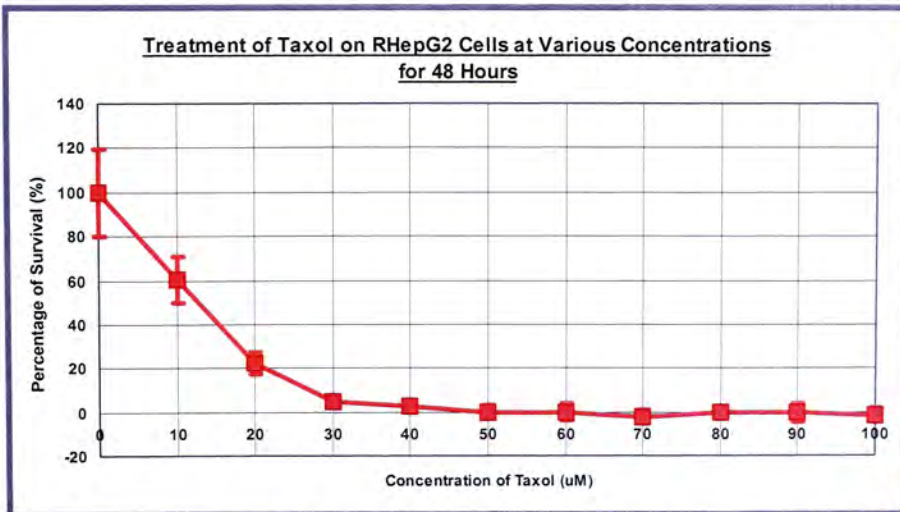


Fig. 3.6.4 Effect of taxol on the proliferation of RHEPG2 cells.

Cells (1×10^4) were seeded in 96-well plates and incubated with different concentrations of taxol for 48 hours at 37°C, 5% CO₂. Cell viability was determined by MTT assay. Results are mean \pm SD of 6 determinations.

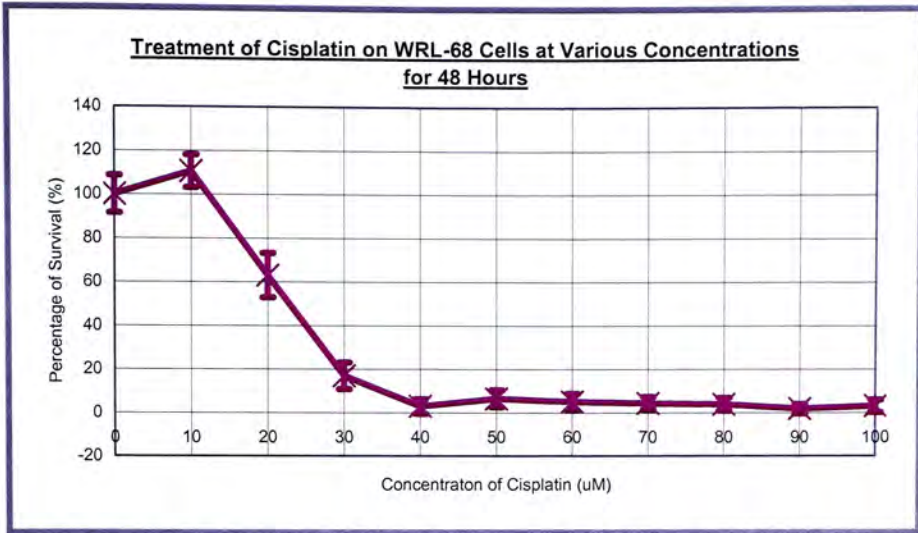


Fig. 3.6.5 Effect of cisplatin on the proliferation of WRL-68 cells.

Cells (1×10^4) were seeded in 96-well plates and incubated with different concentrations of cisplatin for 48 hours at 37°C , 5% CO_2 . Cell viability was determined by MTT assay. Results are mean \pm SD of 6 determinations.

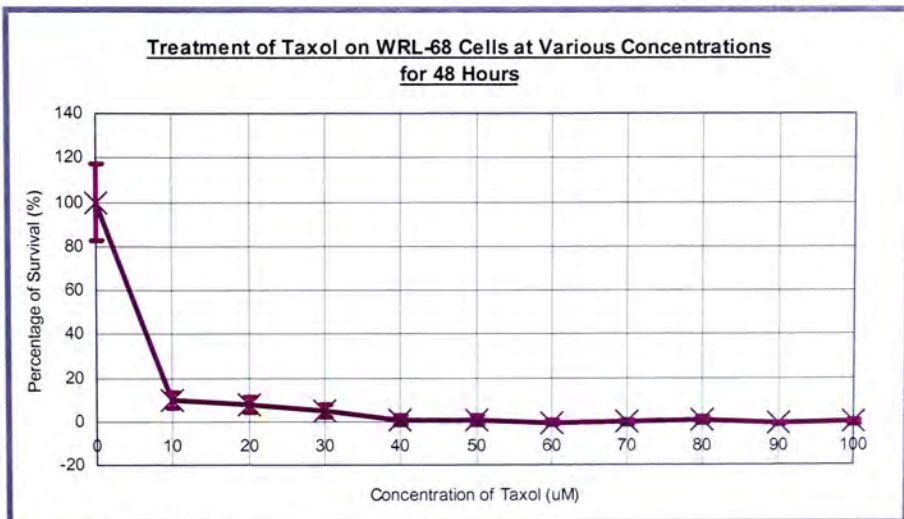


Fig. 3.6.6 Effect of taxol on the proliferation of WRL-68 cells.

Cells (1×10^4) were seeded in 96-well plates and incubated with different concentrations of taxol for 48 hours at 37°C , 5% CO_2 . Cell viability was determined by MTT assay. Results are mean \pm SD of 6 determinations.

3.7 Conclusion

Tabulated in the following were the IC₅₀ values of different combinations of cells and drugs, as determined by the MTT assay (Table 3.2).

	Leachianone A			Sophoraflavone J			Cisplatin	Taxol
	24 hours	48 hours	72 hours	24 hours	48 hours	72 hours	48 hours	48 hours
HepG2 cells	15.75 μM	7.76 μM	6.39 μM	18.49 μM	12.56 μM	12.10 μM	12.5 μM	6 μM
RHepG2 cells	8.68 μM	3.20 μM	3.20 μM	---	---	---	17 μM	13 μM
WRL-68 cells	---	21.69 μM	---	---	20.10 μM	---	23.5 μM	6 μM

Table 3.2 A summary of the results from cell viability assays on the exposure of Leachianone A, Sophoraflavone J and anti-cancer drugs, cisplatin and taxol, to human hepatoma cells and normal liver cells for different time periods.

Remarks :

Conversion of the units from μg/ml into μM was based on the equation:

mass (in μg)/ molar mass]/ volume (in ml) = molarity (in μM), where

the molar masses of Leachianone A and Sophoraflavone J = 438

All in all, both Leachianone A and Sophoraflavone J rendered potent cytotoxic activities on the human hepatoma cell lines HepG2 and RHepG2, in a time- and dose-dependent manner (Fig. 3.2.1, 3.2.2 & 3.3.1). The most

prominent growth-suppressing action, however, appeared at 48-hour exposure. When compared to the currently employed anti-cancer drugs, cisplatin and taxol, Sophoraflavone J presented a comparable degree of cell growth inhibition; whereas Leachianone A owned a much higher efficacy in terms of cytotoxicity (Fig. 3.6.1 – 3.6.4). In consideration with the normal liver cell line WRL-68, treatments of Leachianone A and Sophoraflavone J for 48 hours inevitably induced certain extents of cell loss, dose-dependently (Fig. 3.4.1 & 3.5.1). Yet, such toxicity was relatively inconsequential at their effective dosages against hepatoma cells. In fact, this kind of non-specificity was also displayed in the applications of cisplatin and taxol (Fig. 3.6.5 & 3.6.6). For this reason, Leachianone A and Sophoraflavone J still merited our in-depth research on their action mechanism(s) and possible therapeutic use(s) in liver cancer, if any.

CHAPTER 4

RESULTS and DISCUSSION --

MECHANISTIC STUDY OF LEACHIANONE A-INDUCED CELL DEATH IN

HEPATOMA CELLS, HepG2 and RHepG2

4.1 Promotion of Cell Cycle Arrest

To date, numbers of different approaches are adopted in liver cancer therapy using dietary pharmaceutical agents; one of them is to promote cell cycle arrest.

In cells, the division cycle is grossly comprised of four discrete but well-coordinated processes: cell growth, DNA synthesis (S phase), segregation of duplicated chromosomes as well as cell division (M phase). There are also gap phases, known as G₁, which connects the completion of M phase to the initiation of S phase in next cycle; and G₂, which separates the S and M phases. In response to some developmental and environmental signals, cells in G₁ phase sometimes temporarily or permanently leave the cycle; and enter a quiescent or arrested phase,

known as G_0 . Very often, tumor cells are, however, destined to repeat the cell cycle indefinitely, resulting in an uncontrollable and excessive cell division. As such, blockage or disruption of the cell cycle progression is reckoned as a feasible method to suppress cancer cell growth.

To address this point, we investigated the cell cycle distribution profile of HepG2 and RHepG2 cells, upon treatment with different dosages of Leachianone A by propidium iodide (PI) staining. PI is a dye, which intercalates into the double-stranded nucleic acids and fluoresces strongly, so that DNA contents inside the cells are readily estimated (Godard *et al.*, 1999). A histogram of cell cycle analysis for untreated cells is given in Fig.

4.1.1.

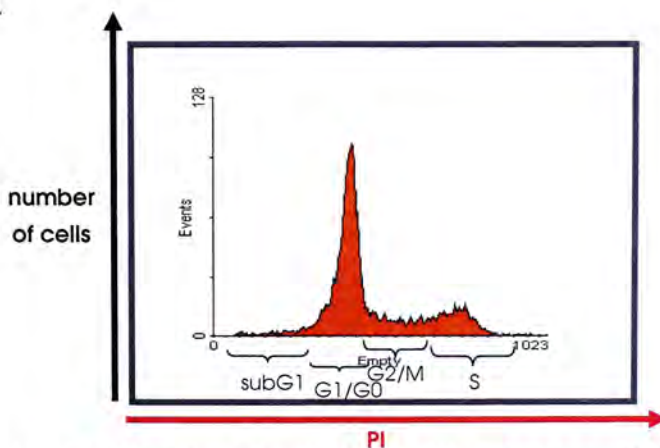


Fig. 4.1.1 A characteristic pattern of untreated cells in the sub-G1, G1/ G0, S and M phases in the cell cycle analysis.

Referring to the results, there was a peak found in the sub-G1 phase, which represented the accumulation of a massive population of cells with hypo-diploid DNA contents, in all Leachianone A-treated panels of cells. As compared to the control, the percentage of cells in the sub-G1 fraction dramatically increased to 35.37% and 53.36% in HepG2 and RHepG2 cells respectively, following a rise in the Leachianone A concentration for 48 hours (Fig. 4.1.2 & 4.1.3). In spite of this, arrest at any phase of the cell cycle did not take place at all. Therefore, we proposed that the growth inhibition of HepG2 and RHepG2 cells elicited by Leachianone A was somehow correlated with apoptosis rather than cell cycle arrest.

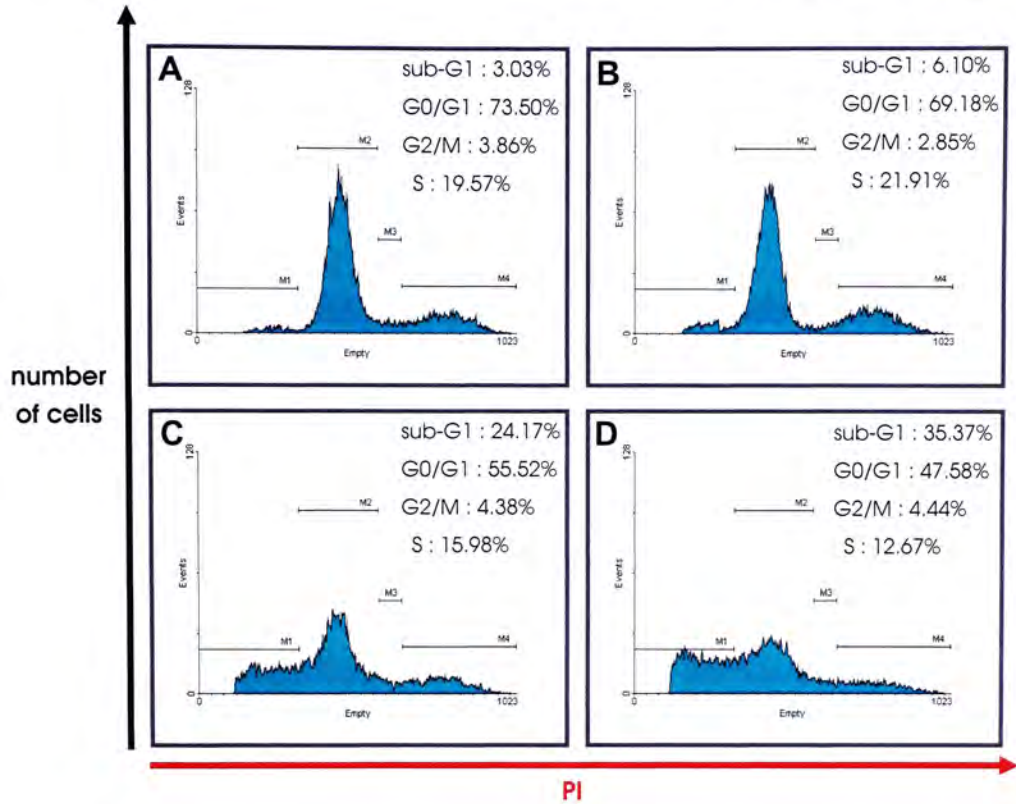


Fig. 4.1.2 Cell cycle analysis of HepG2 cells treated with vehicle or Leachianone A for 48 hours.

Cells (3×10^5) were exposed to vehicle only (A) and Leachianone A at concentrations of 10 $\mu\text{g/ml}$ (B), 20 $\mu\text{g/ml}$ (C) and 30 $\mu\text{g/ml}$ (D) for 48 hours at 37°C, 5% CO₂. Cells harvested were stained with PI and subjected to flow cytometric analysis. Markers M1, M2, M3 and M4 corresponded to the cell fractions at sub-G1, G₀/G₁, G₂/M and S phases, respectively. Results are representative of 4 independent experiments.

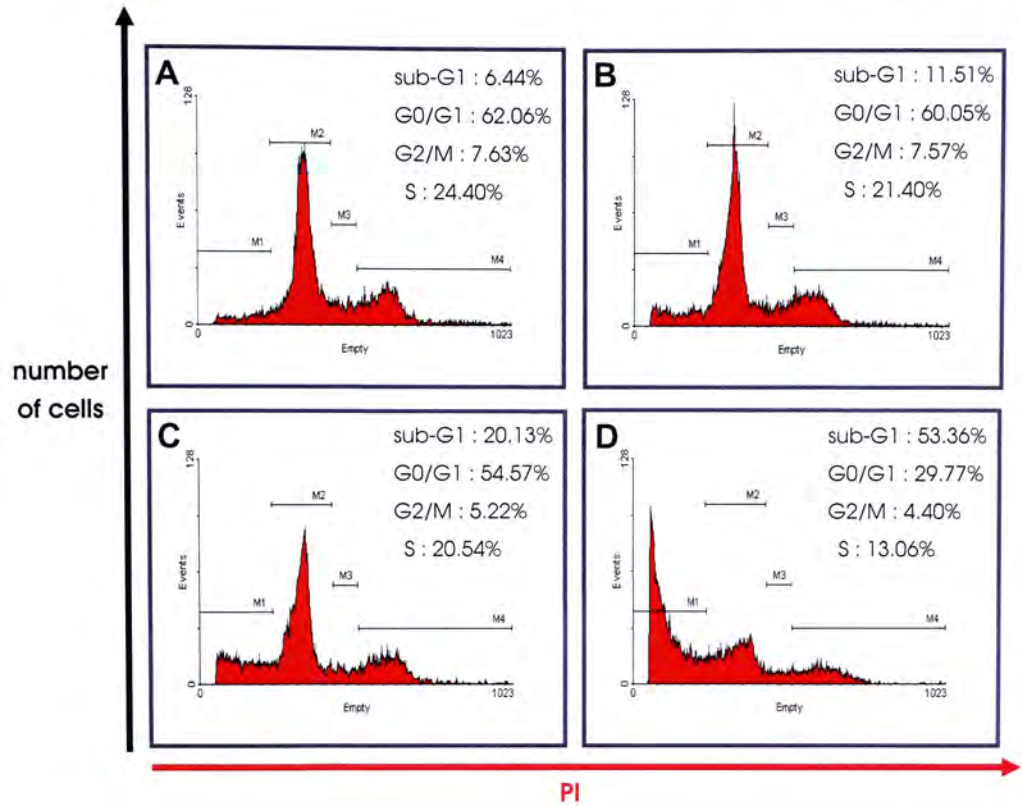


Fig. 4.1.3 Cell cycle analysis of RHePG2 cells treated with vehicle or Leachianone A for 48 hours.

Cells (3×10^5) were exposed to vehicle only (A) and Leachianone A at concentrations of 10 µg/ml (B), 20 µg/ml (C) and 30 µg/ml (D) for 48 hours at 37°C, 5% CO₂. Cells harvested were stained with PI and subjected to flow cytometric analysis. Markers M1, M2, M3 and M4 corresponded to the cell fractions at sub-G1, G₀/G₁, G₂/M and S phases, respectively. Results are representative of 4 independent experiments.

4.2 Induction of Apoptosis as Evidenced by Phosphatidylserine Externalization and DNA Fragmentation

The cell cycle and apoptosis are intimately related. Apoptosis is a kind of programmed cell death (PCD), in which the suicidal process is carried out in an ordered sequence and a regulated manner. In contrast to necrosis, which is considered as a random issue as resulted from acute and violent ruptures, systematic disassembly of a cell by apoptosis reserves a physiological advantage in the cancer therapy because no systemic deleterious inflammatory responses are evoked (Satchell *et al.*, 2003). That explains why exploitation of apoptotic pathway now emerges as a key mechanism, by which cancer cells are eliminated by therapeutic drugs (Solary *et al.*, 2002).

In general, apoptosis is characterized by several distinctive morphological and biochemical changes in cells. The former consists of cell shrinkage, membrane blebbing and chromatin condensation; whereas the latter includes the appearance of phosphatidylserine (PS) on cell membrane surface, DNA fragmentation, protein cleavage at specific locations and increased mitochondrial membrane permeability, etc (Debatin *et al.*, 2001,

Robertson *et al.*, 2002).

4.2.1 Occurrence of Phosphatidylserine Externalization

To elucidate the death type induced by Leachianone A, we next tested for the occurrence of phosphatidylserine (PS) externalization onto the cell surface, an event typically associated with apoptosis (van Engeland *et al.*, 1998). PS is a phospholipid normally restricted to the cytoplasmic surface of the cell membrane in healthy cells. But, when cells undergo apoptosis, PS is flipped and translocated to the outer leaflet of the cell membrane to get exposed to the extra-cellular environment. As a consequence, macrophages come to surround and engulf these apoptotic cells, thus protecting organisms from inflammation, which is always accompanied by necrosis (Bergmann *et al.*, 2002).

Annexin V is a 35kDa Ca^{2+} -dependent human phospholipid-binding protein, which has a high affinity for PS. With a fluorophore FITC conjugated to it, cells with externalized PS confer a distinct green fluorescence signal, as detected by flow cytometry. Since PS translocation also exists during necrosis, a cell impermeant red fluorescence dye PI is used in the assay as an

indicator of membrane structural integrity. Intact cell membrane of viable and early apoptotic cells is simply able to exclude PI; these annexin V(-) PI(-) and annexin V(+) PI(-) populations cluster at the bottom left and right quadrants, respectively. On the other hand, loss of membrane integrity, as displayed in the later stage of apoptosis or necrosis, enables the entry of PI for binding with DNA in the cells. Under these circumstances, both the green and red fluorescence signals are strong, i.e. annexin V(+) PI(+); and cells are mainly localized at the top right quadrant. The general layout of cell distribution in annexin V/ PI staining experiment is depicted in Fig. 4.2.1.1a. Cells incubated with staurosporine (STS), a distinguished apoptosis-inducing agent, serve as the positive control in Fig. 4.2.1.1b.

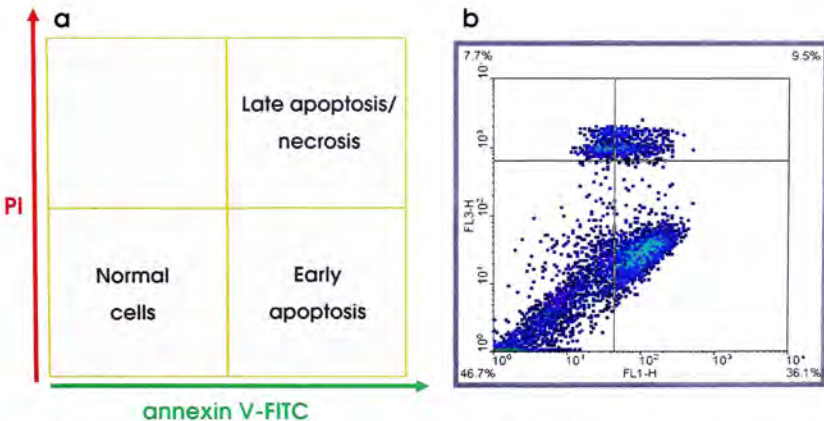


Fig. 4.2.1.1a Schematic diagram of cell distribution of viable, early apoptotic and later apoptotic/ necrotic cells in annexin V-FITC/ PI staining experiment.

Fig. 4.2.1.1b Density plot of cells exposed to 1 μ M staurosporine for 48 hours.

The results herein indicated that the proportion of annexin V-stained cells (signifying both the early and late apoptotic cells) escalated with the concentration of Leachianone A applied (Fig. 4.2.1.2 & 4.2.1.3). At a low concentration (10 $\mu\text{g/ml}$), a substantial quantity of cells was found present in the bottom right quadrant; cells were primarily in the early phase of apoptosis. With higher concentrations (20 $\mu\text{g/ml}$ & 30 $\mu\text{g/ml}$) introduced, a shift of the cell population from the bottom right quadrant to the top right quadrant was demonstrated, dictating that cells were in late apoptotic/ necrotic stage.

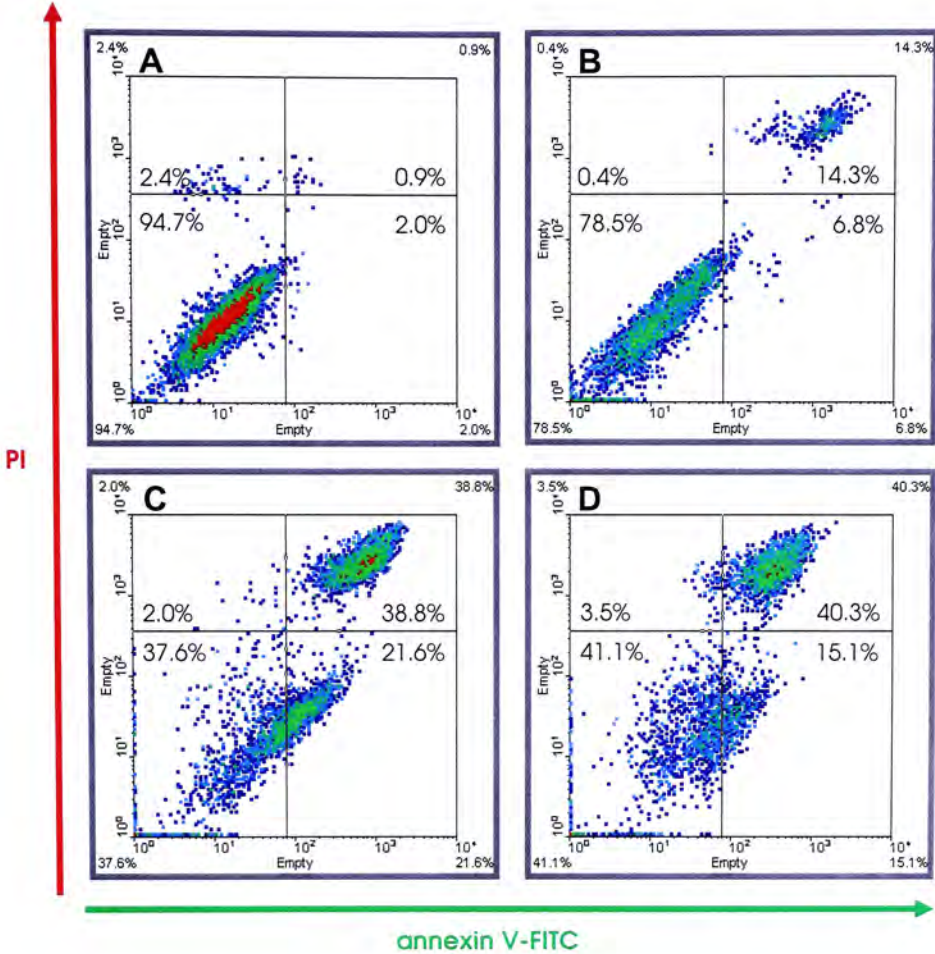


Fig. 4.2.1.2 Annexin V-FITC / PI staining of HepG2 cells treated with vehicle or Leachianone A for 48 hours.

Cells (3×10^5) were exposed to vehicle only (A) and Leachianone A at concentrations of 10 µg/ml (B), 20 µg/ml (C) and 30 µg/ml (D) for 48 hours at 37°C, 5% CO₂. Cells collected were passed to annexin V-FITC and PI staining, followed by flow cytometric analysis. Results are representative of 4 independent experiments.

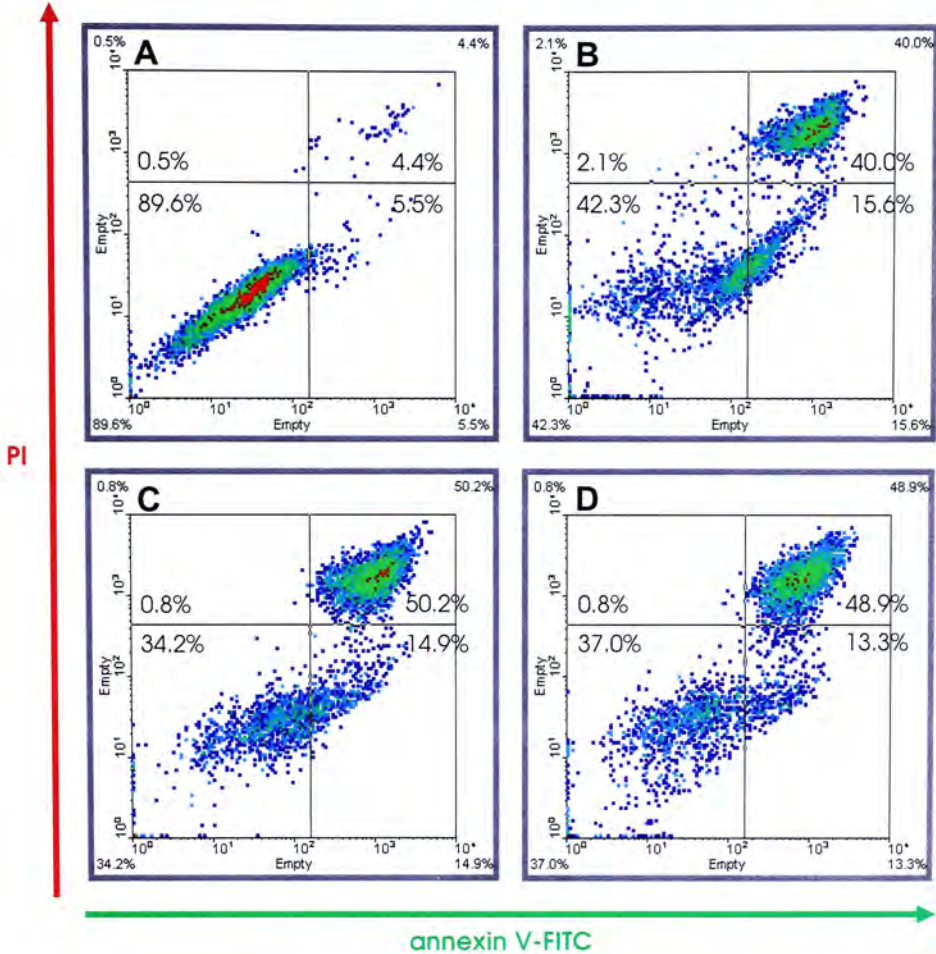


Fig. 4.2.1.3 Annexin V-FITC / PI staining of RHePG2 cells treated with vehicle or Leachianone A for 48 hours.

Cells (3×10^5) were exposed to vehicle only (A) and Leachianone A at concentrations of 10 μ g/ml (B), 20 μ g/ml (C) and 30 μ g/ml (D) for 48 hours at 37°C, 5% CO₂. Cells collected were passed to annexin V-FITC and PI staining, followed by flow cytometric analysis. Results are representative of 4 independent experiments.

4.2.2 DNA Fragmentation Detection

DNA fragmentation is broadly documented as a hallmark of apoptosis (Webb *et al.*, 1997, Yan *et al.*, 2006). During the process, endonucleases are activated to attack the linker region between nucleosomes; and cleave the genomic DNA into small fragments of about 180 to 185 base pairs (bp). The multiple oligomers resulted are detected as an increased fluorescence intensity using flow cytometry in TUNEL assay; or as a laddering pattern in the agarose gel electrophoresis (Saraste *et al.*, 2000).

4.2.2.1 Terminal Deoxynucleotidyl Transferase(TdT)-mediated dUTP

Nick End Labeling (TUNEL) Assay

The TUNEL assay provides a quantitative fluorescence measurement of apoptosis-induced DNA fragmentation. This method fundamentally utilizes the transferase enzyme to fill the exposed 3'-hydroxyl termini in DNA strands directly with conjugated fluorescein-deoxyuridine triphosphate nucleotides (FITC-dUTP) by nicked end labeling. Given DNA degradation present in apoptotic cells, a multitude of these sites are available for the integration of the nucleotide residues into the fragmenting DNA. Conversely, non-apoptotic cells only incorporate a few of FITC-dUTP nucleotides, owing to

the lack of free 3'-hydroxyl DNA ends. The striking difference in the number of 3'-hydroxyl ends, which in turn affects the fluorescence intensity acquired, forms the basis for the identification of healthy cells and dying cells.

Based on the TUNEL study, exposure to Leachianone A at concentrations of 10 µg/ml, 20 µg/ml and 30 µg/ml led to a considerable augment in the amount of cells with fragmented DNA dose-dependently (Fig. 4.2.2.1.1 & 4.2.2.1.2). With the extreme dosage, e.g. 30 µg/ml, over 90% of cells exhibited chromosomal DNA breakages.

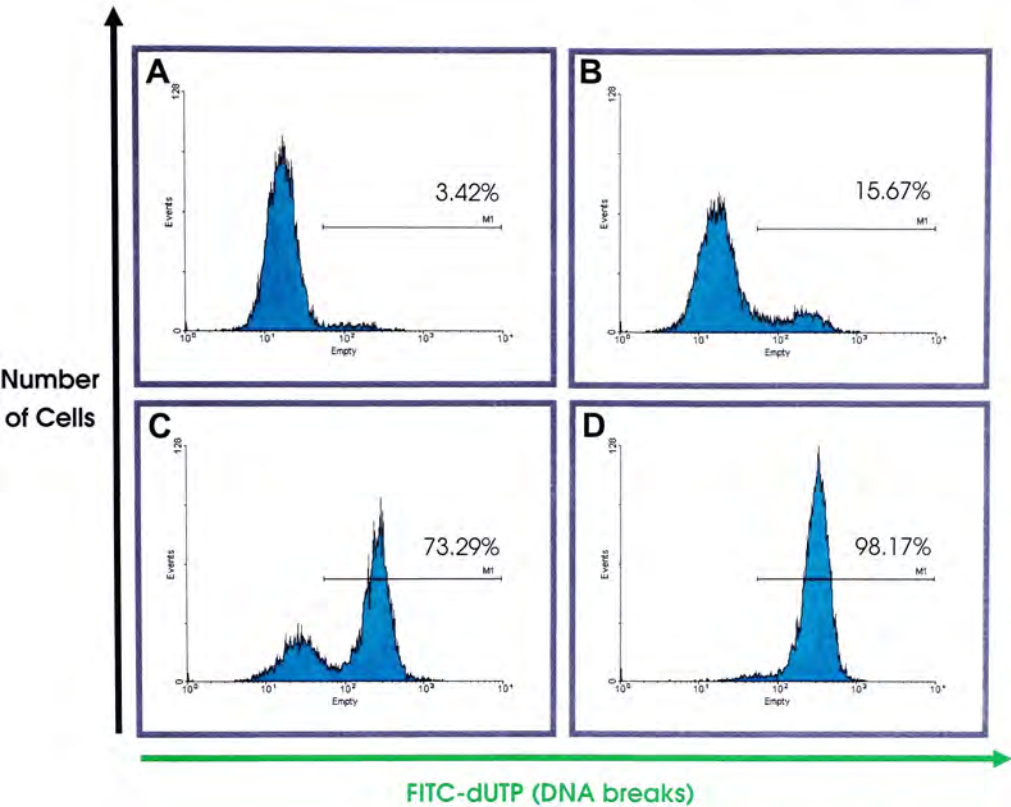


Fig. 4.2.2.1.1 TUNEL assay of HepG2 cells treated with vehicle or Leachianone A for 48 hours.

Cells (1×10^6) were exposed to vehicle only (A) and Leachianone A at concentrations of 10 $\mu\text{g/ml}$ (B), 20 $\mu\text{g/ml}$ (C) and 30 $\mu\text{g/ml}$ (D) for 48 hours at 37°C, 5% CO₂. Numbers of cells with DNA breaks were determined by flow cytometry. Marker M1 corresponded to the cell fraction with DNA breaks labeled with FITC-dUTP nucleotides. Results are representative of 3 independent experiments.

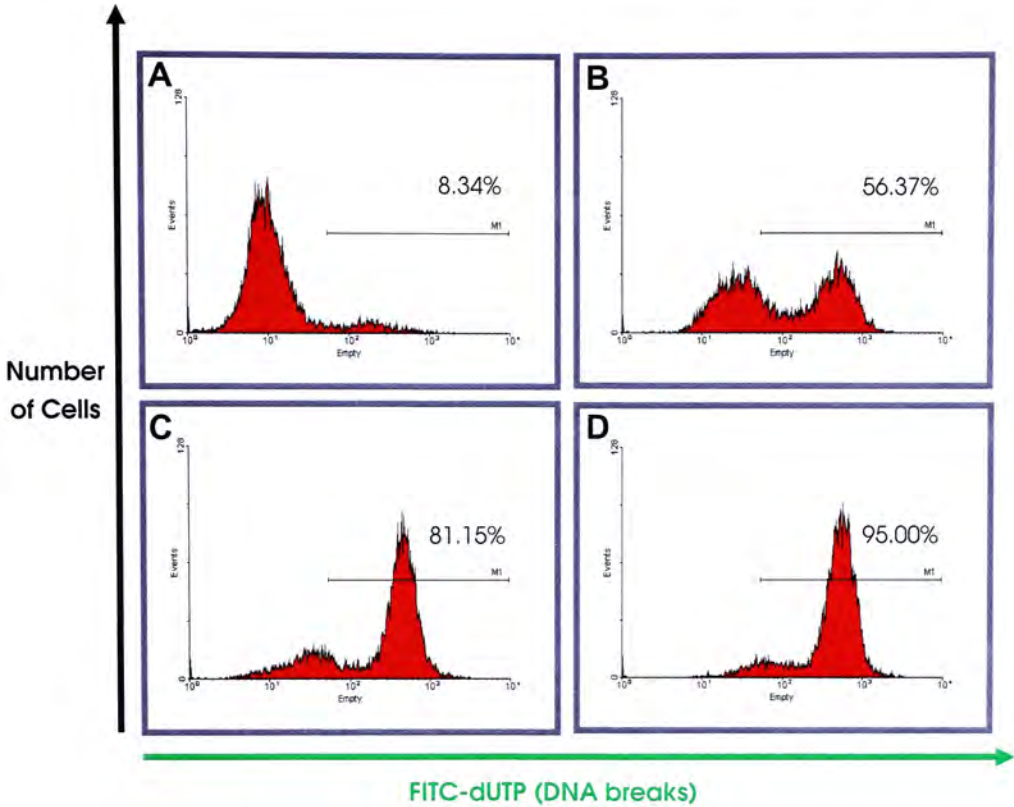


Fig. 4.2.2.1.2 TUNEL assay of RHePG2 cells treated with vehicle or Leachianone A for 48 hours.

Cells (1×10^6) were exposed to vehicle only (A) and Leachianone A at concentrations of 10 $\mu\text{g/ml}$ (B), 20 $\mu\text{g/ml}$ (C) and 30 $\mu\text{g/ml}$ (D) for 48 hours at 37°C, 5% CO₂. Numbers of cells with DNA breaks were determined by flow cytometry. Marker M1 corresponded to the cell fraction with DNA breaks labeled with FITC-dUTP nucleotides. Results are representative of 3 independent experiments.

4.2.2.2 DNA Laddering Pattern in Agarose Gel Electrophoresis

In the majority of cell types, a typical laddering pattern of DNA bands in multiples of approximately 200 bp is indicative of apoptosis. One of the limitations of TUNEL assay is that there is no way to prove the resulting DNA fragments are of which size. Qualitative assessment is hence needed to overcome this shortcoming.

In the agarose gel electrophoresis, a characteristic laddering pattern of DNA was observed at concentrations of 20 $\mu\text{g/ml}$ and 30 $\mu\text{g/ml}$ of Leachianone A in HepG2 cells post-48-hour drug treatment (Fig. 4.2.2.2.1A). Similar pattern was noted in RHepG2 cells too, but at a lower concentration of 10 $\mu\text{g/ml}$ (Fig. 4.2.2.2.1B). These were in agreement with our data obtained previously from TUNEL assay, in which RHepG2 cells were more sensitive than HepG2 cells to Leachianone A treatment in terms of DNA fragmentation (Fig. 4.2.2.1.1 & 4.2.2.1.2). Collectively, we concluded that Leachianone A inhibited the proliferation of HepG2 and RHepG2 cells probably via the induction of apoptosis.

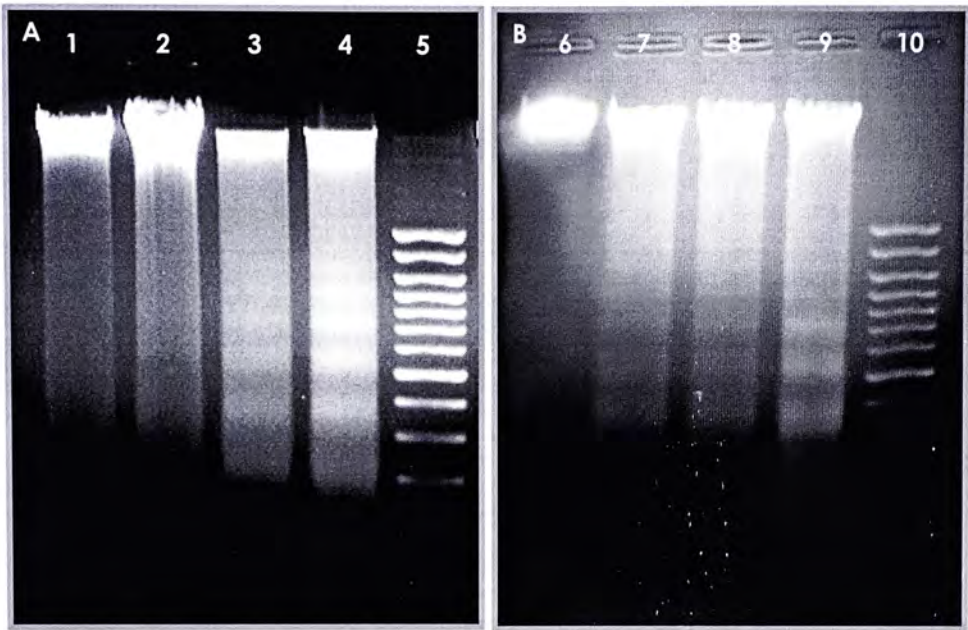


Fig. 4.2.2.2.1 Induction of DNA fragmentation in Leachianone A-treated A) HepG2 and B) RHepG2 cells.

Cells (1×10^6) were incubated with vehicle only (lanes 1 & 6) and Leachianone A at concentrations of 10 $\mu\text{g/ml}$ (lanes 2 & 7), 20 $\mu\text{g/ml}$ (lanes 3 & 8) and 30 $\mu\text{g/ml}$ (lanes 4 & 9) for 48 hours at 37°C, 5% CO₂. DNA laddering pattern was observed by 2% agarose gel electrophoresis. 100bp DNA marker (lanes 5 & 10) was positioned aside for size indication. Results are representative of 3 independent experiments.

4.3 Recruitment of Multiple Signaling Pathways in Leachianone

A-induced Apoptosis

As far as apoptosis was confirmed, we then aimed to work out the underlying mechanisms responsible for this Leachianone A-induced cell death in HepG2 and RHepG2 cells.

Apoptotic cell death is triggered by intra-cellular cues, such as DNA damage and osmotic stress; as well as extra-cellular cues, like growth factor withdrawal, matrix attachment and direct cytokine-mediated killing, etc (Sellers *et al.*, 1999). Two central pathways are identified; one is the extrinsic (death receptor-mediated) pathway and a second, intrinsic (mitochondrial) pathway (Medema *et al.*, 1997, Green *et al.*, 1998). These two pathways converge and connect to each other on the caspase cascade.

4.3.1 Activation of Caspases-3, -8, and -9

The core apoptotic machinery comprises the cysteine-aspartic acid proteases (caspases), members of B-cell lymphoma 2 (Bcl-2) family and apoptosis protease-activating factor-1 (Apaf-1). Caspases are cysteine proteases, which cleave proteins at aspartic acid residues accommodated

within a tetra-peptide recognition motif. Usually, they are classified into initiator caspases (caspases-1, -2, -4, -8, -9, -10 and -14) and effector caspases (caspase-3, -6 and-7) (Muzio *et al.*, 1998, Srinivasula *et al.*, 1998). Proteolytic cleavage of a set of vital substrates by effector caspases largely determines the features of apoptotic cell death (Zimmermann *et al.*, 2001).

Caspase-3, one of the chief effector caspases, plays an indispensable role in the execution of morphological and biochemical changes in apoptosis. In this connection, the level of procaspase-3 in cells before and after Leachianone A application was first examined. As reflected from the results, cleavage of the precursor of caspase-3 happened following the treatment of Leachianone A in a dose-dependent manner (Fig. 4.3.1.1A). Concurrently, a drop in the protein level of the pro-form of both its upstream initiator caspases, caspases-8 and -9, was also seen in the study (Fig. 4.3.1.1B & 4.3.1.1C). These implied that both of the extrinsic and intrinsic pathways were likely to participate in the activation of caspase-3.

With caspase-3 enzyme activated, the follow-up experiment was to explore if there were proteolytic cleavages of its specific downstream substrates, such

as inhibitor of caspase-activated DNase (ICAD) and poly-(ADP-ribose) polymerase (PARP). ICAD is involved to repress the DNase, which otherwise brings about large scale DNA fragmentation (Enari *et al.*, 1998). PARP, on the other hand, aids in protecting the DNA or repairing the damaged DNA (Soldani *et al.*, 2002). When both ICAD and PARP are cleaved, an apoptotic DNA fragmentation means to start. In our study, data from the Western blot analysis clearly illustrated that degradations of ICAD and PARP appeared in a fashion coinciding with the caspase-3 activation (Fig. 4.2.1.1E & 4.3.1.1F).

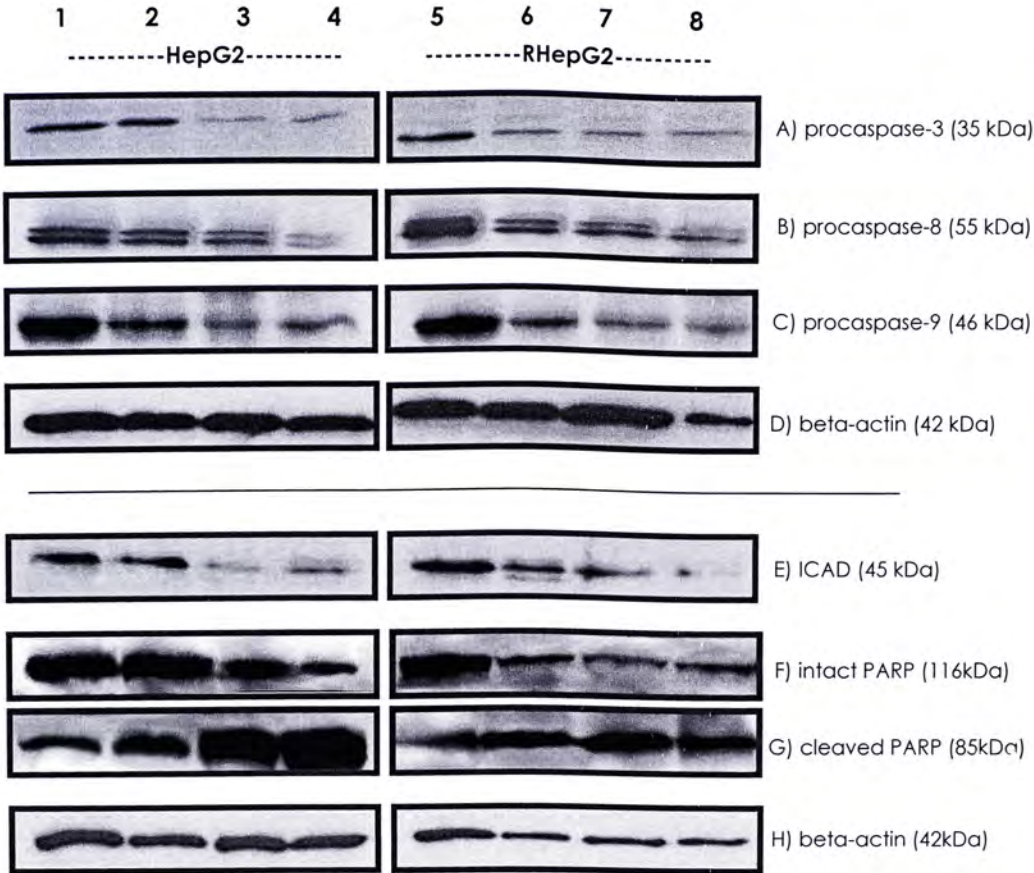


Fig. 4.3.1.1 Activation of caspases-3, 8 and 9 as well as induction of ICAD and PARP cleavages by Leachianone A in HepG2 and RHepG2 cells.

Cells (1×10^6) were incubated with vehicle only (lanes 1 & 5) and Leachianone A at concentrations of $10 \mu\text{g/ml}$ (lanes 2 & 6), $20 \mu\text{g/ml}$ (lanes 3 & 7) and $30 \mu\text{g/ml}$ (lanes 4 & 8) for 48 hours at 37°C , 5% CO_2 . (A) Probed with anti-procaspase-3 (35 kDa) antibody. (B) Probed with anti-procaspase-8 (55 kDa) antibody. (C) Probed with anti-procaspase-9 (46 kDa) antibody. (D) Probed with anti-beta-actin (42 kDa) antibody as loading control. (E) Probed with anti-ICAD (45 kDa) antibody. (F & G) Probed with anti-PARP (116 kDa as intact form and 85kDa as cleaved form) antibody. (H) Probed with anti-beta-actin (42 kDa) antibody as loading control. Data are from a representative of 4 separate experiments.

To further verify the existence of a functionally active caspase-3 in cells, another test was performed in parallel to determine the caspase-3 enzymatic activity. In the course of apoptosis, the activated caspase-3 is recognized and labeled with carboxyfluorescein (FAM)-labeled peptide fluoromethyl ketone (FMK) caspase inhibitors (FAM-peptide-FMK). The peptide sequence aspartate-glutamate-valine-glutamate (DEVD) used in the experiment is specially designed for its tight binding with the activated caspase-3, so that the cells with enhanced fluorescence signals are readily figured out.

Concordant with our findings in the Western blot study (Fig. 4.3.1.1), cells incubated with elevated concentrations of Leachianone A displayed a discernibly greater extent of caspase-3 activation, as compared to the control (Fig. 4.3.1.2 & 4.3.1.3).

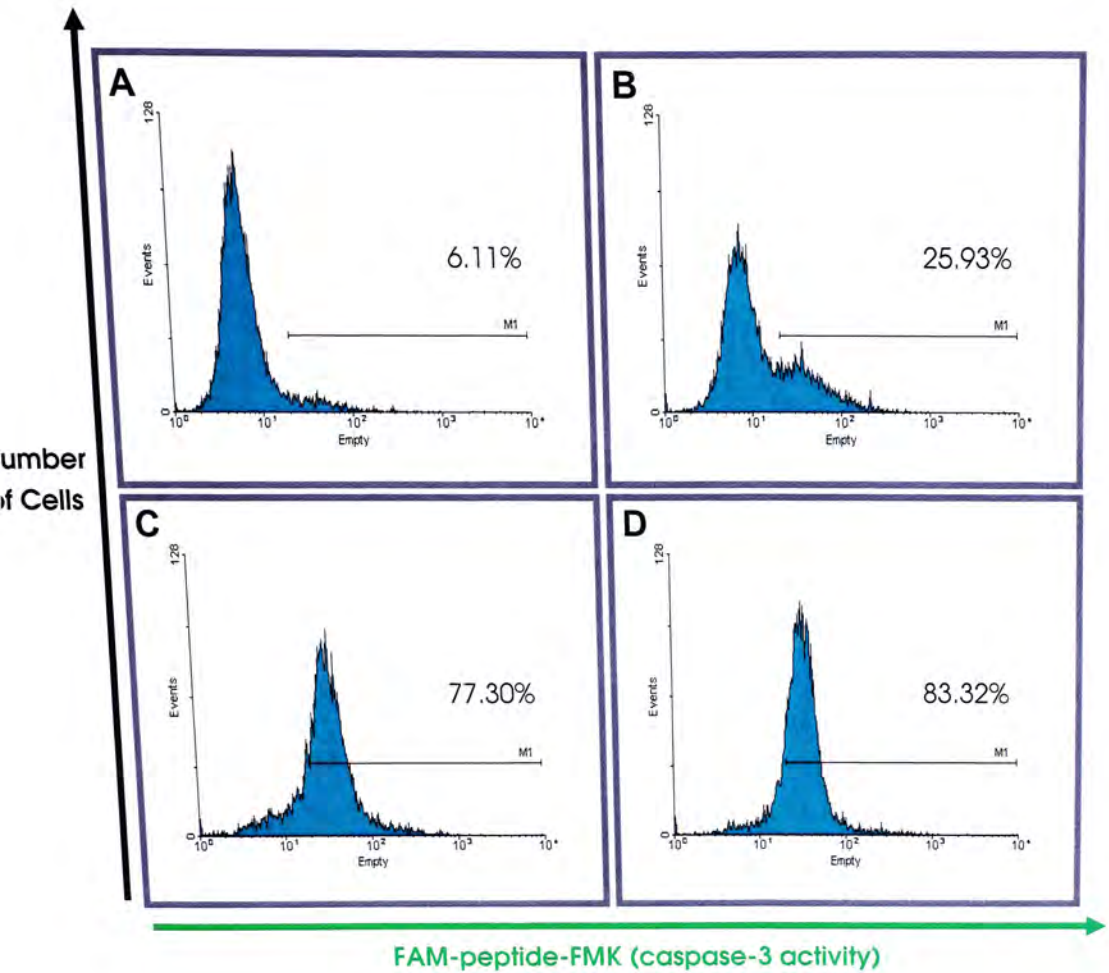


Fig. 4.3.1.2 Study of the enhancement of caspase-3 activity in Leachianone A-treated HepG2 cells.

HepG2 cells (1×10^6) were exposed to vehicle only (A) and Leachianone A at concentrations of $10 \mu\text{g/ml}$ (B), $20 \mu\text{g/ml}$ (C) and $30 \mu\text{g/ml}$ (D) for 48 hours at 37°C , 5% CO_2 . Cells with activated caspase-3 bound to the FAM-peptide-FMK inhibitor were detected using flow cytometry. Marker M1 corresponded to the cell fraction with enhanced caspase-3 activity. Results are representative of 4 independent experiments.

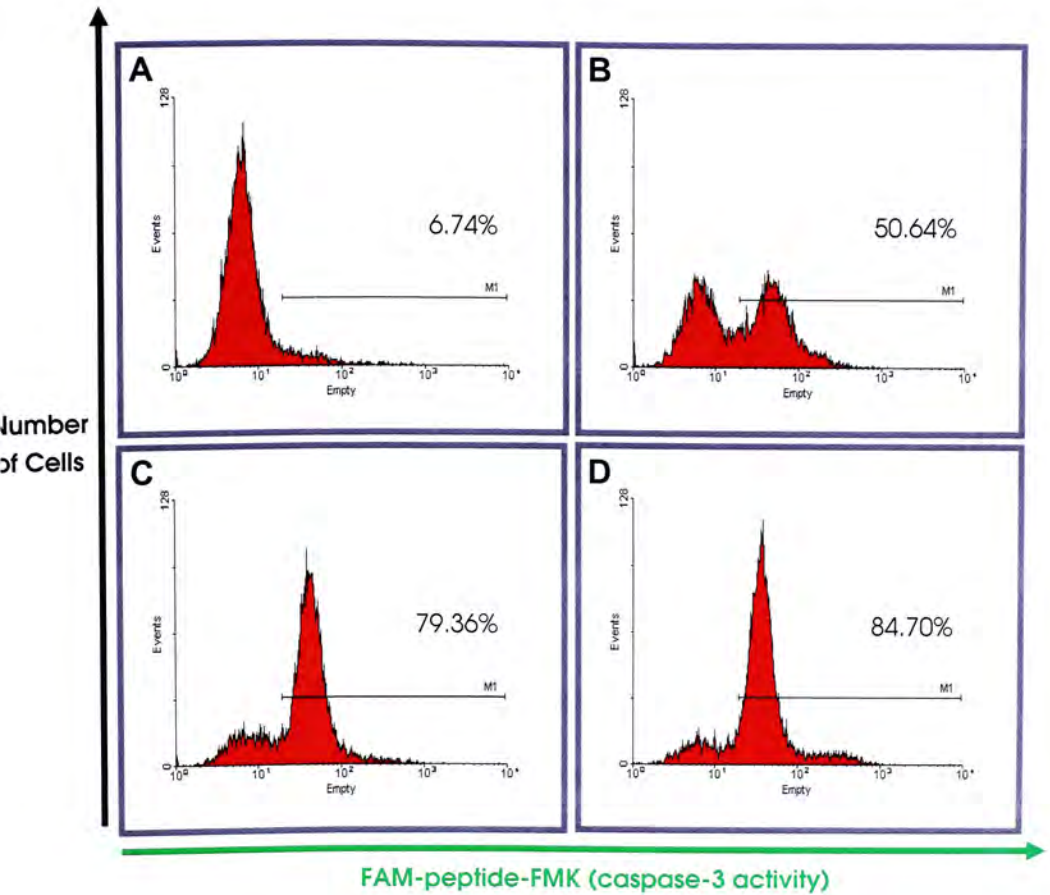


Fig. 4.2.1.3 Study of the enhancement of caspase-3 activity in Leachianone A-treated RHePG2 cells.

RHePG2 cells (1×10^6) were exposed to vehicle only (A) and Leachianone A at concentrations of 10 $\mu\text{g/ml}$ (B), 20 $\mu\text{g/ml}$ (C) and 30 $\mu\text{g/ml}$ (D) for 48 hours at 37°C, 5% CO₂. Cells with activated caspase-3 bound to the FAM-peptide-FMK inhibitor were detected using flow cytometry. Marker M1 corresponded to the cell fraction with enhanced caspase-3 activity. Results are representative of 4 independent experiments.

4.3.2 Altered Expressions of Bcl-2 Family Proteins

Apart from caspases, Bcl-2 family proteins are the essential players to promote or intervene the apoptotic process as well (Jurgensmeier *et al.*, 1998). Bcl-2 family is chiefly consisted of pro-apoptotic factors, like Bad, Bak, Bax, Bcl-Xs, Bik, Bim, Bok, Krk and Mtd; as well as anti-apoptotic factors: A1, Bcl-2, Bcl-XL, Bcl-W and Mcl-1 (Wang *et al.*, 2001). In response to different signals, these proteins interact with each other to form homo-dimers or hetero-dimers, which finally decide the fate of the cells.

Accordingly, the protein expression patterns of certain Bcl-2 family members were evaluated. Results revealed that the expression level of the pro-apoptotic protein, Bid, steadily dwindled as the dosage of Leachianone A raised (Fig. 4.3.2.1A). This was attributed to the processing of Bid into a truncated form, tBid. Down-regulations of anti-apoptotic proteins, for instance Bcl-2 and Bcl-XL; along with an up-regulation of the pro-apoptotic protein, Bad, were also detected in this apoptotic incident (Fig. 4.3.2.1C, 4.3.2.1D, 4.3.2.1F). Notwithstanding, the protein expression of Bax remained almost unchanged (Fig. 4.3.2.1G). Taken together, the net effect herein was to propagate the downstream caspase cascade; and dispose the cells to

apoptosis.

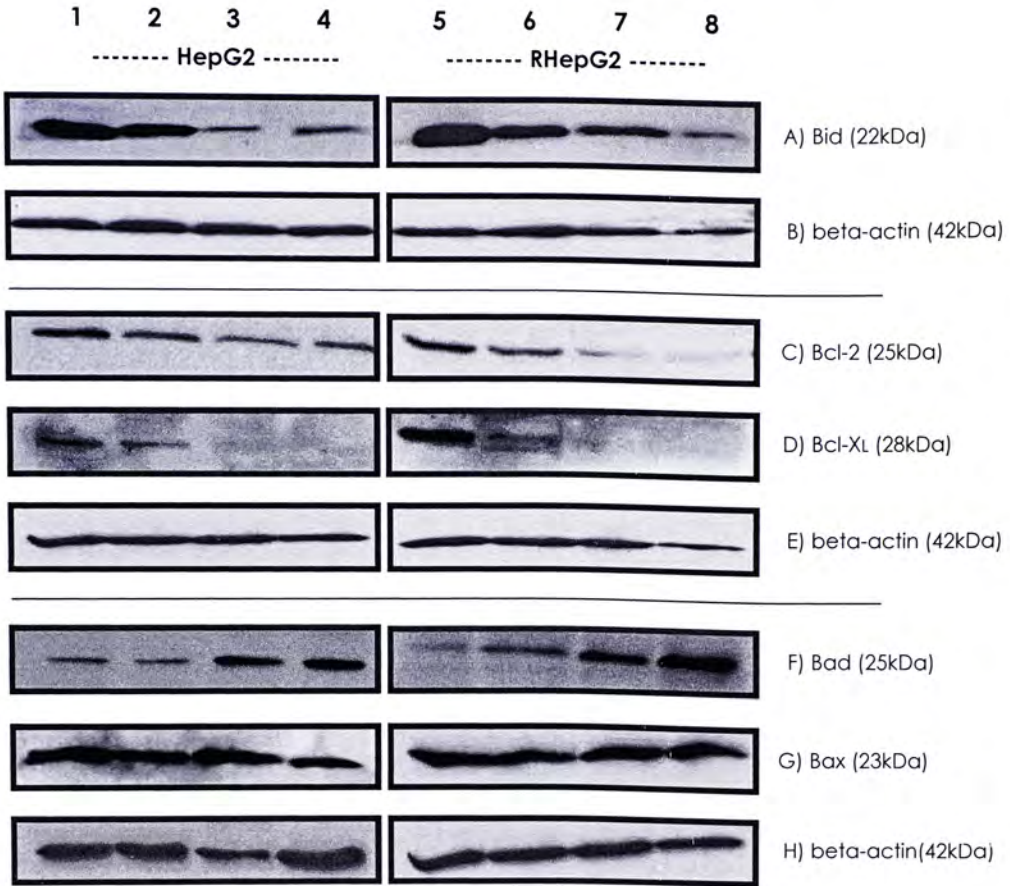


Fig. 4.3.2.1 Alteration of Expression Levels of Bcl-2 family proteins by Leachianone A in HepG2 and RHepG2 cells.

Cells (1×10^6) were incubated with vehicle only (lanes 1 & 5) and Leachianone A at concentrations of $10 \mu\text{g/ml}$ (lanes 2 & 6), $20 \mu\text{g/ml}$ (lanes 3 & 7) and $30 \mu\text{g/ml}$ (lanes 4 & 8) for 48 hours at 37°C , 5% CO_2 . (A) Probed with anti-bid (22 kDa) antibody. (B) Probed with anti-beta-actin (42 kDa) antibody as loading control. (C) Probed with anti-bcl-2 (25 kDa) antibody. (D) Probed with anti-bcl-XL (28 kDa) antibody. (E) Probed with anti-beta-actin (42 kDa) antibody as loading control. (F) Probed with anti-bad (25 kDa) antibody. (G) Probed with anti-bax (23 kDa) antibody. (H) Probed with anti-beta-actin (42 kDa) antibody as loading control. Data are from a representative of 3 separate experiments.

4.3.3 Loss of Mitochondrial Membrane Potential

So far, there are several death signaling pathways reported, including the extrinsic (death receptor-mediated) pathway; and the intrinsic (mitochondrial) pathway. They act in diverse routes; and recruit different molecules to move forward. Yet, they are capable of influencing each other through the Bcl-2 family member, known as Bid. Briefly, caspase-8 cleaves the Bid to produce truncated Bid, which in turn, in co-operation with Bad, facilitates the release of cyt c from mitochondria, thereby causing the caspase adaptor protein Apaf-1 to activate caspase-9. Such kind of inter-connection allows amplification of signals in cells (Kaufmann *et al.*, 2000).

Over the decades, accumulated evidence showed that mitochondria were pivotal in controlling cell life (Grutter *et al.*, 2000). Early initiation of apoptosis is accompanied by the disruption of the mitochondrial membrane integrity, leading to a rapid collapse in the electrochemical gradient (Ly *et al.*, 2003). This prompted us to study the effect of Leachianone A on the mitochondrial trans-membrane potential ($\Delta\Psi_m$) using a mitochondria-specific cationic dye

JC-1. Provided a high $\Delta \Psi_m$ in normal cells, JC-1 predominantly accumulates as J-aggregates in the mitochondria, emitting a red fluorescence. With a declined $\Delta \Psi_m$ in apoptotic cells, however, JC-1 switches to its monomeric form; and stains a green colour.

From the flow cytometric analysis, a remarkable attenuation of $\Delta \Psi_m$ was resulted in cells challenged with Leachianone A; whereas that in untreated cells was well maintained. In fact, presence of increasing concentrations of Leachianone A herein made more and more cells susceptible to mitochondrial membrane depolarization (Fig. 4.3.3.1 & 4.3.3.2).

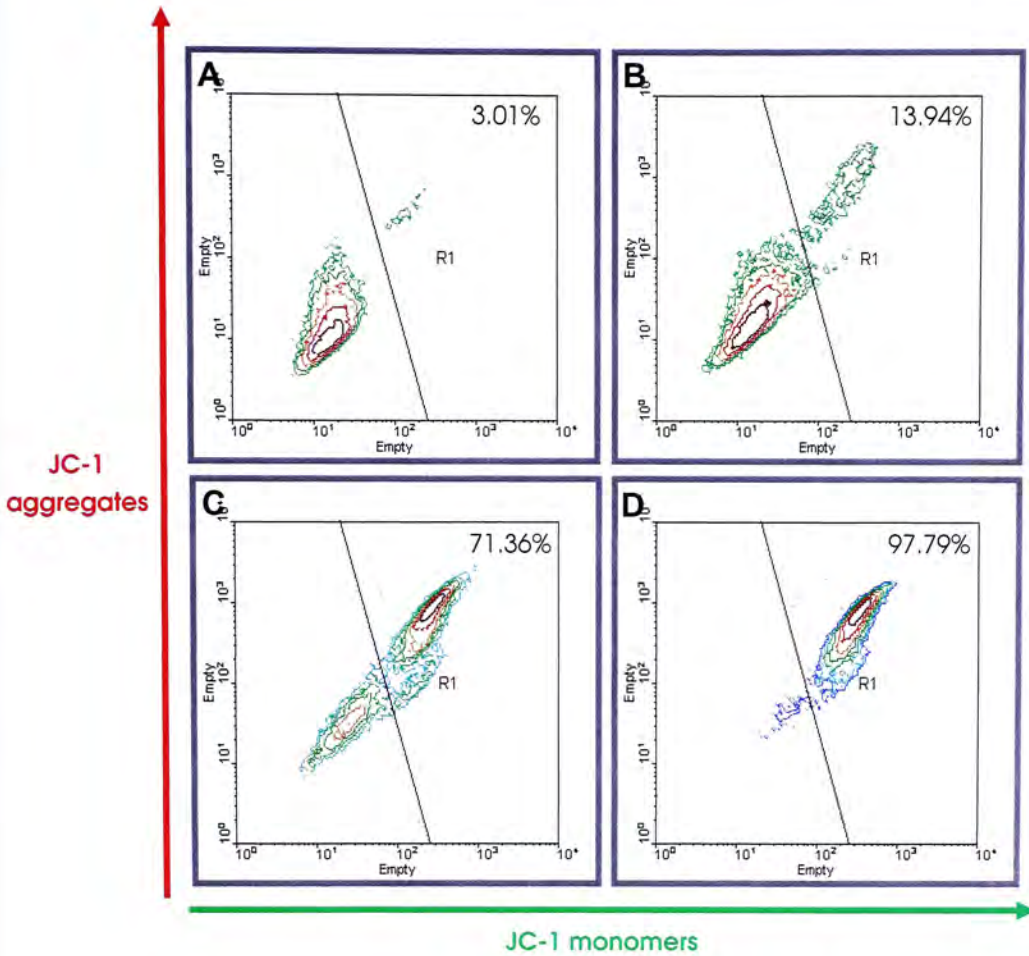


Fig. 4.3.3.1 Study of the loss of mitochondrial membrane potential in Leachianone A-treated HepG2 cells.

HepG2 cells (3×10^5) were exposed to vehicle only (A) and Leachianone A at concentrations of $10 \mu\text{g/ml}$ (B), $20 \mu\text{g/ml}$ (C) and $30 \mu\text{g/ml}$ (D) for 48 hours at 37°C , 5% CO_2 . Cells obtained were incubated with JC-1 dye for staining. Flow cytometry was next used to measure the fluorescence emitted. Region R1 corresponded to the cell fraction with depolarized mitochondrial membrane potential. Results are representative of 5 independent experiments.

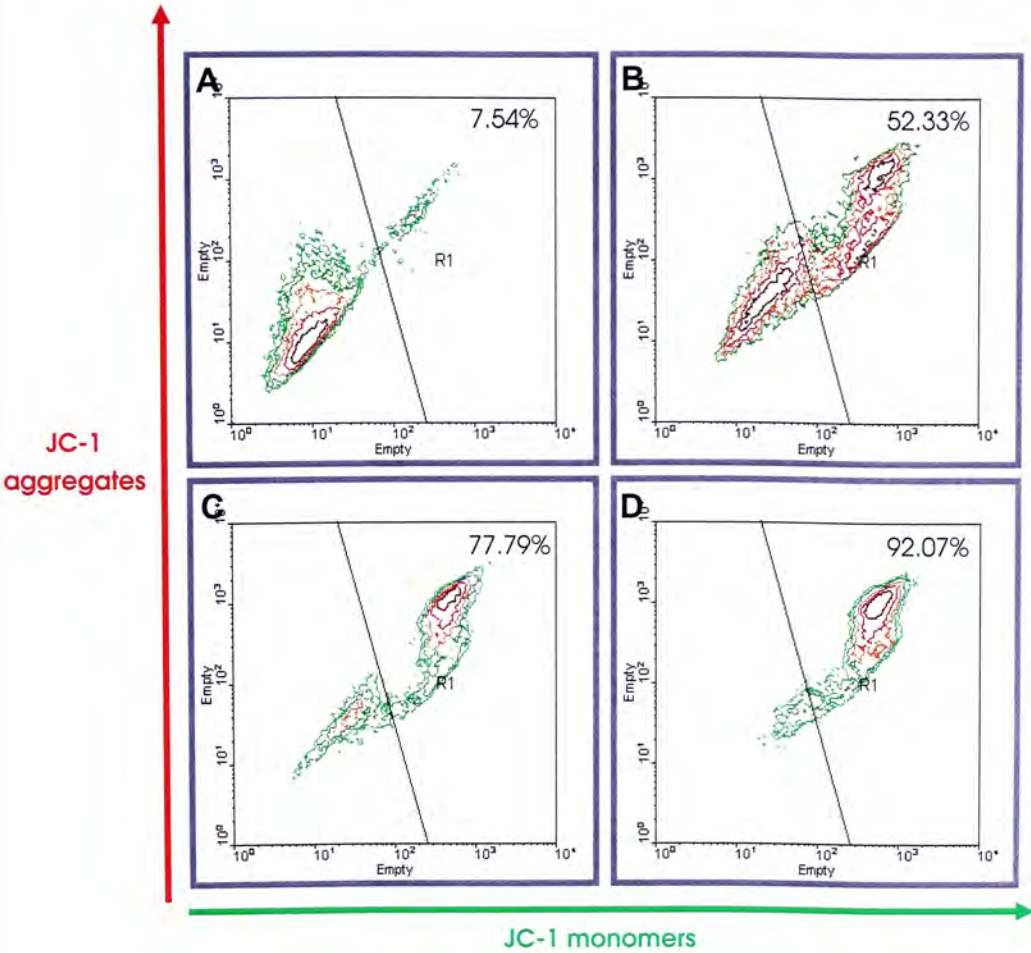


Fig. 4.3.3.2 Study of the loss of mitochondrial membrane potential in Leachianone A-treated RHEpG2 cells.

RHEpG2 cells (3×10^5) were exposed to vehicle only (A) and Leachianone A at concentrations of 10 $\mu\text{g/ml}$ (B), 20 $\mu\text{g/ml}$ (C) and 30 $\mu\text{g/ml}$ (D) for 48 hours at 37°C, 5% CO₂. Cells obtained were incubated with JC-1 dye for staining. Flow cytometry was next used to measure the fluorescence emitted. Region R1 corresponded to the cell fraction with depolarized mitochondrial membrane potential. Results are representative of 5 independent experiments.

In line with the loss of $\Delta\Psi_m$, efflux of some mitochondrial inter-membrane space proteins, like cyt c, apoptosis-inducing factor (AIF), Smac/ DIABLO, Omi/ HtrA2 and endonuclease G (endo G), is also regarded as a key regulatory procedure in the mitochondria-dependent apoptosis (Verhagen *et al.*, 2000). Once released into the cytosol, these apoptogenic proteins assisted to trigger off cellular catabolic destruction (Loeffler *et al.*, 2001).

In light of this, the status of these proteins present in mitochondria and cytosol in each cell panel was checked. It was obvious that incubation of cells with Leachianone A caused a dose-dependent decrease in the mitochondrial cyt c and AIF amounts, with a concomitant increase in the corresponding cytosolic fraction (Fig. 4.3.3.3 A – 4.3.3.3 D).

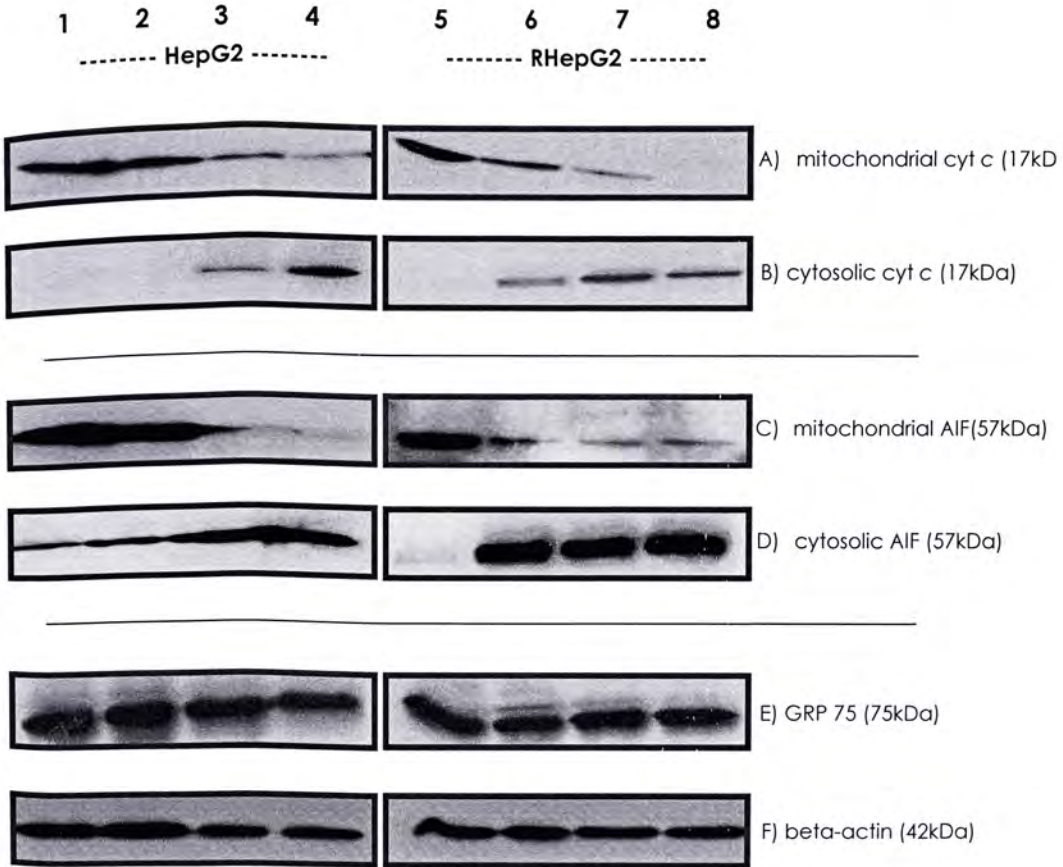


Fig. 4.3.3.3 Release of cytochrome c (cyt c) and apoptosis-inducing factor (AIF) from mitochondria to cytosol in Leachianone A-treated HepG2 and RHepG2 cells.

Cells (1×10^6) were incubated with vehicle only (lanes 1 & 5) and Leachianone A at concentrations of 10 $\mu\text{g}/\text{ml}$ (lanes 2 & 6), 20 $\mu\text{g}/\text{ml}$ (lanes 3 & 7) and 30 $\mu\text{g}/\text{ml}$ (lanes 4 & 8) for 48 hours at 37°C, 5% CO_2 . (A, B) Probed with anti-cytochrome c (17 kDa) antibody. (C, D) Probed with anti-AIF (57 kDa) antibody. (E) Probed with anti-GRP 75 (75 kDa) antibody as loading control for mitochondrial fraction. (F) Probed with anti-beta-actin (42 kDa) antibody as loading control for cytosolic fraction. Data are from a representative of 4 separate experiments.

4.4 *in vivo* Tumor Growth Inhibition in HepG2-bearing Nude Mice

In order to appraise if Leachianone A also reserves the ability to suppress or inhibit tumor growth *in vivo*, a nude mice animal model subcutaneously inoculated with HepG2 cells was employed. Following one month of drug administration, the tumor size was significantly diminished by 17% - 54% in Leachianone A-treated groups of nude mice, when compared to those solely given the vehicle (Fig. 4.4.1). And, the size diminution was just inversely proportional to the dosage of Leachianone A injected, a trend being consistent with the *in vitro* bioassays. Moreover, the plasma activities of the enzymes specific for heart and liver, namely creatine kinase (CK), lactate dehydrogenase (LDH), alanine transaminase (ALT) and aspartate transaminase (AST), in those Leachianone A-treated mice remained at normal levels, suggesting that the use of this compound did not produce any apparent toxicity to the hosts (Fig. 4.4.2). A slight increment in the plasma total LDH activity obtained in control group was possibly an artifact due to the *in vitro* haemolysis during preparation; or otherwise an outcome of the spread of the solid tumor. In such an assumption, calculation of the activity of a certain isoform of the enzyme (that is, LDH-1/ 4H of higher relevance to the heart) was required, so as to have a more precise comment on the effect

of the drug.

Tumor Size (mm³) of Nude Mice Inoculated with HepG2 Cells After 30-Day of Leachianone A Treatment

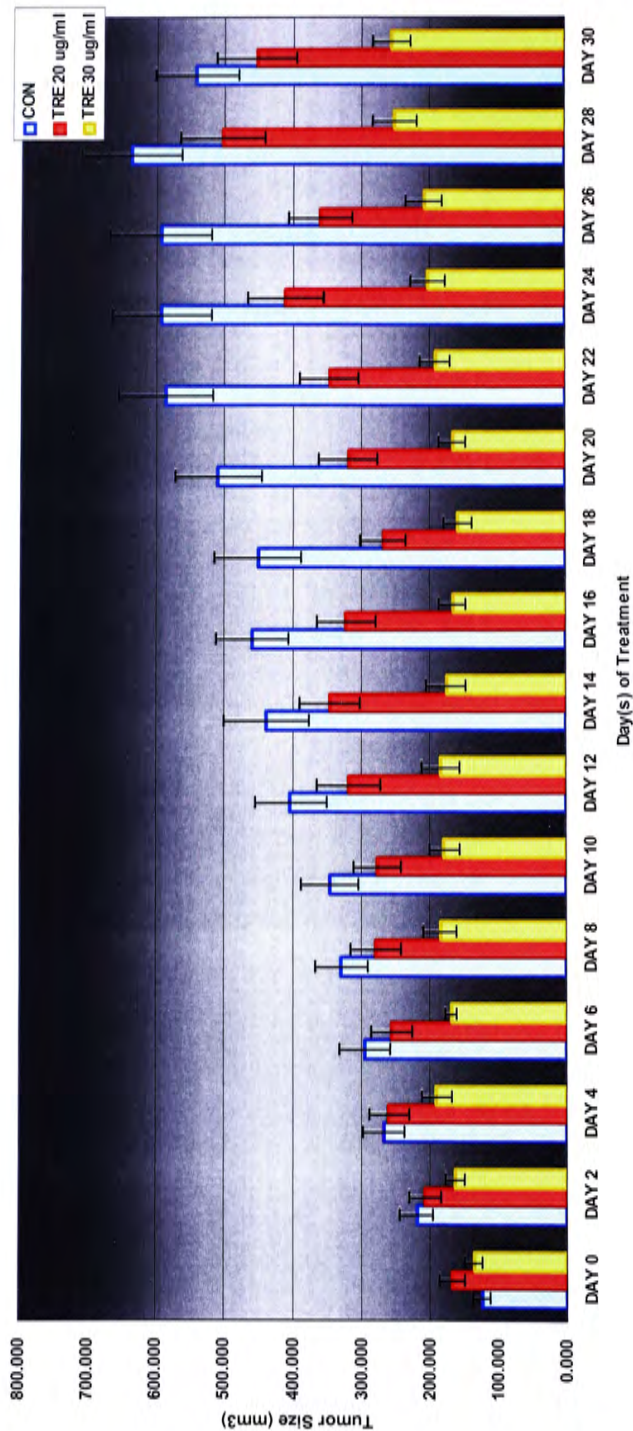


Fig. 4.4.1 Effect of 30-day intra-venous administration of Leachianone A on the size of tumors of HepG2-bearing nude mice.

Nude mice in group of 8 were subcutaneously inoculated with HepG2 cells (1×10^7). After solid tumor formation, nude mice were intra-venously injected with either vehicle or Leachianone A at doses of 20mg/kg/day and 30mg/kg/day on alternate days for 1 month. In the end of experiment, all the animals were sacrificed; and the tumors were dissected and measured. Values are mean \pm SD of 8 determinations.

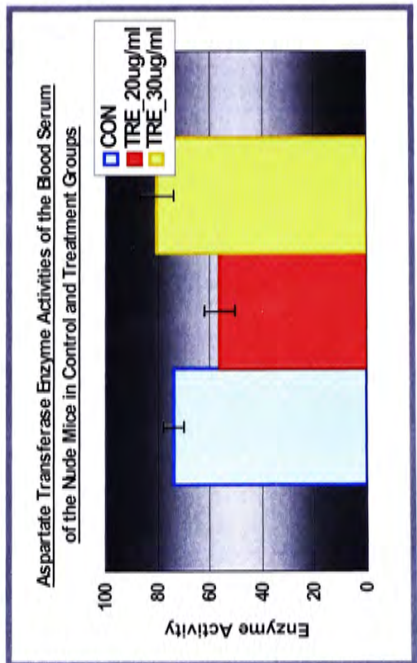
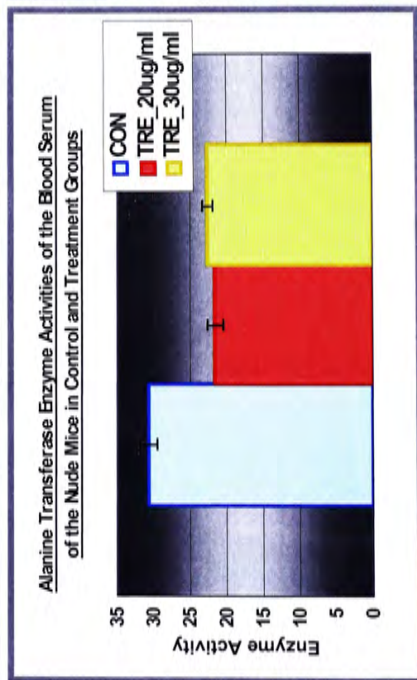
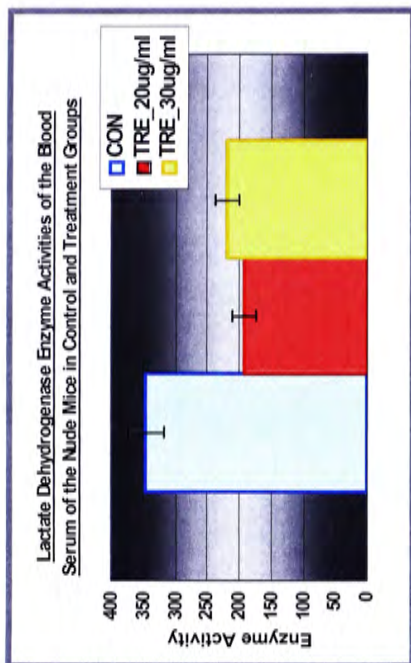
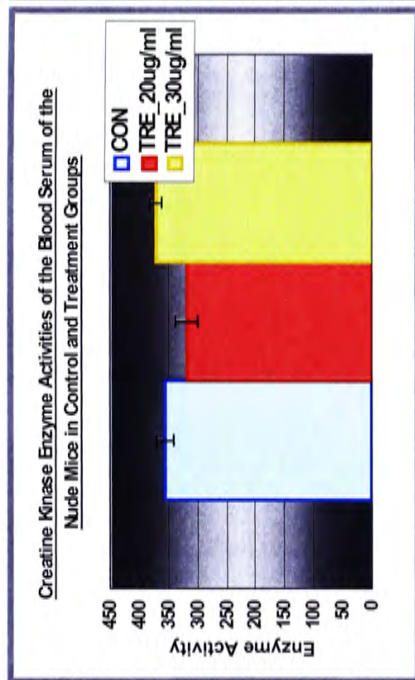


Fig. 4.4.2 Evaluation of the toxicity of Leachianone A on heart and liver of the hosts.

Nude mice were intra-venously injected with either vehicle or Leachianone A at doses of 20mg/kg/day and 30mg/kg/day on alternate days for 1 month. Following treatment, all the animals were sacrificed; and their plasma were collected. Plasma levels of heart specific enzymes creatine kinase (CK) as well as lactate dehydrogenase (LDH); and liver specific enzymes alanine transaminase (ALT) and aspartate transaminase (AST) were measured. Values are mean \pm SD of 8 determinations.

4.5 Conclusion

As a whole, we expounded that Leachianone A treatment was not coupled with any cell cycle arrest in hepatoma cells, HepG2 and RHepG2. Instead, it mediated the activation of apoptotic programme (through both extrinsic and intrinsic pathways) in cells, ascertained by the manifest changes in all the molecular markers analyzed (Fig. 4.1.2 & 4.1.3, 4.2.1.2 & 4.2.1.3, 4.2.2.1.1 & 4.2.2.1.2, 4.2.2.2.1, 4.3.1.1 – 4.3.1.3, 4.3.2.1, 4.3.3.1 – 4.3.3.3, 4.4.1 & 4.4.2).

In many aspects, the killing efficiency of Leachianone A in RHepG2 cells happened to preponderate over that in HepG2 cells. It was substantiated by the vaster population of cells found in the sub-G1 peak and in the annexin V-positive quadrants (inclusive of early and late apoptotic cells), advanced DNA fragmentation and presence of more cells containing active caspase-3 enzyme, etc in RHepG2 cells in comparison to HepG2 cells, as the same concentration of Leachianone A was added. The figures from the *in vitro* apoptotic assays were summarized in the Table 4.1.

CELL CYCLE ANALYSIS

HepG2 cells	sub-G1	G0/G1	G2/M	S	RHepG2 cells	sub-G1	G0/G1	G2/M	S
0	3.03%	73.50%	3.86%	19.57%	0	6.44%	62.06%	7.63%	24.40%
10	6.10%	69.18%	2.85%	21.91%	10	11.51%	60.05%	7.57%	21.40%
20	24.17%	55.52%	4.38%	15.98%	20	20.13%	54.57%	5.22%	20.54%
30	35.37%	47.58%	4.44%	12.67%	30	53.36%	29.77%	4.40%	13.06%

ANNEXIN V/ PI STAINING EXPERIMENT

HepG2 cells	normal	early apoptosis	late apoptosis/ necrosis	others	RHepG2 cells	normal	early apoptosis	late apoptosis/ necrosis	others
0	94.7%	2.0%	0.9%	2.4%	0	89.6%	5.5%	4.4%	0.5%
10	78.5%	6.8%	14.3%	0.4%	10	42.3%	15.6%	40.0%	2.1%
20	37.6%	21.6%	38.8%	2.0%	20	34.2%	14.9%	50.2%	0.8%
30	41.1%	15.1%	40.3%	3.5%	30	37.0%	13.3%	48.9%	0.8%

TUNEL ASSAY

HepG2 cells	normal	with DNA breaks	RHepG2 cells	normal	with DNA breaks
0	96.58%	3.42%	0	91.66%	8.34%
10	74.07%	25.93%	10	43.63%	56.37%
20	26.71%	73.29%	20	18.85%	81.15%
30	16.68%	83.32%	30	5.00%	95.00%

DNA FRAGMENTATION REACTION

HepG2 cells	DNA laddering pattern	RHePG2 cells	DNA laddering pattern
0	no	0	no
10	no	10	yes
20	yes	20	yes
30	yes	30	yes

WESTERN BLOT STUDY – CASPASES AND ICAD/ PARP

HepG2 cells	procaspases-3, -8, -9 cleavages	RHePG2 cells	procaspases-3, -8, -9 cleavages
0	no	0	no
10	no	10	yes
20	yes	20	yes
30	yes	30	yes
HepG2 cells	ICAD/ PARP cleavages	RHePG2 cells	ICAD/ PARP cleavages
0	no	0	no
10	no	10	yes
20	yes	20	yes
30	yes	30	yes

CASPASE-3 ACTIVITY DETERMINATION

HepG2 cells	normal	with enhanced	RHePG2 cells	normal	with enhanced
	normal	with enhanced	RHePG2 cells	normal	with enhanced

	caspase-3 activity			caspase-3 activity		
0	93.89%	6.11%	0	93.26%	6.74%	
10	74.07%	25.93%	10	49.36%	50.64%	
20	22.70%	77.30%	20	20.64%	79.36%	
30	16.68%	83.32%	30	15.3%	84.70%	

WESTERN BLOT STUDY – Bcl-2 FAMILY PROTEINS

HepG2 cells	Bid	Bcl-2	Bcl-XL	Bad	Bax	RHepG2 cells	Bid	Bcl-2	Bcl-XL	Bad	Bax
0	---	---	---	---	---	0	---	---	---	---	---
10	unchanged	unchanged	unchanged	unchanged	unchanged	10	decreased	decreased	decreased	increased	unchanged
20	decreased	decreased	decreased	increased	unchanged	20	decreased	decreased	decreased	increased	unchanged
30	decreased	decreased	decreased	increased	unchanged	30	decreased	decreased	decreased	increased	unchanged

MITOCHONDRIAL MEMBRANE DEPOLARIZATION DETERMINATION

HepG2 cells	normal	with depolarization	RHepG2 cells	normal	with depolarization
0	96.99%	3.01%	0	92.46%	7.54%
10	86.06%	13.94%	10	47.67%	52.33%
20	28.64%	71.36%	20	22.21%	77.79%
30	2.21%	97.79%	30	7.93%	92.07%

WESTERN BLOT STUDY – cyt c AND AIF

HepG2 cells	mitochondrial fraction	cytosolic fraction	RHepG2 cells	mitochondrial fraction	cytosolic fraction

0	---	---	0	---	---
10	unchanged	unchanged	10	decreased	increased
20	decreased	increased	20	decreased	increased
30	decreased	increased	30	decreased	increased

Table 4.1 A summary of the results from the apoptotic bioassays for Leachianone A in HepG2 and RHepG2 cells.

Up till now, the exact reasons for this peculiar phenomenon are not fully understood. We speculate that it has something to do with the drug entry and targeting into and inside the cells. In recent publications, it was mentioned that P-glycoprotein (Pgp) over-expression in clinical cancers simply did not impede the cytotoxicity of flavonoids from *Sophora flavescens*, including Leachianone A (Maia *et al.*, 1998, Choi *et al.*, 1999). Besides, expanding evidence in support of the involvement of lysosome in apoptosis arised lately (Ferri *et al.*, 2001, Bivik *et al.*, 2006, Skommer *et al.*, 2006). It is possible that Leachianone A hastens the lysosomal rupture (LMP) to leak out the digestive enzymes in RHepG2 cells; and helps accelerate the process. Another ground to account for this situation lies on the altered property of mitochondria in RHepG2 cells. Perhaps, Leachianone A modulates the fluidity of biological membranes, which subsequently favors the response of mitochondrial permeability transition (MPT) (Lluis *et al.*, 2003, Colell *et al.*, 2004). In this way, the intrinsic pathway is activated to head towards apoptosis.

CHAPTER 5

RESULTS and DISCUSSION --

MECHANISTIC STUDY OF SOPHORAFLAVONE J-INDUCED CELL DEATH IN HEPATOMA CELLS HepG2

5.1 Execution of Cellular Apoptosis

In the last chapter, we discussed about the assorted bioassays representative of apoptosis. Herein, we followed a similar approach to solve out the effect of Sophoraflavone J on HepG2 cells. (Work on RHepG2 cells was sacrificed owing to the limited availability of Sophoraflavone J.) It was discovered that Sophoraflavone J did not stimulate cell cycle arrest in HepG2 cells (Fig. 5.1.1). But rather, it tipped off an apoptotic cell death, as manifested by PS translocation onto the cell membrane surface and inter-nucleosomal DNA degradation (Fig. 5.1.2 – 5.1.4).

number of cells

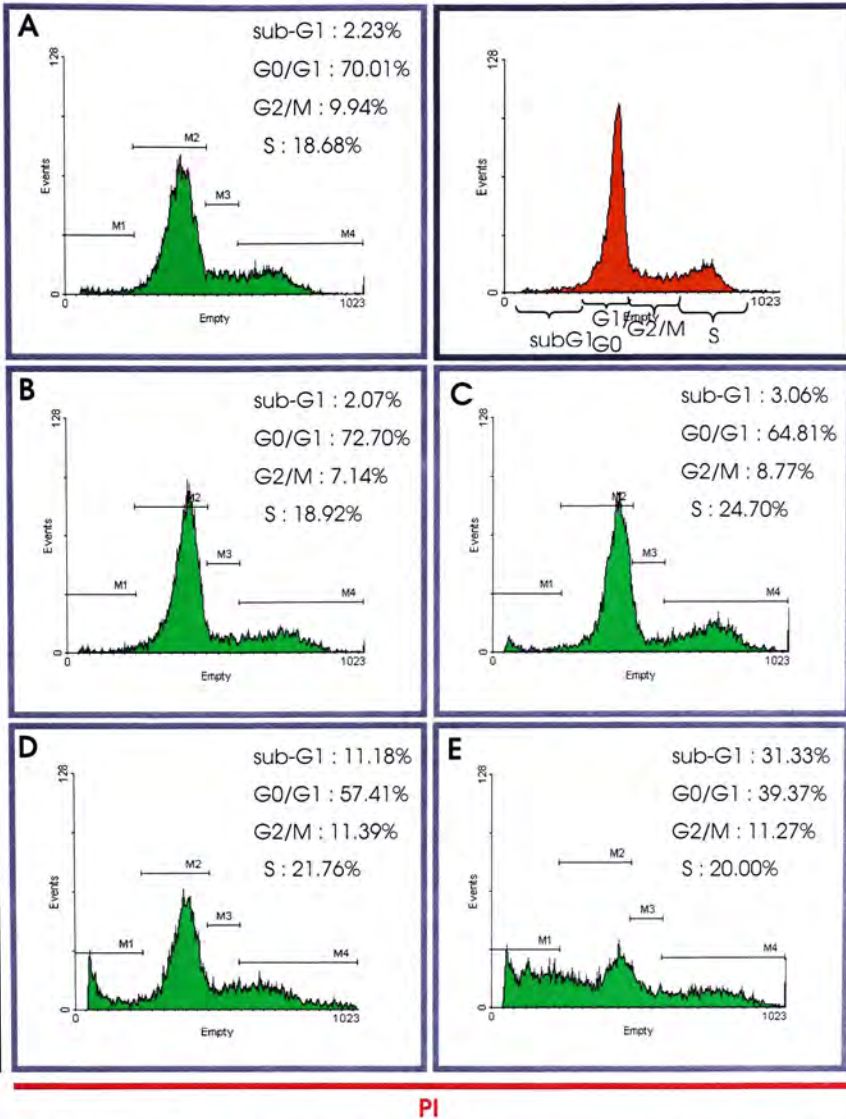


Fig. 5.1.1 Cell cycle analysis of HepG2 cells treated with vehicle or Sophoraflavone J for 48 hours.

Cells (3×10^5) were exposed to vehicle only (A) and Sophoraflavone J at concentrations of 5 $\mu\text{g/ml}$ (B), 10 $\mu\text{g/ml}$ (C), 15 $\mu\text{g/ml}$ (D) and 20 $\mu\text{g/ml}$ (E) for 48 hours at 37°C, 5% CO₂. Cells harvested were stained with PI and subjected to flow cytometric analysis. Markers M1, M2, M3 and M4 corresponded to the cell fractions at sub-G1, G0/ G1, G2/ M and S phases, respectively. Results are representative of 5 independent experiments.

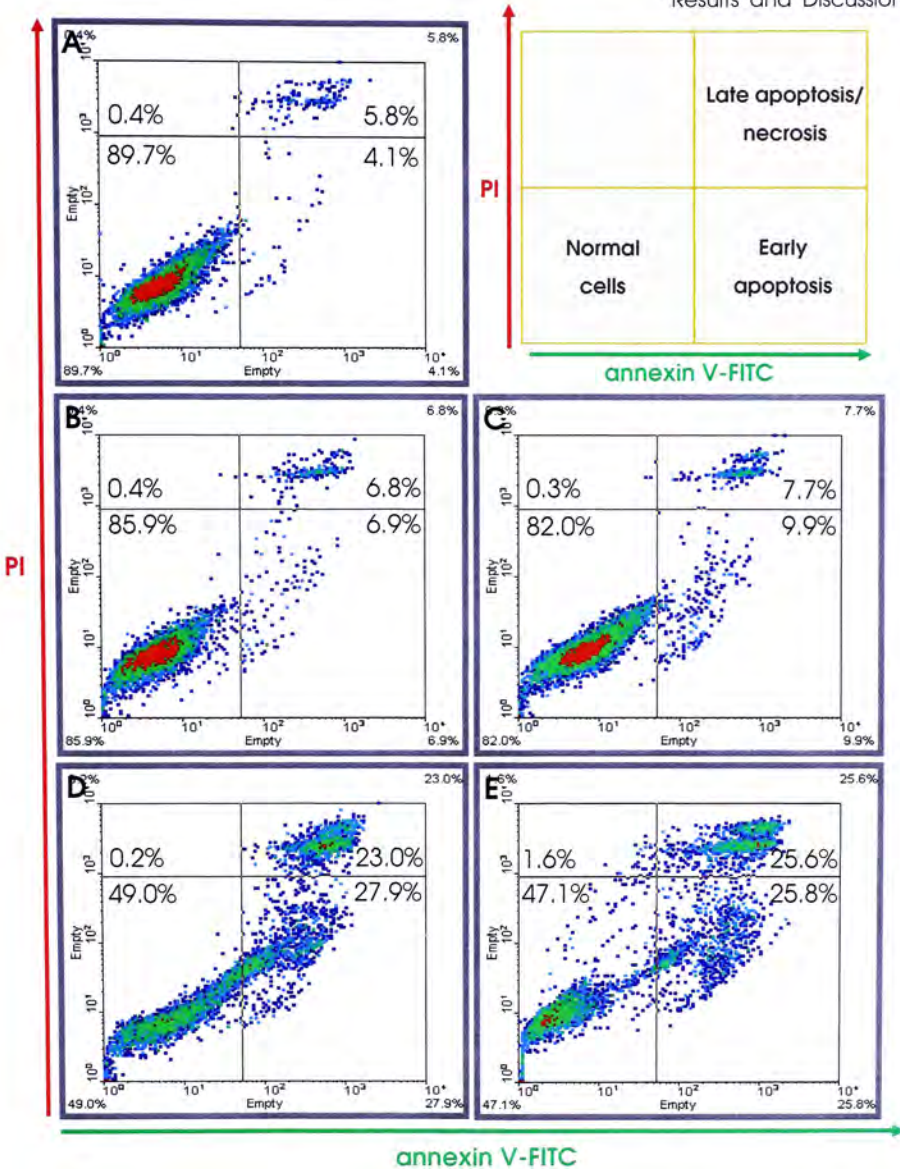


Fig. 5.1.2 Annexin V-FITC / PI staining of HepG2 cells treated with vehicle or Sophoraflavone J for 48 hours.

Cells (3×10^5) were exposed to vehicle only (A) and Sophoraflavone J at concentrations of 5 $\mu\text{g/ml}$ (B), 10 $\mu\text{g/ml}$ (C), 15 $\mu\text{g/ml}$ (D) and 20 $\mu\text{g/ml}$ (E) for 48 hours at 37°C, 5% CO₂. Cells collected were passed to annexin V-FITC and PI staining, followed by flow cytometric analysis. Results are representative of 5 independent experiments.

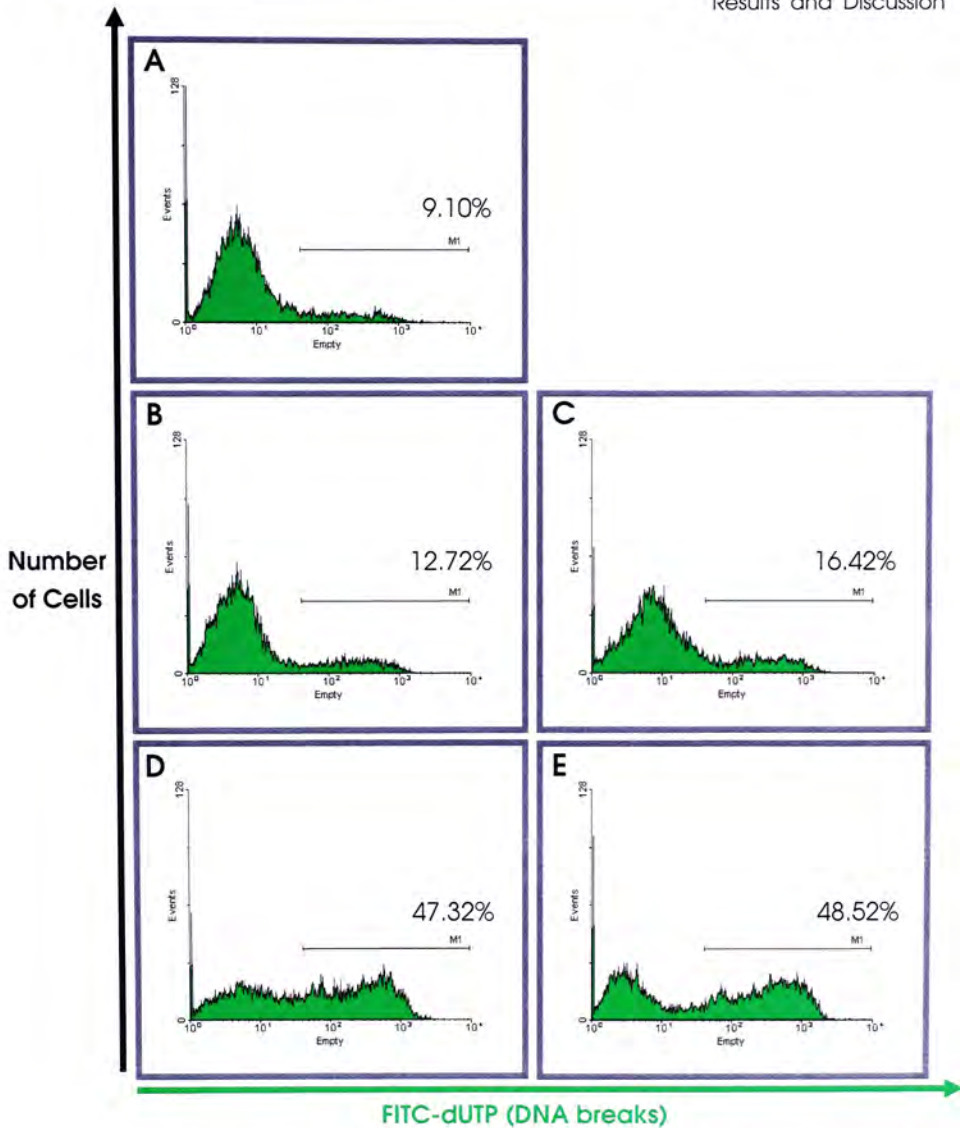


Fig. 5.1.3 TUNEL assay of HepG2 cells treated with vehicle or Sophoraflavone J for 48 hours.

Cells (1×10^6) were exposed to vehicle only (A) and Sophoraflavone J at concentrations of 5 $\mu\text{g/ml}$ (B), 10 $\mu\text{g/ml}$ (C), 15 $\mu\text{g/ml}$ (D) and 20 $\mu\text{g/ml}$ (E) for 48 hours at 37°C, 5% CO₂. Numbers of cells with DNA breaks were determined by flow cytometry. Marker M1 corresponded to the cell fraction with DNA breaks labeled with FITC-dUTP nucleotides. Results are representative of 4 independent experiments.

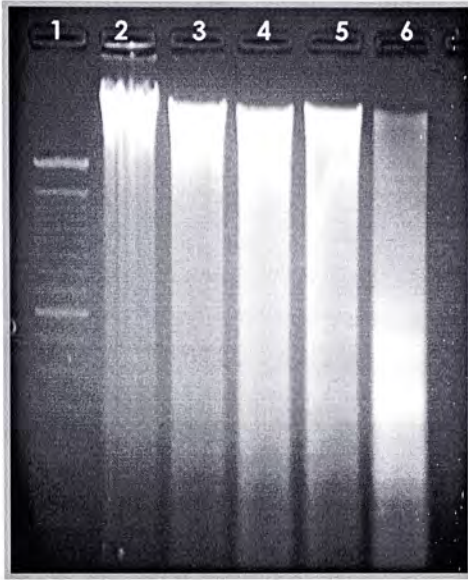


Fig. 5.1.4 Induction of DNA fragmentation in Sophoraflavone J-treated HepG2 cells.

Cells (1×10^6) were incubated with vehicle only (lane 2) and Sophoraflavone J at concentrations of 5 $\mu\text{g/ml}$ (lane 3), 10 $\mu\text{g/ml}$ (lane 4), 15 $\mu\text{g/ml}$ (lane 5) and 20 $\mu\text{g/ml}$ (lane 6) for 48 hours at 37°C, 5% CO₂. DNA laddering pattern was observed by 2% agarose gel electrophoresis. 100bp DNA marker (lane 1) was positioned aside for size indication. Results are representative of 4 independent experiments.

5.2 Involvement of Multiple Signaling Pathways in Sophoraflavone

J-induced Apoptosis

In the course of apoptosis, we noticed that cleavages of pro-caspases-8 and -9 came up in Sophoraflavone J-treated cells at concentrations of 15 $\mu\text{g/ml}$ or higher (Fig. 5.2.1B & 5.2.1C). Consequently, they brought about the proteolytic processing of caspase-3 zymogens into active enzymes (Fig. 5.2.1A). The activity of activated caspase-3 was seen with the cleavages of downstream substrates, ICAD and PARP, in Western blotting and the enhanced fluorescence signal in enzymatic activity assay (Fig. 5.2.1 E & 5.2.1F, 5.2.2).

For the expression patterns of Bcl-2 protein family members, there was a dose-dependent lessening in the level of Bid upon exposure to Sophoraflavone J (Fig. 5.2.3 A). Meanwhile, under-expressions of anti-apoptotic proteins Bcl-2 and Bcl-X_L; together with over-expressions of pro-apoptotic proteins Bad and Bax, were also attended (Fig. 5.2.3 C – 5.2.3F). These directed the disorganization of mitochondrial membrane, thereby causing the dissipation of membrane potential ($\Delta\Psi_m$) as well as the release of apoptogenic proteins, such as cyt c and AIF, from mitochondria into

cytosol (Fig. 5.2.4 & 5.2.5 A – 5.2.5D).

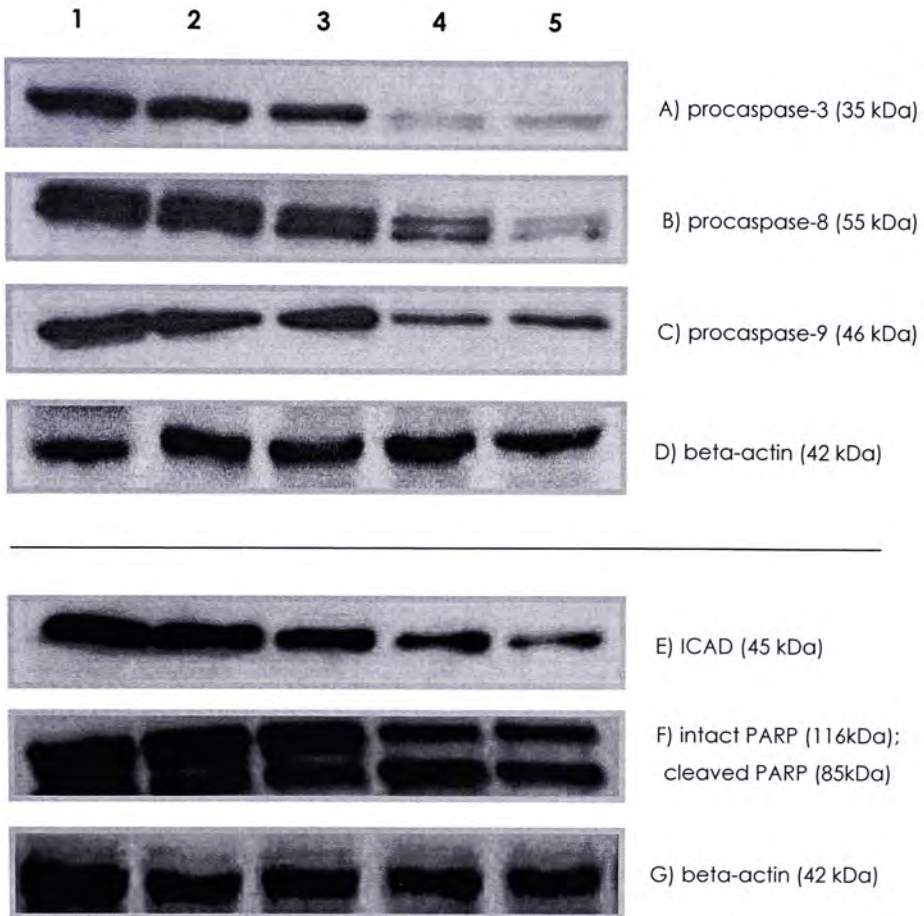


Fig. 5.2.1 Activation of caspases-3, 8 and 9 as well as induction of ICAD and PARP cleavages by Sophoraflavone J in HepG2 cells.

Cells (1×10^6) were incubated with vehicle only (lane 1) and Sophoraflavone J at concentrations of 5 $\mu\text{g/ml}$ (lane 2), 10 $\mu\text{g/ml}$ (lane 3), 15 $\mu\text{g/ml}$ (lane 4) and 20 $\mu\text{g/ml}$ (lane 5) for 48 hours at 37°C, 5% CO₂. (A) Probed with anti-procaspase-3 (35 kDa) antibody. (B) Probed with anti-procaspase-8 (55 kDa) antibody. (C) Probed with anti-procaspase-9 (46 kDa) antibody. (D) Probed with anti-beta-actin (42 kDa) antibody as loading control. (E) Probed with anti-ICAD (45 kDa) antibody. (F) Probed with anti-PARP (116 kDa as intact form and 85kDa as cleaved form) antibody. (G) Probed with anti-beta-actin (42 kDa) antibody as loading control. Data are from a representative of 3 separate experiments.

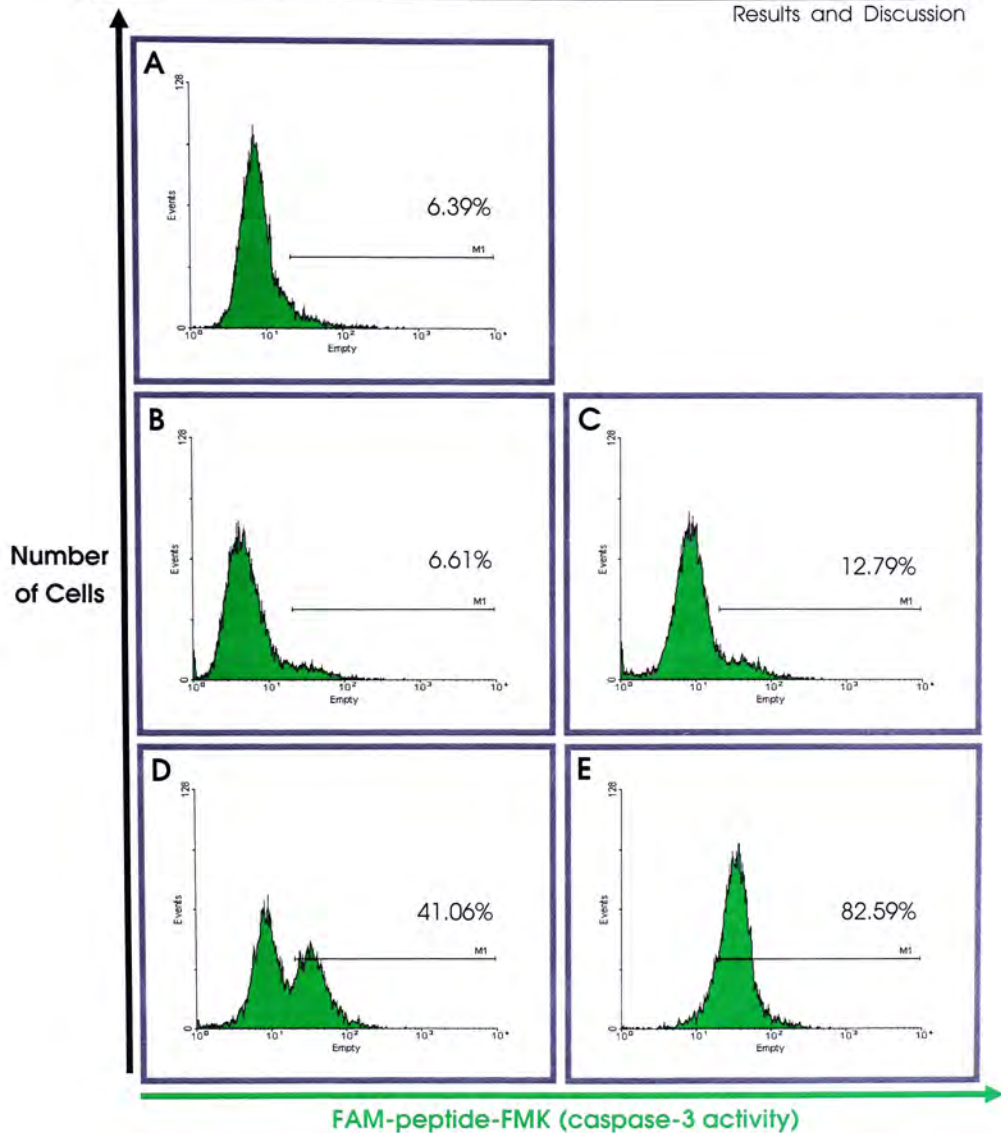


Fig. 5.2.2 Study of the enhancement of caspase-3 activity in Sophoraflavone J-treated HepG2 cells.

HepG2 cells (1×10^6) were exposed to vehicle only (A) and Sophoraflavone J at concentrations of 10 $\mu\text{g/ml}$ (B), 20 $\mu\text{g/ml}$ (C) and 30 $\mu\text{g/ml}$ (D) for 48 hours at 37°C, 5% CO₂. Cells with activated caspase-3 bound to the FAM-peptide-FMK inhibitor were detected using flow cytometry. Marker M1 corresponded to the cell fraction with enhanced caspase-3 activity. Results are representative of 3 independent experiments.

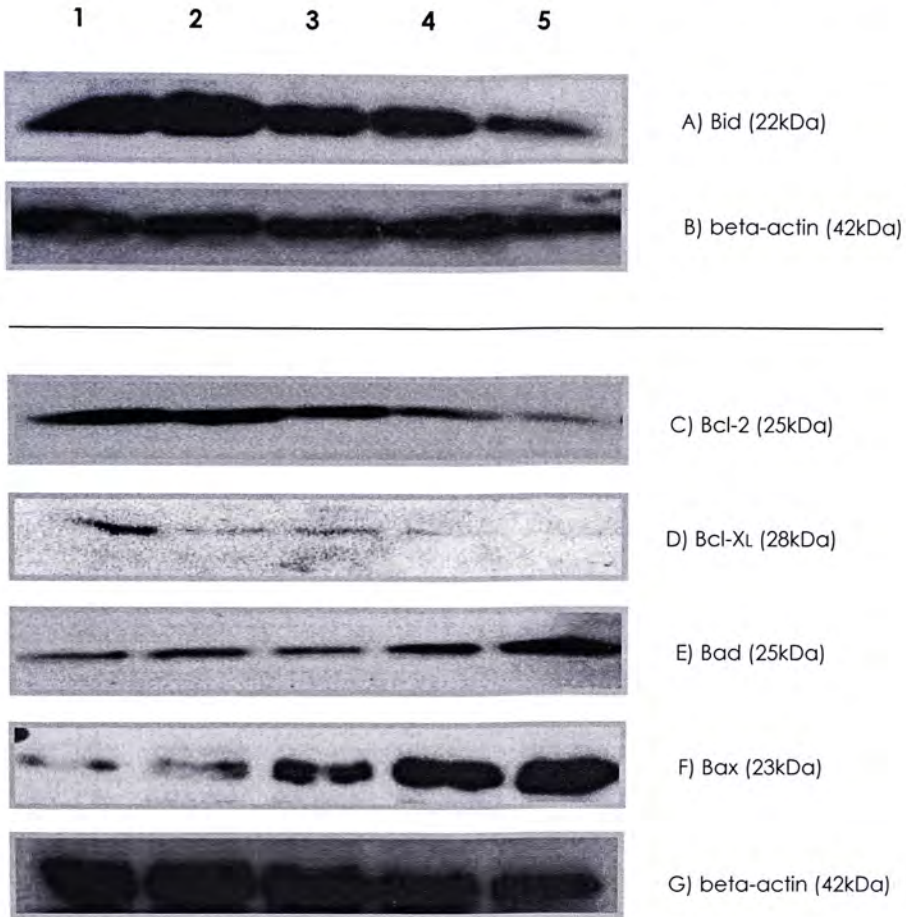


Fig. 5.2.3 Alteration of Expression Levels of Bcl-2 family proteins by Sophoraflavone J in HepG2 cells.

Cells (1×10^6) were incubated with vehicle only (lane 1) and Sophoraflavone J at concentrations of 5 $\mu\text{g/ml}$ (lane 2), 10 $\mu\text{g/ml}$ (lane 3), 15 $\mu\text{g/ml}$ (lane 4) and 20 $\mu\text{g/ml}$ (lane 5) for 48 hours at 37°C, 5% CO₂. (A) Probed with anti-bid (22 kDa) antibody. (B) Probed with anti-beta-actin (42 kDa) antibody as loading control. (C) Probed with anti-bcl-2 (25 kDa) antibody. (D) Probed with anti-bcl-XL (28 kDa) antibody. (E) Probed with anti-beta-actin (42 kDa) antibody as loading control. (F) Probed with anti-bad (25 kDa) antibody. (G) Probed with anti-bax (23 kDa) antibody. (H) Probed with anti-beta-actin (42 kDa) antibody as loading control. Data are from a representative of 3 separate experiments.

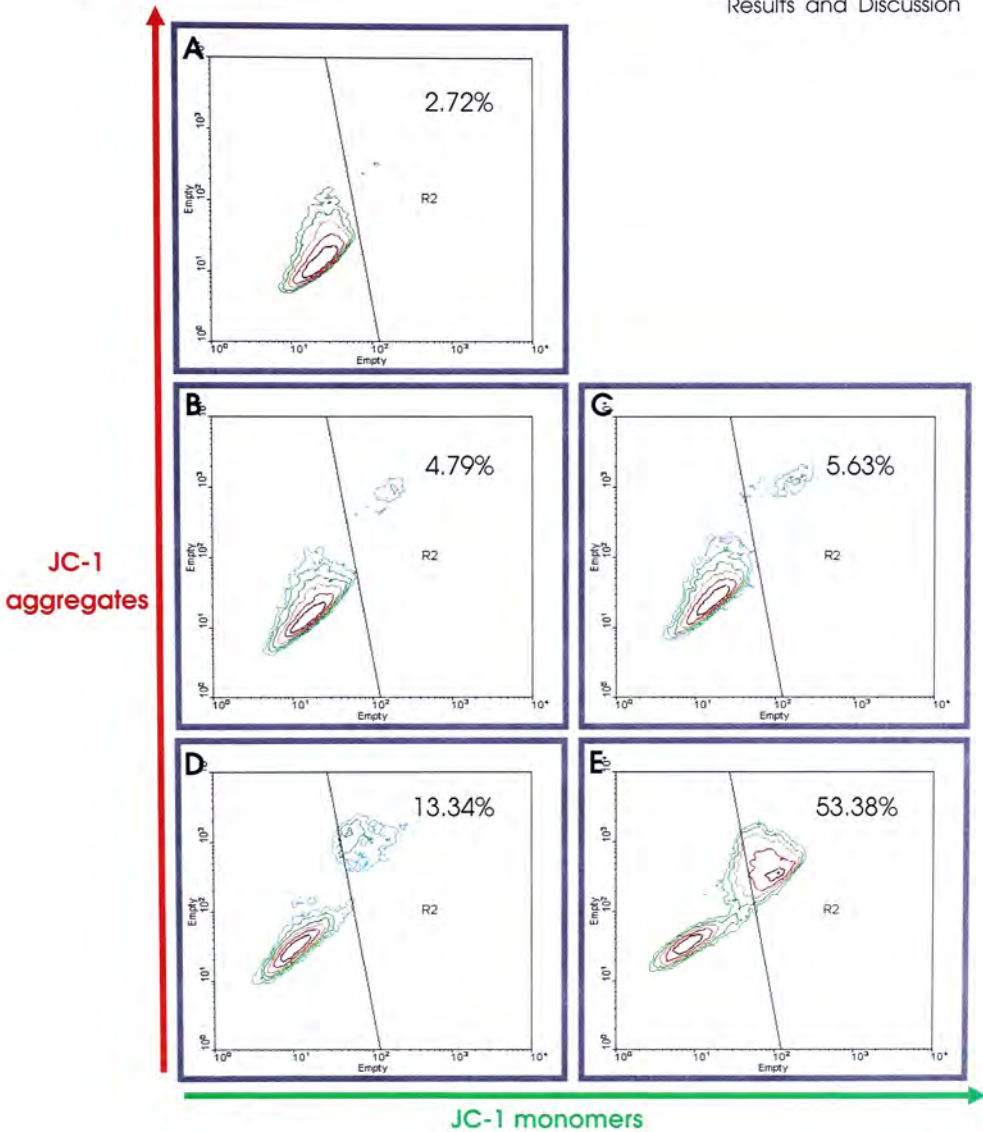


Fig. 5.2.4 Study of the loss of mitochondrial membrane potential in Sophoraflavone J-treated HepG2 cells.

HepG2 cells (3×10^5) were exposed to vehicle only (A) and Sophoraflavone J at concentrations of 5 $\mu\text{g/ml}$ (B), 10 $\mu\text{g/ml}$ (C), 15 $\mu\text{g/ml}$ (D) and 20 $\mu\text{g/ml}$ (E) for 48 hours at 37°C, 5% CO_2 . Cells obtained were incubated with JC-1 dye for staining. Flow cytometry was next used to measure the fluorescence emitted. Region R2 corresponded to the cell fraction with depolarized mitochondrial membrane potential. Results are representative of 3 independent experiments.

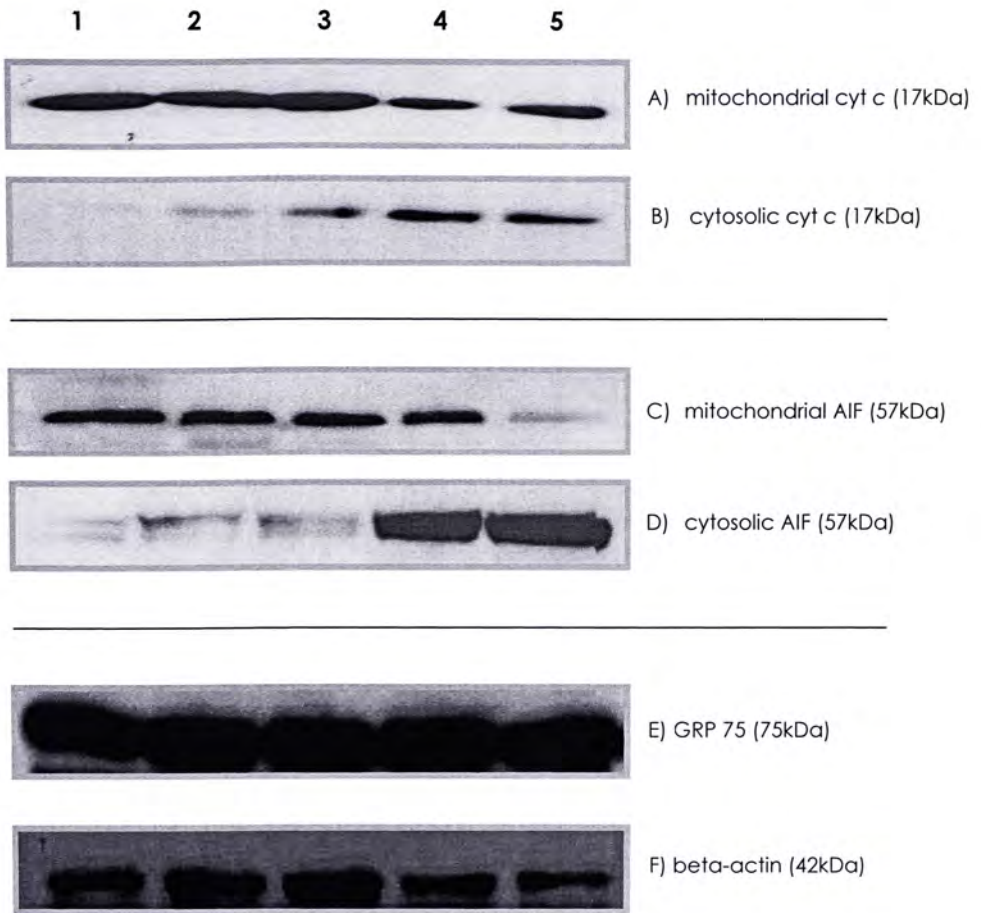


Fig. 5.2.5 Release of cytochrome c (cyt c) and apoptosis-inducing factor (AIF) from mitochondria to cytosol in Sophoraflavone J-treated HepG2 cells.

Cells (1×10^6) were incubated with vehicle only (lane 1) and Sophoraflavone J at concentrations of $5 \mu\text{g/ml}$ (lane 2), $10 \mu\text{g/ml}$ (lane 3), $15 \mu\text{g/ml}$ (lane 4) and $20 \mu\text{g/ml}$ (lane 5) for 48 hours at 37°C , 5% CO_2 . (A, B) Probed with anti-cytochrome c (17 kDa) antibody. (C, D) Probed with anti-AIF (57 kDa) antibody. (E) Probed with anti-GRP 75 (75 kDa) antibody as loading control for mitochondrial fraction. (F) Probed with anti-beta-actin (42 kDa) antibody as loading control for cytosolic fraction. Data are from a representative of 3 separate experiments.

CELL CYCLE ANALYSIS					ANNEXIN V/ PI STAINING EXPERIMENT				
	sub-G1	G0/G1	G2/M	S		normal	early apoptosis	late apoptosis/ necrosis	others
0	2.23%	70.01%	9.94%	18.68%	0	89.7%	4.1%	5.8%	0.4%
5	2.07%	72.70%	7.14%	18.92%	5	85.9%	6.9%	6.8%	0.4%
10	3.06%	64.81%	8.77%	24.70%	10	82.0%	9.9%	7.7%	0.3%
15	11.18%	57.41%	11.39%	21.76%	15	49.0%	27.9%	23.0%	0.2%
20	31.33%	39.37%	11.27%	20.00%	20	47.1%	25.8%	25.6%	1.6%
TUNEL ASSAY					DNA FRAGMENTATION REACTION				
	normal		with DNA breaks					DNA laddering pattern	
0	90.9%		9.10%	0				no	
5	87.28%		12.72%	5				no	
10	83.58%		16.42%	10				no	
15	52.68%		47.32%	15				no	
20	51.48%		48.52%	20				yes	
WESTERN BLOT STUDY – CASPASES AND ICAD/ PARP									

	procaspases-3, -8, -9 cleavages		ICAD/ PARP cleavages	
0	no	0	no	
5	no	5	no	
10	no	10	no	
15	yes	15	yes	
20	yes	20	yes	
CASPASE-3 ACTIVITY DETERMINATION		WESTERN BLOT STUDY – Bcl-2 FAMILY PROTEINS		
	normal			
0	93.61%	with enhanced caspase-3 activity		
		6.39%	Bid	---
5	93.39%	6.61%	unchanged	---
			Bcl-2	unchanged
10	87.21%	12.79%	unchanged	unchanged
			Bcl-Xl	unchanged
15	58.94%	41.06%	unchanged	unchanged
			Bad	increased
20	17.41%	82.59%	decreased	increased
			Box	unchanged
MITOCHONDRIAL MEMBRANE DEPOLARIZATION DETERMINATION		WESTERN BLOT STUDY – cyt c AND AIF		
	normal			
		with depolarization		
0	97.28%	2.72%	mitochondrial fraction	cytosolic fraction
			---	---

5	95.21%	4.79%	5	unchanged	unchanged
10	94.37%	5.63%	10	unchanged	unchanged
15	86.66%	13.34%	15	decreased	increased
20	46.62%	53.38%	20	decreased	increased

Table 5.1 A summary of the results from the apoptotic bioassays for Sophorolflavone J in HepG2 cells.

5.3 Differential Proteomes of Control and Sophoraflavone J-treated

HepG2 Cells

Today, advances in genomics and proteomics hold huge potentials for prognostic, diagnostic and therapeutic applications (Srinivas *et al.*, 2001).

Active genes, their corresponding protein products and other organic chemicals impart the molecular signposts of the biologic state of a cell at a specific circumstance. Thus, the global gene and protein expression studies are always of a great value in searching for the biomarkers important for early disease detection as well as identification (Chambers *et al.*, 2000, Ryu *et al.*, 2003).

Proteomics is one of the popular technologies recently emerged in the field of cancer research over genomics (Seow *et al.*, 2000). It is believed that proteins are the functional outputs of expressed genes; and the proteomic method enables the differential display of the proteomic asset of normal and carcinoma cells in response to the genetic and environmental impacts, and establishes a direct means to delineate the exact role of genes (Pandey *et al.*,

2000). In principal, the proteomics is dominated by two techniques, the first being the array of complex samples by two-dimensional gel electrophoresis (2-DE); and the other, the computational interpretation of the proteins by matrix-assisted laser desorption ionization time-of-flight mass spectrometry (MALDI-TOF-MS). In this project, we made use of the proteomics; and obtained the characteristic 2-DE maps of the whole lysates of control and Sophoraflavone J-treated (20 $\mu\text{g}/\text{ml}$; 48 hours) HepG2 cells (Fig. 5.3.1). The dosage and time adopted were the ones conferring a marked change in cells challenged with Sophoraflavone J, as referred to the previous apoptotic study. In an overview, a total of 22 (14 up-regulated and 8 down-regulated) protein spots were annotated; their respective identities and reported functions for altered expressions were summarized (Fig. 5.3.2 & Table 5.1).

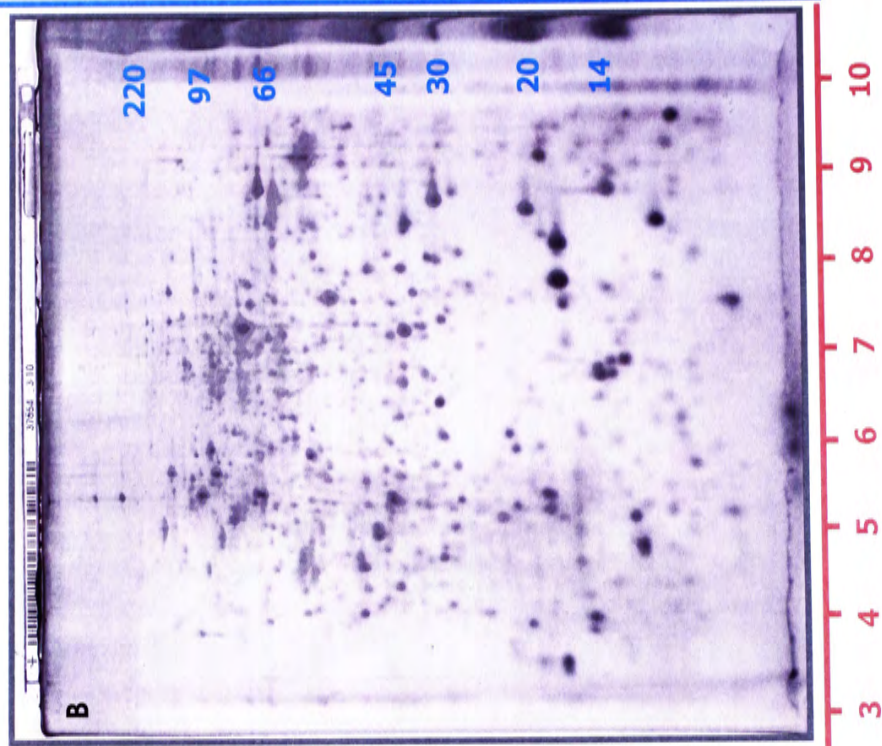
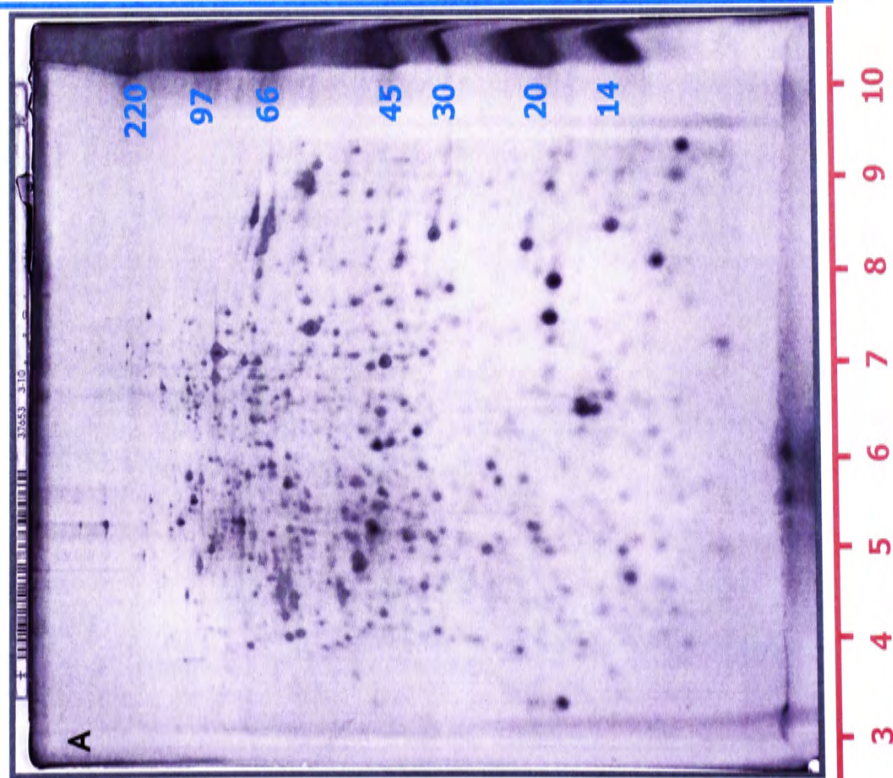
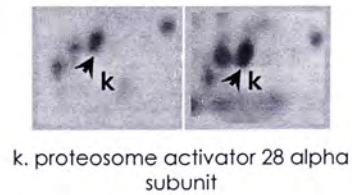
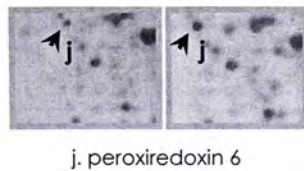
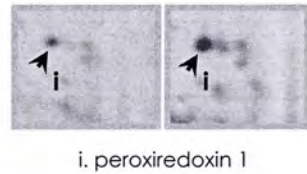
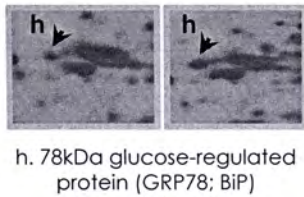
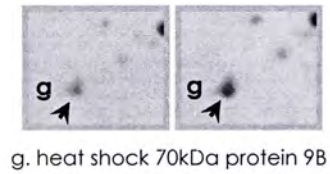
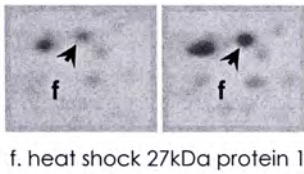
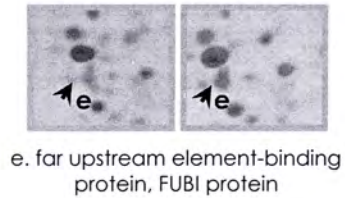
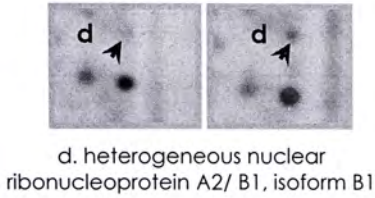
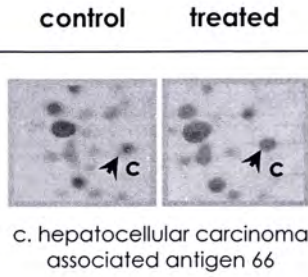
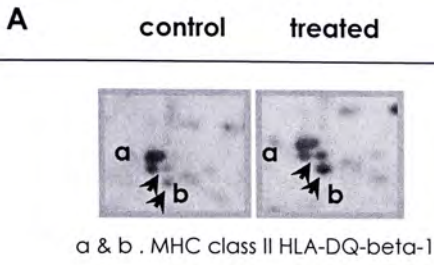
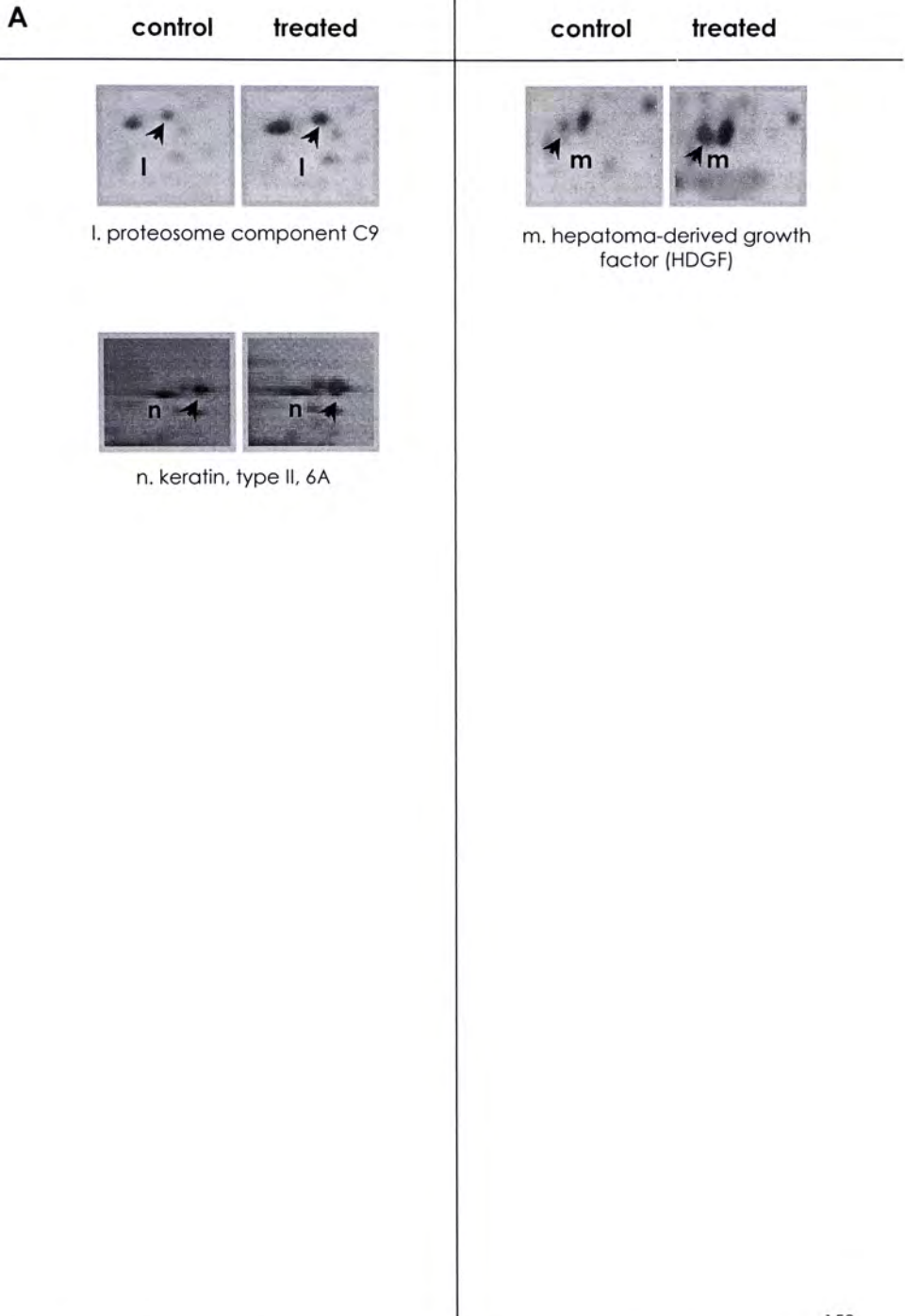


Fig. 5.3.1 Representative overview of 2D-gel images of control and Sophoraflavone J-treated HepG2 cell samples.

Cells (2×10^6) were disrupted in a lysis buffer cocktail. Approximately 300 μg of protein lysates (incubated with vehicle only (A) and Sophoraflavone J at a concentration of 20 $\mu\text{g}/\text{ml}$ (B)) were focused on a pH 3 – 10 linear IPG strip; and then separated by a 12% polyacrylamide gel. Protein expression patterns were subsequently visualized by silver staining method.





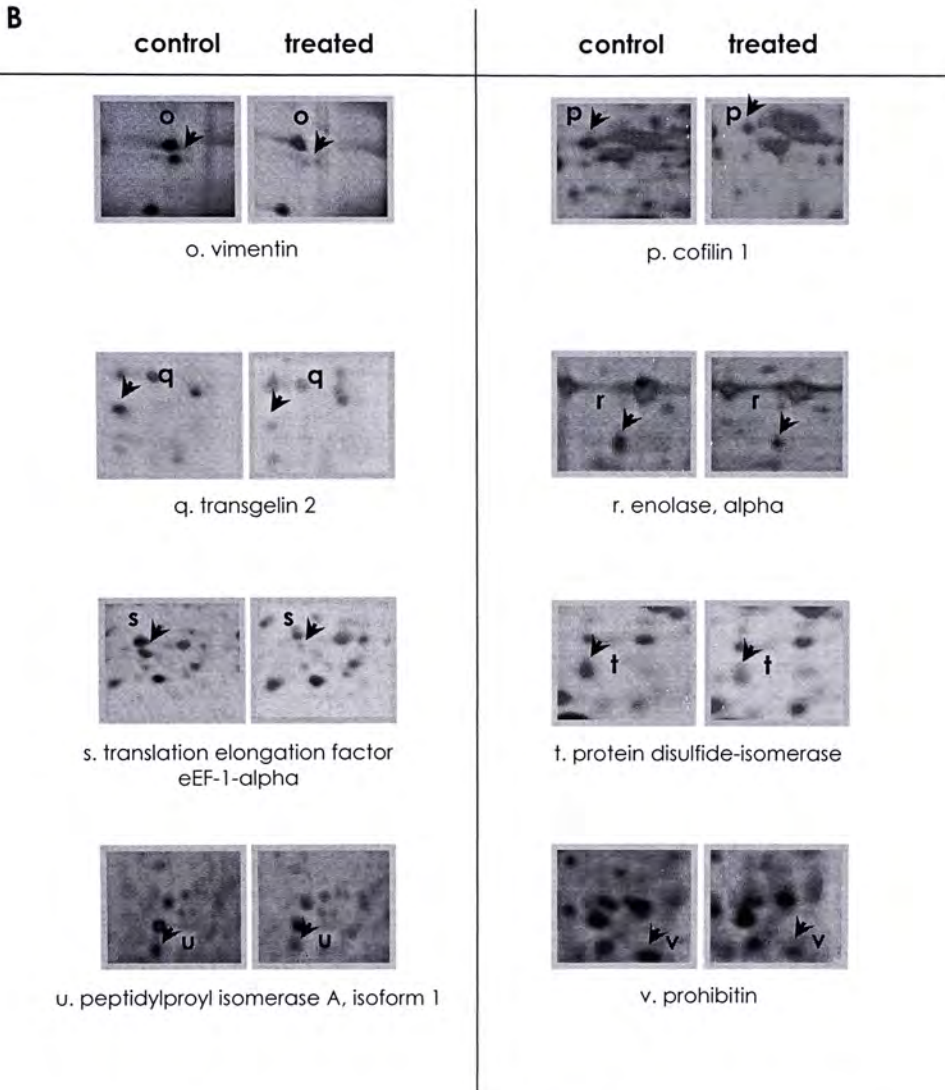


Fig. 5.3.2 Comparison of the protein expression profiles of control and Sophoraflavone J-treated HepG2 cell samples.

Image analysis of the stained 2D-gels was performed using computer software (ImageMaster 2D Platinum; version 5.0). Spots with over-expressed (A) and under-expressed (B) levels were indicated by arrows. Their identities (a – v) were searched in SWISS-PROT and NCBI non-redundant databases, respectively. Results are representative of 5 independent experiments.

Spot	SWISS-PROT/ NCBI Accession Number	Protein	Score	Isoelectric Point, pI	Molecular Weight, MW	Reported Function for Altered Expression
Up-regulated in Treated Panel						
a & b	619854/ 619856	MHC class II HLA-DQ-beta-1	57	6.67/6.73	26319/26309	enhance tumor immunogenicity upon antigen presentation
c	7670836	hepatocellular carcinoma (HCC)-associated antigen 66	54	7.19	70167	a member of the cancer/testis (CT) antigens frequently present in HCC
d	14043072	heterogeneous nuclear ribonucleoprotein (hnRNP) A2/ B1, isoform B1	106	8.97	37406	facilitate the packaging of pre-messenger RNA (mRNA) into hnRNP particles, transport of poly(A) mRNA from nucleus to cytoplasm; and modulate the splice site selection
e	17402900	far upstream element-binding protein, FUBI protein	74	7.18	67518	stimulate the activity of c-myc gene to control and regulate multiple aspects of biological processes
f	662841	heat shock 27kDa protein 1	61	7.83	22313	a stress protein to tolerate/ protect against numbers of cellular stresses
g	24234688	heat shock 70kDa protein 9B	82	5.87	73634	a stress protein to tolerate/ protect against numbers of cellular stresses
h	16507237	78kDa glucose-regulated protein [GRP78; BiP]	279	5.07	72288	a chaperon protein required for proper protein folding
i	32455266	peroxiredoxin (Prx) 1	140	6.00	25019	a redox enzyme to scavenge reactive oxygen species (ROS)
j	1718024	peroxiredoxin (Prx) 6	94	8.27	22096	a redox enzyme to scavenge reactive oxygen species (ROS)
k	P97371	proteasome activator 28 alpha subunit	68	5.70	28673	bind to and activate proteasome for internal protein degradation
l	P25767	proteasome component C9	56	6.91	25898	a subunit of proteasome enzyme complex to destabilize and destroy proteins
m	P51858	hepatoma-derived growth factor (HDGF)	77	4.70	26771	unknown; reported to be over-expressed during melanoma development and progression [Bernard et al., 2003]

Down-regulated in Treated Panel						
n	14318422	keratin, type II, 6A	65	8.14	59877	unknown; reported to be highly expressed in myeloma cells treated with arsenic trioxide (Li et al., 2005)
o	P08670	vimentin	80	5.06	53686	a cancer-related protein; reported to be up-regulated in malignant, transformed hepatocytes; positively related to drug resistance ability (Fella et al., 2005)
p	26400725	cofilin 1	119	5.42	271385	a cytoskeletal protein participated in the initiation of mitochondrial apoptosis pathway
q	4507357	transgelin 2	204	8.41	22377	a cytoskeletal protein related to cell morphology and metastatic potential
r	29292061	enolase, alpha	95	7.01	47139	a glycolytic enzyme to catalyze the inter-conversion of 2-phosphoglycerate and phosphoenolpyruvate for carbohydrate metabolism
s	2119925	translation elongation factor eEF-1-alpha	52	9.61	24180	entailed in protein translation
t	2135267	protein disulfide-isomerase	58	6.23	56715	an enzyme to catalyze the thiol/disulfide exchange for protein assembly
u	13937981	peptidylprolyl isomerase A, isoform 1	55	7.68	17999	promote cell proliferation and differentiation
v	P35232	prohibitin	102	5.57	29804	negatively influence cell-cycle progression and DNA synthesis for cell growth

Table 5.2 A complete list of the altered expressed protein molecules in Sophor flavone J-treated HepG2 cells.

Proteins with at least 2-fold difference of alteration in the expression levels were of study interest. The column "score [the probability based mouse score]" was computed from $-10 \times \log(P)$, where P is the absolute probability that the observed match is a random event. Score greater than 41 pretended an identity or extensive homology. The 4 candidates highlighted in gray boxes above were chosen for further experiment.

Out of these candidates, we picked four – heat shock protein 70 (HSP70), glucose-regulated protein 78 (GRP78), transgelin 2 (TAGLN2) and alpha enolase (ENO1) – to have Western blotting for validation of their differential expressions, subsequent to 48-hour Sophoraflavone J incubation (Fig. 5.3.3). Besides, we also conducted real-time PCR to examine whether the regulation lied at the transcriptional level or not. Interestingly, our findings pinpointed that mRNA and protein patterns were quite correlative with each other; an exception was HSP70 (Fig. 5.3.4 & Table 5.3). The discrepancy was possibly due to some other regulatory units in cells, which contributed to the increased translation of the existing mRNA and the decreased elimination of the encoded protein (Nordengren et al., 1998, Pradet-Balade et al., 2001).

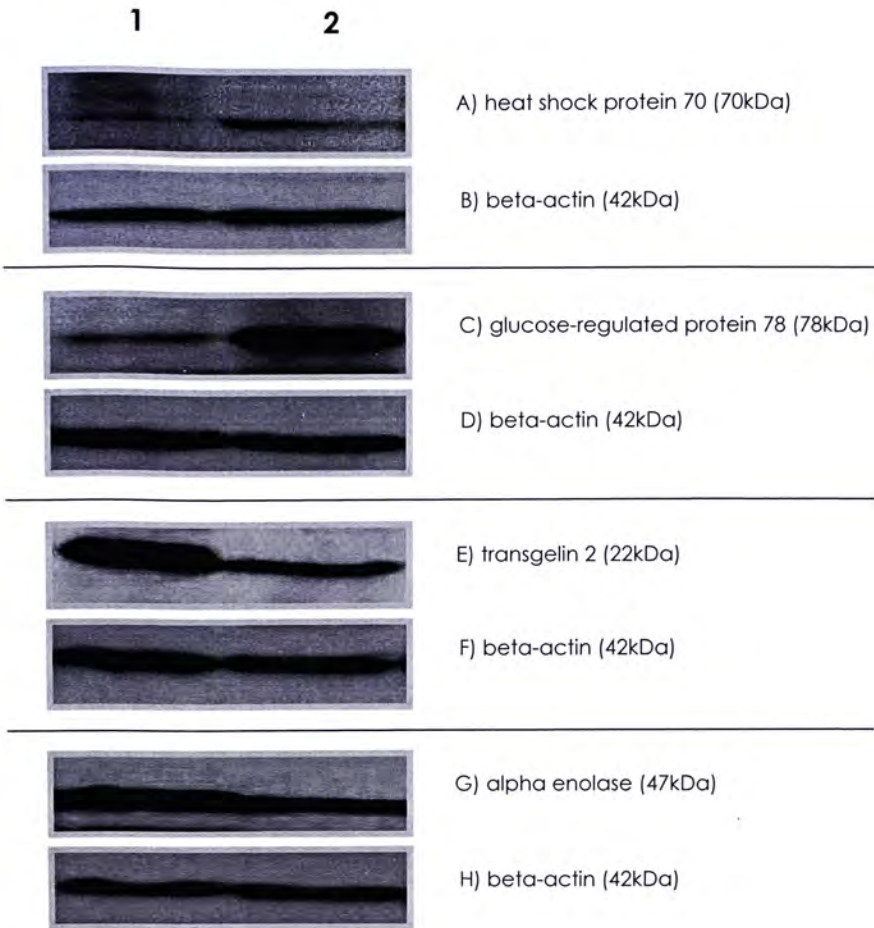


Fig. 5.3.3 Confirmation of the altered expressed protein molecules in Sophoraflavone J-treated HepG2 cells by Western blotting.

Cells (1×10^6) were incubated with vehicle only (lane 1) and Sophoraflavone J at a concentration of $20 \mu\text{g/ml}$ (lane 2) for 48 hours at 37°C , 5% CO_2 . (A) Probed with anti-HSP 70 (70 kDa) antibody. (C) Probed with anti-GRP 78 (78 kDa) antibody. (E) Probed with anti-TAGLN 2 (22 kDa) antibody. (G) Probed with anti-ENO 1 (47 kDa) antibody. (B, D, F & G) Probed with anti-beta-actin (42 kDa) antibody as loading control. Results are representative of 5 independent experiments.

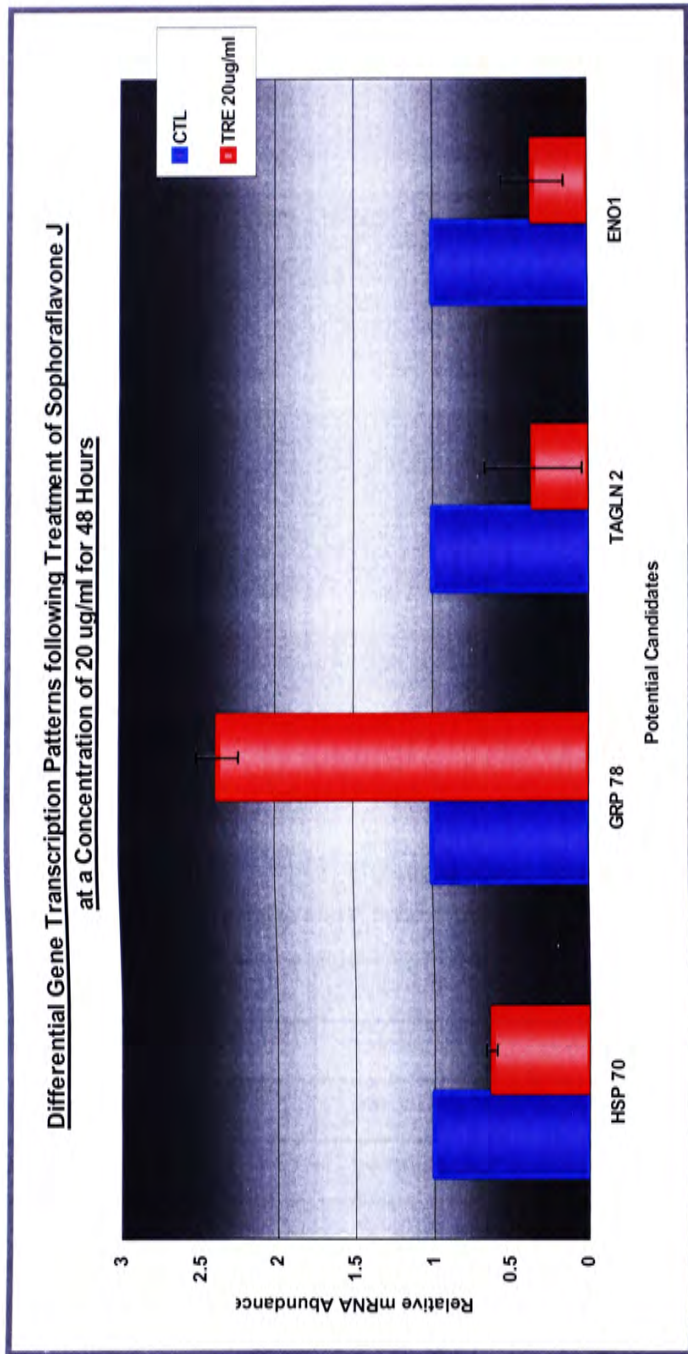


Fig. 5.3.4 Investigation of modulated mRNA transcripts in Sophorafflavone J-treated HepG2 cells using real-time PCR.

Cells (1×10^5) were incubated with vehicle only and Sophorafflavone J at a concentration of 20 $\mu\text{g/ml}$ for 48 hours at 37°C, 5% CO₂. Total mRNA was extracted and reverse-transcribed for cDNA for real-time PCR quantification under optimized condition. Values are mean \pm SD of 3 determinations.

	PROTEN LEVELS		mRNA LEVELS	
	control	treated	control	treated
HSP70	---	increased	---	decreased
GRP78	---	increased	---	increased
TAGLN2	---	decreased	---	decreased
ENO1	---	decreased	---	decreased

Table 5.3 A review of the mRNA and protein levels of the 4 candidates in control and Sophoraflavone J-treated HepG2 cells.

In encounter with Sophoraflavone J, lots of proteins in cells were switched up or down to make up the branching, complicated cellular response in return. These proteins are thought to be linked with a wide range of human tumors in many facets. However, there is no precise sequence for each protein coming between one and the other; they are instead inter-reliant and multi-directional.

From literature review, **HSP70** is an anti-apoptotic chaperon protein abundantly and preferentially expressed in human cancers (Kaur *et al.*, 2000, Nylandsted *et al.*, 2000). Neutralization of its function and/ or repression of its expression often ends up in a yet unknown caspase-independent death pathway, in which other anti-apoptotic proteins, like Bcl-2 and Bcl-XL, etc failed to rescue the cells (Zhao *et al.*, 2005). More to this, inactivated HSP70 results in a high rate of spontaneous chromosomal aberrations and genome instability (Pandita *et al.*, 2004). These tell that HSP70 over-expression is a prerequisite for the survival of cancer cells against host defense system as well as various sorts of therapy.

In our situation, HSP70 up-regulation was presumably a mechanism employed by the cells to counteract with the lethal stresses from driving them to die. In fact, acute production of HSP proteins was repeatedly found in patients following diverse forms of cancer treatments as a very short-termed response. On recovery, such proteins were continuously down-regulated to allow selective tumor cell death (Schueller *et al.*, 2004). Possibly, Sophoraflavone J got a time lag in depleting endogenous HSP70 to a minimal level yet to be observed post-48-hour application.

GRP78 is another chaperon protein located at the endoplasmic reticulum (ER) lumen for nascent polypeptide folding and secretion (Rao *et al.*, 2002). Unlike HSP70, GRP78 is unresponsive to heat stress; but is induced by glucose deprivation. **ENO1** is characterized as an evolutionarily conserved cytoplasmic enzyme involved in catalyzing the inter-conversion reaction of 2-phosphoglycerate and phosphoenolpyruvate in glycolysis. There are three isoenzymes of enolase, namely alpha- (α -), beta- (β -) and gamma- (γ -) enolase. The former is detected in most tissues; whereas the latter two are

utterly in muscle and neural tissues, respectively (Piast *et al.*, 2005). Herein, up-regulation of GRP78 and down-regulation of ENO1 revealed that the cells were short of energy source supply in the presence of Sophoraflavone J.

TAGLN2 is a 22kDa monomeric protein containing nuclear factor-binding motifs to modulate transcription in cells (Camoretti-Mercado *et al.*, 1998). It is capable of gelling actin filaments rapidly; and affecting the expression of actin-associated proteins. Changed actin network was constantly accompanied by neoplasia and metastasis (Frances *et al.*, 2006). So far, TAGLN2 over-expression is considered as a molecular signature for carcinoma cells (Chen *et al.*, 2005, Qi *et al.*, 2005). From our data, its down-regulation after the addition of Sophoraflavone J acted to help prevent the condition from deteriorating.

Apart from Western blot experiment, we included a functional study to explicate the strong expression of peroxiredoxin (Prx) proteins as well. It was postulated that Sophoraflavone J boosted up the generation of reactive

oxygen species (ROS) in cells, which subsequently enriched the ROS-sensitive Prx proteins for an antagonizing action. Usually, cellular ROS level was negatively associated with the glutathione (GSH) changes (Fujii *et al.*, 2002). And, in our analysis, abated glutathione was described with a fall in the fluorescence signals, because of the poor formation of monochlorobimane (MCB)-glutathione adducts (Fig. 5.3.5). As such, we knew that the up-regulation of Prx proteins was accredited to the escalated ROS level in Sophoraflavone J-treated cells.

To conclude, the ultimate goal of this part was to find out the novel non-apoptotic cell-killing mechanism(s) allied to drug treatment. Down-regulation of ENO1 and TAGLN2 proteins herein inferred a nutrient/ energy dispossession and cytoskeletal reorganization within the cells by Sophoraflavone J. At the same moment, apoptosis-related molecules, including HSP70 and Prx 1 and 6 proteins, also shown to join in the process. HSP70 was versatile in annulling the apoptotic machinery either through binding with Bax to stop its translocation to mitochondria; or through

interacting with Apaf-1 to avert the formation of apoptosome. Despite this, HSP70 in company with Prx 1 and 6 up-regulations were rather a fall-out feedback from the intensive ROS development. Many commercial anti-cancer drugs (e.g. camptothecin and actinomycin D) engaged to activate the mitochondrial apoptotic pathway through introduction of cells with free radicals (Creagh *et al.*, 1999, Murakami *et al.*, 2006). In this regard, more work is necessary to draw a full conclusion in the future.

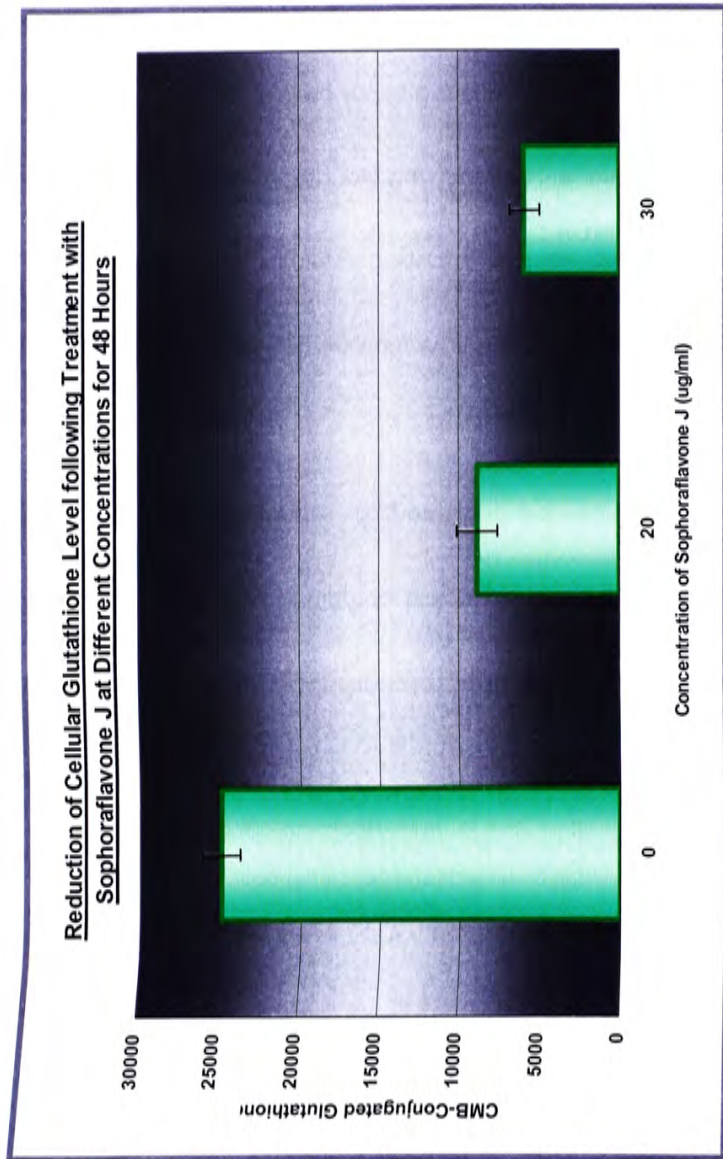


Fig. 5.3.5 Change of cellular glutathione level contributed partly to the Sophoraflavone J-induced cell death.

Cells (1×10^6) were incubated with vehicle only and Sophoraflavone J at concentrations of 20 µg/ml and 30 µg/ml for 48 hours at 37°C, 5% CO₂. Protein lysates were assayed for the glutathione levels with the use of a fluorescent dye. Values are mean \pm SD of 3 determinations.

5.4 Conclusion

As a whole, we clarified that Sophoraflavone J elicited apoptosis in HepG2 cells, dependent of both extrinsic and intrinsic pathways (Fig. 5.1.2 – 5.1.4, 5.2.1 – 5.2.5). However, it demonstrated minute effect on cell cycle progression; the distribution of cells in the G1 or G2 phases was more or less the same with or without drug treatment (Fig. 5.1.1).

To further supplement the detailed mechanism behind the Sophoraflavone J-induced cell death, we undertook a combined proteomic analysis; and spotted out manifold genes of differentially expressed proteins (Fig. 5.3.1 & 5.3.2). These proteins were classified into several categories based on their major biological roles, for instance membrane proteins/ antigens, structural proteins, transcriptional factors, glycolytic enzymes, heat-shock chaperon proteins (HSP), reactive oxygen species (ROS)-related proteins and proteosomes, etc (Table 5.2). From a set of preliminary tests, we deduced that the cytotoxicity of Sophoraflavone J partially counted on its ability to incur nutrient deficiency and intra-cellular oxidation in HepG2 cells (Fig.

5.3.3 – 5.3.5).

CHAPTER 6

OVERALL CONCLUSION and FUTURE PERSPECTIVES

Apoptotic Study

The use of Chinese herbal ingredient(s) alone or in conjunction with some conventional drugs is a new trend in the contemporary clinical medicine to circumvent malignant cancers (Hemalswarya *et al.*, 2006, Inanc *et al.*, 2006, Xie *et al.*, 2006). In the present research, we unraveled that both Leachianone A and Sophoraflavone J from Radix *Sophorae* were specific in their *in vitro* and *in vivo* cytotoxic activities against human hepatoma cells HepG2 and RHepG2; but not its normal liver cell counterpart WRL-68. Additionally, they were of extreme potency preceding the anti-cancer agents, cisplatin and taxol.

Mechanistically, the two compounds worked to arrest cell proliferation and cause cell death through apoptosis, in which both the extrinsic (death

receptor-mediated) and intrinsic (mitochondrial) pathways were undergone. The proposed mode of action was that 1) Leachianone A or Sophoraflavone J interacted with the cognate receptors and initiated receptor trimerization; 2) trimerized receptors either recruited caspase-8 directly or in aid with some adaptor molecules; 3) activated caspase-8 then cleaved Bid into tBid; 4) tBid migrated to mitochondria and rendered the efflux of cyt c and AIF to cytosol; 5) Apaf-1, cyt c and pro-caspase-9 next joined up for apoptosome, which gave rise to activated caspases-9 and -3 sequentially; 6) active caspase-3 enzyme lastly mediated ICAD and PARP processing for DNA fragmentation as well as other morphological and biochemical changes during apoptosis.

Proteomic Study

Proteomics possesses the advantage of viewing all the protein species within a single cell or tissue simultaneously (Towbin *et al.*, 2003). In practical, this methodology was most appreciated in biological science to, for example, elucidate protein changes between healthy and diseased subjects as well as during disease staging (Colantonio *et al.*, 2005).

In the section of proteomics, we hunted out a total of 22 protein spots expressed differentially in control and Sophoraflavone J-treated HepG2 cells. These proteins managed miscellaneous tasks, as grouped into: 1) membrane proteins/ antigens (MHC class II HLA-DQ-beta-1, HCC-associated antigen 66), 2) structural proteins (vimentin, cofilin 1, TAGLN2), 3) transcriptional factors (translation elongation factor eEF-1-alpha, hn RNP A2/ B1 isoform B1, FUBI protein), 4) glycolytic enzymes (ENO1), 5) heat-shock chaperon proteins (HSP) (HSP27, HSP70, GRP78), 6) reactive oxygen species (ROS)-related proteins (Prx1, Prx6) and 7) proteosomes (proteosome activator 28 alpha subunit, proteosome component C9), etc (hepatoma-derived growth factor, keratin type II 6A, protein disulfide-isomerase, peptidylproyl isomerase A isoform 1, prohibitin). According to

the experimental findings, we surmised that Sophoraflavone J treatment directly or indirectly imposed on the cancer cells difficulties in consuming food sources and coping with oxygen species, before straightly getting to induce apoptosis.

In the near future, effort will be extended to the characterization of the identified proteins so as to gain more insights in the comprehensive action mechanism of Sophoraflavone J in HepG2 cells. For instance, immunostaining will be manipulated to highlight the intra-cellular localization(s) of the candidate protein(s); and RNA interference (RNAi) will also be utilized to knock down certain gene(s) in cells for further exploration.

REFERENCES

- ARCECI RJ. (2000)** Can multidrug resistance mechanisms be modified? *Br J Haematol.* 110(2): 285-91.
- BERGMANN A, TUGENTMAN M, SHILO BZ, STELLER H. (2002)** Regulation of cell number by MAPK-dependent control of apoptosis: a mechanism for trophic survival signaling. *Dev Cell.* 2(2): 159-70.
- BERNARD K, LITMAN E, FITZPATRICK JL, SHELLMAN YG, ARGAST G, POLVINEN K, EVERETT AD, FUKASAWA K, NORRIS DA, AHN NG, RESING KA. (2003)** Functional proteomic analysis of melanoma progression. *Cancer Res.* 63(20): 6716-25.
- BIVIK CA, LARRSON PK, KAGEDAL KM, ROSDAHL IK, OLLINGER KM. (2006)** UVA/B-induced apoptosis in human melanocytes involves translocation of cathepsins and Bcl-2 family members. *J Invest Dermatol.* 126(5): 1119-27.
- BLAGOSKLONNY MV. (2003)** Targeting cancer cells by exploiting their resistance. *Trends Mol Med.* 9(7): 307-12.
- CAMORETTI-MERCADO B, FORSYTHE SM, LEBEAU MM, ESPINOSA R 3RD, VIEIRA JE, HALAYKO AJ, WILLADSEN S, KURTZ B, OBER C, EVANS GA, THWEATT R, SHAPIRO S, NIU Q, QIN Y, PADRID PA, SOLWAY J. (1998)** Expression and cytogenetic localization of the human SM22 gene (TAGLN). *Genomics.* 49(3): 452-7.
- CARROLL DG. (2006)** Nonhormonal therapies for hot flashes in menopause. *Am Fam Physician.* 73(3): 457-64.
- CHAMBERS G, LAWRIE L, CASH P, MURRAY GI. (2000)** Proteomics: a new approach to the study of disease. *J Pathol.* 192(3): 280-8.
- CHAN JY, CHU AC, FUNG KP. (2000)** Inhibition of P-glycoprotein expression and reversal of drug resistance of human hepatoma HepG2 cells by

multidrug resistance gene (*mdr1*) antisense RNA. *Life Sci.* 67(17): 2117-24.

CHEN H, WANG M, WANG XY, GAO S, WANG J, GUAN XM. (2005) Identification of differential genes in ovarian cancer using representational difference analysis of cDNA. *Chin Med Sci J.* 20(3): 185-9.

CHIPUK JE, CORNELIUS SC, PULTZ NJ, JORGENSEN JS, BONHAM MJ, KIM SJ, DANIELPOUR D. (2002) The androgen receptor represses transforming growth factor-beta signaling through interaction with Smad3. *J Biol Chem.* 277(2): 1240-8.

CHOI SU, KIM KH, CHOI EJ, PARK SH, LEE CO, JUNG NP, YOON SK, RYU SY. (1999) P-glycoprotein (Pgp) does not affect the cytotoxicity of flavonoids from *Sophora flavescens*, which also have no effects on Pgp action. *Anticancer Res.* 19(3A): 2035-40.

COLANTONIO DA, CHAN DW. (2005) The clinical application of proteomics. *Clin Chim Acta.* 357(2): 151-8.

COLELL A, GARCIA-RUIZ C, MARI M, FERNANDEZ-CHECA JC. (2004) Mitochondrial permeability transition induced by reactive oxygen species is independent of cholesterol-regulated membrane fluidity. *FEBS Lett.* 560(1-3): 63-8.

COLGATE EC, MIRANDA CL, STEVENS JF, BRAY TM, HO E. (2006) Xanthohumol, a prenylflavonoid derived from hops induces apoptosis and inhibits NF-kappaB activation in prostate epithelial cells. *Cancer Lett.* [Epub ahead of print]

CREAGH EM, COTTER TG. (1999) Selective protection by hsp 70 against cytotoxic drug-, but not Fas-induced T-cell apoptosis. *Immunology.* 97(1): 36-44.

DEBATIN KM. (1999) The role of CD95 system in chemotherapy. *Drug Resist Updat.* 2(2): 85-90.

DE NAEYER A, VANDEN BERGHE W, POCOCK V, MILLIGAN S, HAEGEMAN G, DE

KEUKELEIRE D. (2004) Estrogenic and anticarcinogenic properties of kurarinone, a lavandulyl flavanone from the roots of *Sophora flavescens*. *J Nat Prod.* 67(11): 1829-32.

ENARI M, SAKAHIRA H, YOKOYAMA H, OKAWA K, IWAMATSU A, NAGATA S. (1998) A caspase-activated DNase that degrades DNA during apoptosis, and its inhibitor ICAD. *Nature.* 391(6662): 43-50.

FELLA K, GLUCKMANN M, HELLMANN J, KARAS M, KRAMER PJ, KROGER M. (2005) Use of two-dimensional gel electrophoresis in predictive toxicology: identification of potential early protein biomarkers in chemically induced hepatocarcinogenesis. *Proteomics.* 5(7): 1914-27.

FERRI KF, KROEMER G. (2001) Organelle-specific initiation of cell death pathways. *Nat Cell Biol.* 3(11): E255-63.

FRANCES R, TUMANG JR, KAKU H, GURDAK SM, ROTHSTEIN TL. (2006) B-1 cells express transgelin 2: Unexpected lymphocyte expression of a smooth muscle protein identified by proteomic analysis of peritoneal B-1 cells. *Mol Immunol.* 43(13): 2124-9.

FRANKEL A, BUCKMAN R, KERBEL RS. (1997) Abrogation of taxol-induced G2-M arrest and apoptosis in human ovarian cancer cells grown as multicellular tumor spheroids. *Cancer Res.* 57(12): 2388-93.

FUJII J, IKEDA Y. (2002) Advances in our understanding of peroxiredoxin, a multifunctional, mammalian redox protein. *Redox Rep.* 7(3): 123-30.

GERBER M, BOUTRON-RUAULT MC, HERCBERG S, RIBOLI E, SCALBERT A, SIESS MH. (2002) Food and cancer: state of the art about the protective effect of fruits and vegetables. *Bull Cancer.* 89(3): 293-312.

GODARD T, DESLANDES E, LEBAILLY P, VIGREUX C, POULAIN L, SICHEL F, POUL JM, GAUDUCHON P. (1999) Comet assay and DNA flow cytometry analysis of staurosporine-induced apoptosis. *Cytometry.* 36(2): 117-22.

GOUAZE V, MIRault ME, CARPENTIER S, SALVAYRE R, LEVADE T,

- ANDRIEU-ABADIE N. (2001)** Glutathione peroxidase-1 overexpression prevents ceramide production and partially inhibits apoptosis in doxorubicin-treated human breast carcinoma cells. *Mol Pharmacol.* 60(3): 488-96.
- GREEN DR, AMARANTE-MENDES GP. (1998)** The point of no return: mitochondria, caspases, and the commitment to cell death. *Results Probl Cell Differ.* 24: 45-61.
- GRUDE P, CONTI F, MENNECIER D, LOUVEL A, HOUSSIN D, WEILL B, CALMUS Y. (2002)** MDR1 gene expression in hepatocellular carcinoma and the peritumoral liver of patients with and without cirrhosis. *Cancer Lett.* 186(1): 107-13.
- GRUTTER MG. (2000)** Caspases: key players in programmed cell death. *Curr Opin Struct Biol.* 10(6): 649-55.
- GUIMARAES CA, BENCHIMOL M, AMARANTE-MENDES GP, LINDEN R. (2003)** Alternative programs of cell death in developing retinal tissue. *J Biol Chem.* 278(43): 41938-46.
- GUPTA S. (2001)** Molecular steps of death receptor and mitochondrial pathways of apoptosis. *Life Sci.* 69(25-26): 2957-64.
- HAGHIAC M, WALLE T. (2005)** Quercetin induces necrosis and apoptosis in SCC-9 oral cancer cells. *Nutr Cancer.* 53(2): 220-31.
- HEMALSWARYA S, DOBLE M. (2006)** Potential synergism of natural products in the treatment of cancer. *Phytother Res.* 20(4): 239-49.
- HOESSEL R, LECLERC S, ENDICOTT JA, NOBEL ME, LAWRIE A, TUNNAH P, LEOST M, DAMIENS E, MARIE D, MARKO D, NIEDERBERGER E, TANG W, EISENBRAND G, MEIJER L. (1999)** Indirubin, the active constituent of a Chinese antileukaemia medicine, inhibits cyclin-dependent kinases. *Nat Cell Biol.* 1(1): 60-7.
- HUANG JC, ZAMBLE DB, REARDON JT, LIPPARD SJ, SANCAR A. (1994)**

HMG-domain proteins specifically inhibit the repair of the major DNA adduct of the anticancer drug cisplatin by human excision nuclease. *Proc Natl Acad Sci USA*. 91(22): 10394-8.

HUANG X, ZHAI D, HUANG Y. (2000) Study on the relationship between calcium-induced calcium release from mitochondria and PTP opening. *Mol Cell Biochem*. 213(1-2): 29-35.

INANC N, SAHIN H, CICEK B, TASC S. (2006) Use of herbs or vitamin/mineral supplements by patients with cancer in Kayseri, Turkey. *Cancer Nurs*. 29(1): 17-20.

JOAQUIN AM, GOLLAPUDI S. (2001) Functional decline in aging and disease: a role for apoptosis. *J Am Geriatr Soc*. 49(9): 1234-40.

JOHNSON K, LLOYD-PURYEAR MA, MANN MY, ROMAS LR, THERRELL BL. (2006) Financing state newborn screening programs: sources and uses of funds. *Pediatrics*. 117(5 Pt 2): S270-9.

JORDAN MA, WENDELL K, GARDINER S, DERRY WB, COPPH, WILSON L. (1996) Mitotic block induced in HeLa cells by low concentrations of paclitaxel (Taxol) results in abnormal mitotic exit and apoptotic cell death. *Cancer Res*. 56(4): 816-25.

JURGENSMEIER JM, XIE Z, DEVERAUX Q, ELLERBY L, BREDESEN D, REED JC. (1998) Bax directly induces release of cytochrome c from isolated mitochondria. *Proc Natl Acad Sci USA*. 95(9): 4997-5002.

KANG TH, JEONG SJ, KO WG, KIM NY, LEE BH, INAGAKI M, MIYAMOTO T, HIGUCHI R, KIM YC. (2000) Cytotoxic lavandulyl flavanones from *Sophora flavescens*. *J Nat Prod*. 63(5): 680-1.

KAUFMANN SH, GORES GJ. (2000) Apoptosis in cancer: cause and cure. *Bioessays*. 22(11): 1007-17.

KAUR J, KAUR J, RALHAN R. (2000) Induction of apoptosis by abrogation of HSP70 expression in human oral cancer cells. *Int J Cancer*. 85(1): 1-5.

KERR JF, SEARLE J (1972) A mode of cell loss in malignant neoplasms. *J Pathol.* 106(1): Pxi.

KIM GS, PARK YA, CHOI YS, CHOI YH, CHOI HW, JUNG YK, JEONG S. (2006) Suppression of receptor-mediated apoptosis by death effector domain recruiting domain binding peptide aptamer. *Biochem Biophys Res Commun.* 343(4): 1165-70.

KIM YC, KIM HS, WATAYA Y, SOHN DH, KANG TH, KIM MS, KIM YM, LEE GM, CHANG JD, PARK H. (2004) Antimalarial activity of lavandulyl flavanones isolated from the roots of *Sophora flavescens*. *Biol Pharm Bull.* 27(5): 748-50.

KO S, YUEN WF, FUNG KP, LEE CY, CHOY YM, CHENG HK, KWOK TT, KONG SK. (2000) Reversal of TNF-alpha resistance by hyperthermia: role of mitochondria. *Life Sci.* 67(25): 3113-21

KOEBNICK C, GARCIA AL, DAGNELIE PC, STRASSNER C, LINDEMANS J, KATZ N, LEITZMANN C, HOFFMANN I. (2005) Long-term consumption of a raw food diet is associated with favorable serum LDL cholesterol and triglycerides but also with elevated plasma homocysteine and low serum HDL cholesterol in humans. *J Nutr.* 135(10): 2372-8.

LEE WP, LEE CL, LIN HC. (1996) Glutathione S-transferase and glutathione peroxidase are essential in the early stage of adriamycin resistance before P-glycoprotein overexpression in HOB1 lymphoma cells. *Cancer Chemother Pharmacol.* 38(1): 45-51.

LEONARD JP. (2003) Improved outcomes from dose-dense adjuvant chemotherapy for breast cancer with growth factor support. *Curr Hematol Rep.* 2(6): 451-2.

LI CL, CHEN SL, CHEN WM, LIU JZ, XIAO B, ZHANG HB. (2005) Detection of gene expression alteration of myeloma cells treated with arsenic trioxide. *Zhonghua Xue Ye Xue Za Zhi.* 26(4): 209-13.

LI F, AMBROSINI G, CHU EY, PLESCIA J, TOGNIN S, MARCHISIO PC, ALTIERI DC. (1998) Control of apoptosis and mitotic spindle checkpoint by survivin.

Nature. 396(6711): 580-4.

LIVAK KJ, SCHMITTGEN TD. (2001) Analysis of relative gene expression data using real-time quantitative PCR and the 2(-Delta Delta C(T)) Method. *Methods*. 25(4): 402-8.

LLUIS JM, COLCELL A, GARCIA-RUIZ C, KAPLOWITZ N, FERNANDEZ-CHECA JC. (2003) Acetaldehyde impairs mitochondrial glutathione transport in HepG2 cells through endoplasmic reticulum stress. *Gastroenterology*. 124(3): 708-24.

LOEFFLER M, DAUGAS E, SUSIN SA, ZAMAMI N, METIVIER D, NIEMINEN AL, BROTHERS G, PENNINGER JM, KROMER G. (2001) Dominant cell death induction by extramitochondrially targeted apoptosis-inducing factor. *FASEB J*. 15(3): 758-67.

LOWE SW, RULEY HE, JACKS T, HOUSMAN DE. (1993) p53-dependent apoptosis modulates the cytotoxicity of anticancer agents. *Cell*. 74(6): 957-67.

LY JD, GRUBB DR, LAWEN A. (2003) The mitochondrial membrane potential ($\Delta\psi(m)$) in apoptosis; an update. *Apoptosis*. 8(2): 115-28.

MAIA RC, VASCONCELOS FC, HARAB RC, COELHO AM, DOBBIN JA, RUMJANEK VM. (1998) Comparison between anthracyclines and rhodamine-123 accumulation in chronic lymphoid leukemia: effect of cyclosporin A and verapamil. *Tumour Biol*. 19(1): 41-51.

MEDEMA JP, SCAFFIDI C, KISCHKE FC, SHEVCHENKO A, MANN M, KRAMMER PH, PETER ME. (1997) FLICE is activated by association with the CD95 death-inducing signaling complex (DISC). *EMBO J*. 16(10): 2794-804.

MOSMANN T. (1983) Rapid colorimetric assay for cellular growth and survival: application to proliferation and cytotoxicity assays. *J Immunol Methods*. 65(1-2): 55-63.

MURAKAMI A, OHIGASHI H. (2006) Cancer-preventive anti-oxidants that

attenuate free radical generation by inflammatory cells. *Bio Chem.* 387(4): 387-92.

MUZIO M. (1998) Signalling by proteolysis: death receptors induce apoptosis. *Int J Clin Lab Res.* 28(3): 141-7.

NORDENGREN J, CASSLEN B, CUSTAVSSON B, EINARSOTTIR M, WILLEN R. (1998) Discordant expression of mRNA and protein for urokinase and tissue plasminogen activators (u-PA, t-PA) in endometrial carcinoma. *Int J Cancer.* 79(2): 195-201.

NOWAK AK, CHOW PK, FINDLAY M. (2004) Systemic therapy for advanced hepatocellular carcinoma: a review. *Eur J Cancer.* 40(10): 1474-84.

NYLANDSTED J, ROHDE M, BRAND K, BASTHOLM L, ELLING F, JAATELA M. (2000) Selective depletion of heat shock protein 70 (Hsp70) activates a tumor-specific death program that is independent of caspases and bypasses Bcl-2. Selective depletion of heat shock protein 70 (Hsp70) activates a tumor-specific death program that is independent of caspases and bypasses Bcl-2. *Prot Natl Acad Sci USA.* 97(14): 7871-6.

OBERLIES NH, KROLL DJ. (2004) Camptothecin and taxol: historic achievements in natural products research. *J Nat Prod.* 67(2): 129-35.

OMATA M, TATEISHI R, YOSHIDA H, SHIINA S. (2004) Treatment of hepatocellular carcinoma by percutaneous tumor ablation methods: Ethanol injection therapy and radiofrequency ablation. *Gastroenterology.* 127(5 Suppl 1): S159-66.

PAGLIACCI MC, SPINOZZI F, MIGLIORATI G, FUMI G, SMACCHIA M, GRIGNANI F, RICCARDI C, NICOLETTI I. (1993) Genistein inhibits tumour cell growth in vitro but enhances mitochondrial reduction of tetrazolium salts: a further pitfall in the use of the MTT assay for evaluating cell growth and survival. *Eur J Cancer.* 29A(11): 1573-7.

PANDEY A, MANN M. (2000) Proteomics to study genes and genomes. *Nature.* 405(6788): 837-46.

- PANDITA TK, HIGSHIKUBO R, HUNT CR. (2004)** HSP70 and genomic stability. *Cell Cycle*. 3(5): 591-2.
- PIAST M, KUSTRZEBA-WOJCICKA I, MATUSIEWICZ M, BANAS T. (2005)** Molecular evolution of enolase. *Acta Biochem Pol*. 52(2): 507-13.
- PRADET-BALADE B, BOULME F, BEUG H, MULLNER EW, GARCIA-SANZ JA. (2001)** Translation control: bridging the gap between genomics and proteomics? *Trends Biochem Sci*. 26(4): 225-9.
- PRU JK, TILLY JL. (2001)** Programmed cell death in the ovary: insights and future prospects using genetic technologies. *Mol Endocrinol*. 15(6): 845-53.
- QI Y, CHIU JF, WANG L, KWONG DL, HE QY. (2005)** Comparative proteomic analysis of esophageal squamous cell carcinoma. *Proteomics*. 5(11): 2960-71.
- RAO RV, PEEL A, LOGVINOVA A, DEL RIO G, HERMEL E, YOKOTA T, GOLDSMITH PC, ELLERBY LM, ELLERBY HM, BREDESEN DE. (2002)** Coupling endoplasmic reticulum stress to the cell death program: role of the ER chaperone GRP78. *FEBS Lett*. 514(2-3): 122-8.
- RIEDER CL, COLE R. (2000)** Microtubule disassembly delays the G2-M transition in vertebrates. *Curr Biol*. 10(17): 1067-70.
- ROBERTSON JD, ORRENIUS S. (2002)** Role of mitochondria in toxic cell death. *Toxicology*. 181-182: 491-6.
- RYU JW, KIM HJ, LEE YS, MYONG NH, HWANG CH, LEE GS, YOM HC. (2003)** The proteomics approach to find biomarkers in gastric cancer. *J Korean Med Sci*. 18(4): 505-9.
- SARASTE A, PULKKI K. (2000)** Morphologic and biochemical hallmarks of apoptosis. *Cardiovasc Resc*. 45(3): 528-37.
- SARTORIUS U, SCHMITZ I, KRAMMER PH. (2001)** Molecular mechanisms of death-receptor-mediated apoptosis. *Chembiochem*. 2(1): 20-9.

- SATCHELL PG, GUTMANN JL, WITHERSPOON DE. (2003)** Apoptosis: an introduction for the endodontist. *Int Endod J.* 36(4): 237-45.
- SCAFFIDI C, SCHMITZ I, ZHA J, KORSMEYER SJ, KRAMMER PH, PETER ME. (1999)** Differential modulation of apoptosis sensitivity in CD95 type I and type II cells. *J Biol Chem.* 274(32): 22532-8.
- SCHMIDT S, MICHNA H, DIEL P. (2005)** Combinatory effects of phytoestrogens and 17beta-estradiol on proliferation and apoptosis in MCF-7 breast cancer cells. *J Steroid Biochem Mol Biol.* 94(5): 445-9.
- SCHOTT AF, APEL IJ, NUNEZ G, CLARKE MF. (1995)** Bcl-XL protects cancer cells from p53-mediated apoptosis. *Oncogene.* 11(7): 1389-94.
- SCHUELLER G, KETTENBACH J, SEDIVY R, STIFT A, FRIEDL J, GNANT M, LAMMER J. (2004)** Heat shock protein expression induced by percutaneous radiofrequency ablation of hepatocellular carcinoma in vivo. *Int J Oncol.* 24(3): 609-13.
- SEGLEN PO, BOHLEY P. (1992)** Autophagy and other vacuolar protein degradation mechanisms. *Experientia.* 48(2): 158-72.
- SELLERS WR, FISHER DE. (1999)** Apoptosis and cancer drug targeting. *J Clin Invest.* 104(12): 1655-61.
- SEOW TK, ONG SE, LIANG RC, REN EC, CHAN L, OU K, CHUNG MC. (2000)** Two-dimensional electrophoresis map of the human hepatocellular carcinoma cell line, HCC-M, and identification of the separated proteins by mass spectrometry. *Electrophoresis.* 21(9): 1787-813.
- SIMON SM, SCHINDLER M. (1994)** Cell biological mechanisms of multidrug resistance in tumors. *Proc Natl Acad Sci USA.* 91(9): 3497-504.
- SINGH B, BHAT TK, SINGH B. (2003)** Potential therapeutic applications of some antinutritional plant secondary metabolites. *J Agric Food Chem.* 51(19): 5579-97.

- SKOMMER J, WLODKOWIC D, PELKONEN J. (2006)** Cellular foundation of curcumin-induced apoptosis in follicular lymphoma cell lines. *Exp Hematol.* 34(4): 463-74.
- SOLARY E, PLENCHETTE S, SORDET O, REBE C, DUCOROY P, FILOMENKO R, BRUEY JM, DROIN N, CORCOS L. (2001)** Modulation of apoptotic pathways triggered by cytotoxic agents. *Therapie.* 56(5): 511-8.
- SOLDANI C, SCOVASSI AI. (2001)** Poly(ADP-ribose) polymerase-1 cleavage during apoptosis: an update. *Apoptosis.* 7(4): 321-8.
- SORRENTINO BP. (2002)** Gene therapy to protect haematopoietic cells from cytotoxic cancer drugs. *Nat Rev Cancer.* 2(6): 431-41.
- SRINIVAS PR, SRIVASTAVA S, HANASH S, WRIGHT GL JR. (2001)** Proteomics in early detection of cancer. *Clin Chem.* 47(10): 1901-11.
- SRINIVASULA SM, AHMAD M, FERNANDES-ALNEMRI T, ALNEMRI ES. (1998)** Autoactivation of procaspase-9 by Apaf-1-mediated oligomerization. *Mol Cell.* 1(7):949-57.
- STANGL V, LORENZ M, STANGL K. (2006)** The role of tea and tea flavonoids in cardiovascular health. *Mol Nutr Food Res.* 50(2): 218-28.
- STAVROVSKAYA AA. (2000)** Cellular mechanisms of multidrug resistance of tumor cells. *Biochemistry (Mosc).* 65(1): 95-106.
- STROH C, SCHULZE-OSTHOFF K. (1998)** Death by a thousand cuts: an ever increasing list of caspase substrates. *Cell Death Differ.* 5(12): 997-1000.
- TOMIDA S, HANDI T, HONDA H, KOBAYASHI T. (2002)** Analysis of expression profile using fuzzy adaptive resonance theory. *Bioinformatics.* 18(8): 1073-83.
- TOWBIN H, BAIR KW, DECAPRIO JA, ECK MJ, KIM S, KINDER FR, MOROLLO A, MUELLER DR, SCHINDLER P, SONG HK, VAN OOSTRUM J, VERSACE RW, VOSHOL H, WOOD J, ZABLUDOFF S, PHILLIPS PE. (2003)** Proteomics-based target

identification: bengamides as a new class of methionine aminopeptidase inhibitors. *J Biol Chem.* 278(52): 52964-71.

UENG YF, TASI TH, DON MJ, CHEN RM, CHEN TL. (2005) Alteration of the pharmacokinetics of theophylline by rutaecarpine, an alkaloid of the medicinal herb *Evodia rutaecarpa*, in rats. *J Pharm Pharmacol.* 57(2): 227-32.

VAN ENGELAND M, NIELAND LJ, RAMAEKERS FC, SCHUTTE B, REUTELINGSPERGER CP. (1998) Annexin V-affinity assay: a review on an apoptosis detection system based on phosphatidylserine exposure. *Cytometry.* 31(1): 1-9.

VERHAGEN AM, EKERT PG, PAKUSCH M, SILKE J, CONNOLLY LM, REID GE, MORITZ RL, SIMPSON RJ, VAUX DL. (2000) Identification of DIABLO, a mammalian protein that promotes apoptosis by binding to and antagonizing IAP proteins. *Cell.* 102(1): 43-53.

WALCZAK H, BOUCHON A, STAHL H, KRAMMER PH. (2000) Tumor necrosis factor-related apoptosis-inducing ligand retains its apoptosis-inducing capacity on Bcl-2- or Bcl-xL-overexpressing chemotherapy-resistant tumor cells. *Cancer Res.* 60(11): 3051-7.

WANG M, WANG B, WANG X. (2001) A novel antiapoptosis gene, survivin, bcl-2, p53 expression in cervical carcinomas. *Zhonghus Fu Chan Ke Za Zhi.* 36(9): 546-8.

XIE JT, WANG CZ, WICKS S, YIN JJ, KONG J, LI J, LI YC, YUAN CS. (2006) Ganoderma lucidum extract inhibits proliferation of SW 480 human colorectal cancer cells. *Exp Oncol.* 28(1): 25-9.

XU GL, YAO L, YU SQ, WANG YF, GONG ZN, ZHANG SQ. (2005) Effect of epigallocatechingallate on acute lung injury induced by oleic acid in mice. *Yao Xue Xue Bao.* 40(3): 231-5.

WANG J, BIJU MP, WANG MH, HAASE VH, DONG Z. (2006) Cytoprotective Effects of Hypoxia against Cisplatin-Induced Tubular Cell Apoptosis:

Involvement of Mitochondrial Inhibition and p53 Suppression. *J Am Soc Nephrol.* 17(7): 1875-85.

WEBB SJ, HARRISON DJ, WYLLIE AH. (1997) Apoptosis: an overview of the process and its relevance in disease. *Adv Pharmacol.* 41: 1-34.

WYLLIE AH, BEATTIE GJ, HARGREAVES AD. (1981) Chromatin changes in apoptosis. *Histochem J.* 13(4): 681-92.

YAMAHARA J, MOCHIZUKI M, FUJIMURA H, TAKAISHI Y, YOSHIDA M, TOMIMATSU T, TAMAI Y. (1990) Antiulcer action of *Sophora flavescens* root and an active constituent. I. *J Ethnopharmacol.* 29(2): 173-7.

YAN B, WANG H, PENG Y, HU Y, WANG H, ZHANG X, CHEN Q, BEDFORD JS, DEWHIRST MW, LI CY. (2006) A unique role of the DNA fragmentation factor in maintaining genomic stability. *Proc Natl Acad Sci USA.* 103(5): 1504-9.

YEN A, ROBERSON MS, VARVAYANIS S, LEE AT. (1998) Retinoic acid induced mitogen-activated protein (MAP)/extracellular signal-regulated kinase (ERK) kinase-dependent MAP kinase activation needed to elicit HL-60 cell differentiation and growth arrest. *Cancer Res.* 58(14): 3163-72.

YU A, MCMASTER CR, BYERS DM, RIDGWAY ND, COOK HW. (2004) Resistance to UV-induced apoptosis in Chinese-hamster ovary cells overexpressing phosphatidylserine synthases. *Biochem J.* 381(Pt 3): 609-18.

ZAMBLE DB, MU D, REARDON JT, SANCAR A, LIPPARD SJ. (1996) Repair of cisplatin-DNA adducts by the mammalian excision nuclease. *Biochemistry.* 35(31): 10004-13.

ZAVERI NT. (2006) Green tea and its polyphenolic catechins: medicinal uses in cancer and noncancer applications. *Life Sci.* 78(18): 2073-80.

ZHAO X, WEI Y, PENG Z. (2000) Induction of apoptosis in ovarian carcinoma cells by HSP70 antisense oligodeoxynucleotides. *Zhonghua Yi Xue Yi Chuan Xue Za Zhi.* 17(1): 32-5.

ZIMMERMANN KC, BONZON C, GREEN DR. (2001) The machinery of

programmed cell death. *Pharmacol Ther.* 92(1): 57-70.

CUHK Libraries



004359141